International Journal of
Young Scientist Research

Vol 7, No 2, Dec 2023
ISSN: 2588- 5111

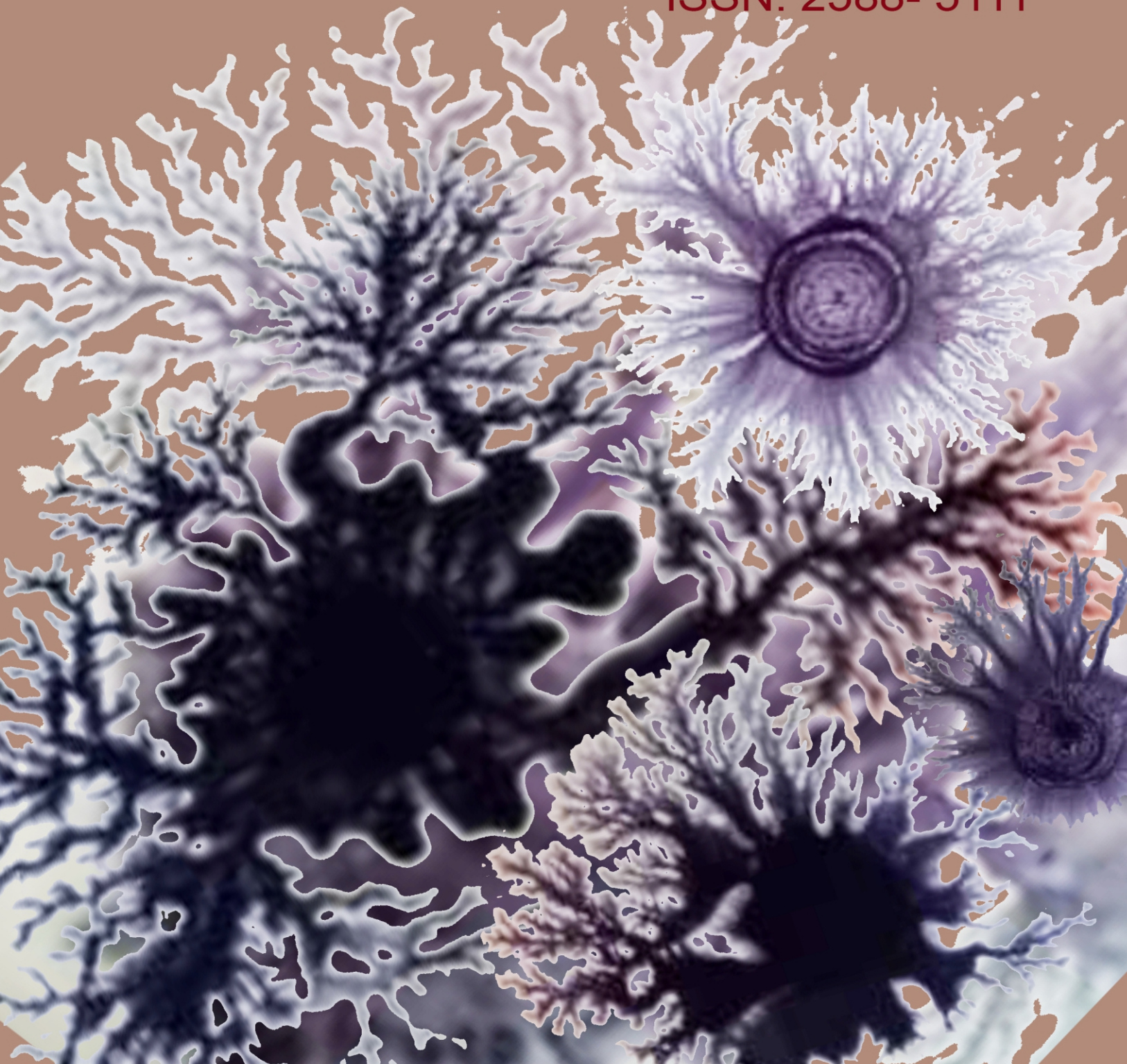

Contents

Literature Review on Lunar Plant Cultivation..... (4-7)

The Physics in Science Fiction Movies..... (8-17)

Colored Line.....(18-21)

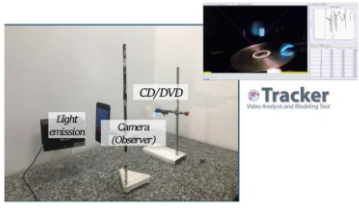

Short Length Wire as an Electrical Fuse..... (22-25)

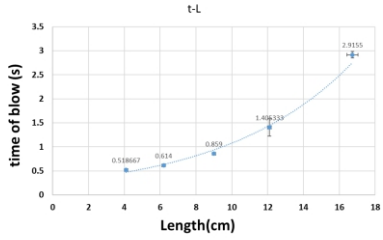

Teaching Material for Environmental Literacy..... (26-30)

Oscillating Screw..... (31-34)

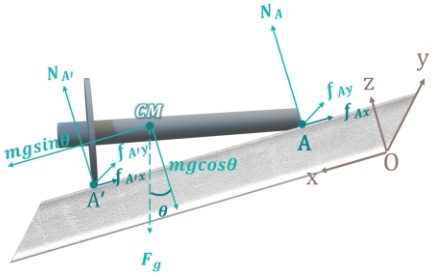

The Effect of Ammonia on Flowers with .....(35-37)

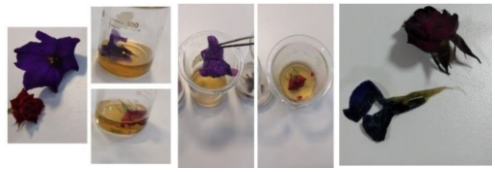

.

The Effect of Different Jumping Techniques .....(38-40)

How Does a Magnetic Field Affect ..... (41-42)

Geometry and Dynamics of the Fractal Fingers.....(43-46)

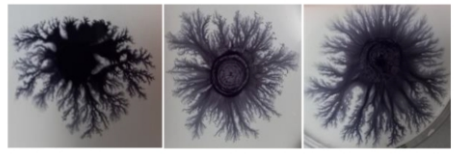

Paper Wrinkles..... (47-50)

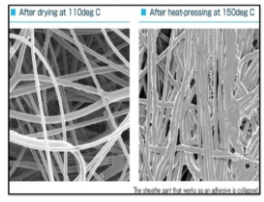

Investigating Growing plants in Different Kinds of Light..... (51-52)

Investigating an Intriguing Effect When One.....(53-55)

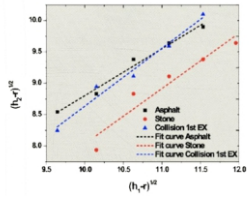

Microscopic Swimmers..... (56-57)

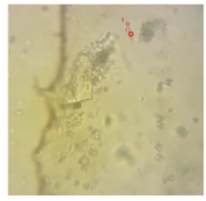

Arrester Bed..... (58-61)

Young Scientist Research

Title proper: Young scientist research

Subject: NATURAL SCIENCES, ART, ENGINEERING AND TECHNOLOGY

Corporate contributor: Ariaian Young Innovative Minds Institute

Publisher: Tehran: Ariaian Young Innovative Minds Institute

Dates of publication: 2017- Present

Frequency: Annual

Type of resource: Periodical

Language: English

Country: Iran

Medium: Online

Indexed by: ROAD (The Directory of Open Access Resources)

ISSN- 2588-5111
ISSN International Centre
45 rue de Turbigo
75003 Paris
France

Address:

Unit 14, No.32, Malek Ave., Shariati St.

Post Code: 1565843537

Tel:+9821-77507013, 77522395

WELCOME TO THE INTERNATIONAL JOURNAL of YOUNG SCIENTIST RESEARCH

Young Scientist Research is a research journal based on scientific projects and we are pleased to present our students' work in scientific activities. This open-access journal includes young students' research in any field of science which publishes full-length and abstract research on any aspects of applied sciences in relation to work presented in both national and international conferences, competitions and tournaments of all types.

Programs that have educational opportunities for high school students to present their distinguished projects from regional, national and international events such as International Conference of Young Scientists (ICYS), International / Persian Young Physicists' Tournament (IYPT/ PYPT), International / Iran Physics' Tournament (IPT/ IRPT), International / Persian Young Naturalists' Tournament (IYNT/ PYNT) and International ISAC Olympiad .

New manuscripts sent to the Journal will be handled by the Editorial Office who checks compliance with the guidelines to authors. Then a rapid screening process at which stage a decision to reject or to go to full review is made.

By submission of a manuscript to the Journal, all authors warrant that they have the authority to publish the material and that the paper, or one substantially the same, has neither been published previously, nor is being considered for publication elsewhere.

This journal belongs to Ariaian Young Innovative Minds Institute, AYIMI, and one to two issues are published in a year. All details are on the YOUNG SCIENTIST RESEARCH Journal website (http://journal.ayimi.org).

Editor in Chief
Dr. Dina Izadi
Researcher & President of
Ariaian Young Innovative Minds Institute, AYIMI
ADIB, Cultural and Artistic Institute
http://www.ayimi.org
http://adib.ayimi.org
http://journal.ayimi.org
Email: info@ayimi.org
Unit 14, No. 32, Malek Ave., Shariati St.,
Post Code: 1565843537, Tehran/ Iran
Young Scientist Research Journal, ISSN: 2588-5111

CURRENT ISSUE
Vol 7 NO2 Dec. 2023

Literature Review on Lunar Plant Cultivation: Seed Storage, Plant Maintenance, Electromagnetic Protection Dome Construction

Sarah Yim,Seoul, South Korea, sarahyim26@gmail.com

ARTICLE INFO

Accepted by Ariaian Young Innovative Minds Institute , AYIMI

http://www.ayimi.org ,info@ayimi.org

ABSTRACT

During the early days of the space age (Apollo era), the visionary plan was to bring samples of the lunar regolith back to Earth, but thoroughly studying them with advanced equipment and saving them for future research was not yet imagined. It was important to store seeds in a secure airtight packet because they help reduce humidity, which is key to storing seeds effectively. Issues such as climate change, global warming, and food insecurity worsen every year, so in this study lunar plant cultivation has been considered to mitigate these issues.

Keywords : *Space, Seeds, Cultivation, Climate Change*

1. Introduction

People, including scientists, have long regarded lunar plant cultivation as mere science fiction and far-reaching into the future. However, as issues such as climate change, global warming, and food insecurity worsen every year, lunar plant cultivation has become a reality and a potential solution considered by many to mitigate these issues. Lunar plant cultivation, the growth and production of crops on the Moon's surface, is a nascent topic that many scientists have begun to research on.

During the early days of the space age (Apollo era), the visionary plan was to bring samples of the lunar regolith back to Earth, but thoroughly studying them with advanced equipment and saving them for future research was not yet imagined. Fifty years later in the Artemis era, three of the regolith samples have been used to successfully grow plants. NASA Administrator Bill Nelson states that "this research is critical to NASA's long-term human exploration goals as we'll need to use resources found on the Moon and Mars to develop food sources for future astronauts living and operating in deep space. This fundamental plant growth research is also a key example of how NASA is working to unlock agricultural innovations that could help us understand how plants might overcome stressful conditions in food-scarce areas here on Earth" [1].

According to previous research, lunar soil is cultivable but not as robust as growth from Earth soil. Several aerospace agencies such as the Japan Aerospace Exploration Agency (JAXA), China's Lunar Exploration Program (CLEP), and the National Aeronautics and Space. Administration (NASA) have experimented with both simulated lunar regolith and lunar regolith. In January of 2019, China's Chang'e 4 spacecraft landed on the far side of the Moon, carrying with it a biosphere that contained five sets of plants and some insects in order to test sustainability of long-term settlements in space. Although the cotton plant successfully sproutedon the Moon's surface, it shortly died after, unable to withstand the Moon's extreme environmental conditions [2]. Additionally, in May of 2022, NASA planted seeds of the flowering weed called Arabidopsis thaliana in lunar soil samples of which were retrieved back in 1969 and 1972. These seeds successfully sprouted, but what was interesting was that the plants reacted differently depending on which soil sample the growth was supported by. In other words, the location where soil samples were collected mattered [3].

In order to construct a sustainable and efficient lunar planting system, this paper divides the process into three different sections: the seed storage process, necessary maintenance (temperature, water, light, fertilizer), and the construction of an electromagnetic protection dome.

2. Seed Storage Process

It is important to store seeds in a secure airtight packet because they help reduce humidity, which is key to storing seeds effectively. Reducing humidity will also reduce the risk of mold and premature sprouting in seeds. Not only do seeds need to be stored in an airtight packet, but they also need to be frozen. Freezing seeds not only helps with seed germination but also helps with long term seed storage, which is particularly handy for space travelers. Seeds will usually be placed near the back of the fridge/freezer to avoid temperature fluctuations from opening and closing its doors. Since 2020, astronauts have used two food fridges called the Freezer Refrigerator Incubator Device for Galley and Experimentation (FRIDGE) on the ISS [4]. The ideal freezing temperature for seed storage is 0 to 10 degrees C. It is very important to set a consistent range of cool temperatures during seed storage. Every 5-6 degree C change in temperature could cost seeds half their storage life.

3. Plant Maintenance

3.1. Temperature

Problems in plant growth most often occur when plants are grown in extreme temperatures that are not ideal for plants. This will most likely be the case on the Moon, for temperature fluctuates between -183 degrees C and 106 degrees C on the Moon [5]. So, what could be solutions to this temperature problem? Firstly, replanting the roots somewhere else on the Moon will not solve this problem because the plants will still experience extreme temperature fluctuations.

Additionally, harvest will also be an infeasible solution, for the plants will not be ready because they have stopped growing prematurely. Thirdly, transporting the plants back

to Earth could be a possible solution but could aggravate their growth due to sudden changes in the environment.

Therefore, if current technology and mechanisms allow, adjusting the temperature of the surrounding environment in a separately constructed dome will be the ideal solution. Currently, scientists have used the Active Thermal Control System (ATCS), using a mechanically pumped fluid in closed-loop circuits to perform three functions: heat collection, transportation, and rejection. The remaining waste heat is subsequently eliminated using cold plates and heat exchangers, both of which are cooled by circulating ammonia loops on the station's exterior [6].

While most plants grow best in temperatures ranging from 15 to 30 degrees C, some plants such as wheat thrive in a hot and humid climate. For example, wheat plants thrive in an environment with the average temperature ranging from 21 to 37 degrees C. These plants can tolerate temperatures up to 42 degrees C. To grow wheat on the Moon, optimal temperature must be adjusted accordingly.

3.2. Water

The most common explanation for the wilting of plant leaves is lack of water. While plants need at least 2 inches (5 cm) of water a week, the lack of liquid water found on the Moon poses a foreseeable problem of underwatering for plants. Thus, astronauts must find alternative ways to water their plants on the Moon.

Instead of water, ice (could be used after harvest) is present on the moon and has been found in dark, cold areas such as deep craters or near the Moon's poles. However, the ice on the moon is demineralized, so the minerals and nutrients (nitrogen, phosphorus, potassium) that compost from human feces are very valuable. Additionally, recent technology shows evidence of water molecules on the Moon, especially near some of the moon's large craters such as the Clavius crater in the moon's southern hemisphere. To detect water molecules, NASA's Stratospheric Observatory for Infrared Astronomy (SOFIA) used a special infrared camera that could distinguish between water's specific wavelength of 6.1 microns and the wavelength of hydroxyl, or OH. "Data from this location reveal water in concentrations of 100 to 412 parts per million — roughly equivalent to a 12-ounce bottle of water — trapped in a cubic meter of soil spread across the lunar surface," NASA says [7]. However, these are not puddles of water; but instead, they are water molecules that are so spread apart. Scientists continue to research ways to use these water molecules for plant watering.

NASA offers two possible explanations for the peculiar appearance of water in these regions. First, micrometeorites, carrying small amounts of water, could be raining down on the lunar surface. When micrometeorites collide with the moon, water may be left behind on the surface. Secondly, there could be a two-step process by which the solar wind from the Sun transports hydrogen to the lunar surface and reacts with oxygen-bearing minerals in the soil to produce hydroxyl. It is possible that the radiation from the impact of micrometeorites is turning that hydroxyl into water.

Another important question is how the water is stored and accumulated. The high heat produced by micrometeorite strikes may cause small structures in the soil that resemble tiny beads to develop, trapping the water. Another possibility is that the water may be shielded from sunlight and concealed between grains of lunar soil, making it slightly more accessible than water trapped in bead-like structures [8].

Although ice is a potential source of water that could be used after it is liquefied, a pragmatic question that emerges is: how will humans access these water ice resources buried so deeply in dark craters where temperatures are as low as 400 K? NASA's Jet Propulsion Lab proposes reflecting solar energy using giant mirror reflectors (transported from Earth) into the dark craters, allowing for robotic mining vehicles to dig into the deep craters to extract the hidden water ice.

These mirrors, which will supply energy to overcome ice's high heat capacity, will help sublimate and liquify the solid water ice for plant watering [9].

Another key question then emerges: how will the methods for plant watering be altered to address the different gravitational conditions on Mars? Astronauts actually use a special syringe to inject water directly into "plant pillows," which are special bags that contain the seed. A major concern for many astronauts today is finding a balance between aeration (getting the right amount of air to a plant) and hydration (getting sufficient amount of water to a plant). NASA astronauts discovered that imbalanced air flow could result in high levels of humidity, resembling tropical rainforest conditions that would put plants under a lot of stress. High humidity levels could cause guttation, which is when a plant's internal pressure builds up, forcing excess water out of the leaves. Overhydration also resulted in some plants growing mold or bacteria. Through research projects such as the Plant Water Management (PWM) project, astronauts continue to investigate the best way to water plants in space that address both aeration and hydration [10].

3.3. Light

Although most plants can grow in the shade without light, they need to get enough light to grow large heads and healthy leaves. Moreover, plant growth is slower without light compared to with light (full or partial sun conditions). It is recommended that plants are grown in sunny spots that receive at least 6 hours of sun daily. Similar to Earth, the Moon spins on its axis and goes through daytime and dark cycles. However, the cycles on the Moon are longer than on Earth, as the mean solar day on the Moon is 29.5306 Earth days (meaning 14-15 days of daytime and night time each) [11]. Plants cannot survive 14-15 days without light, so an external light source (other than natural sunlight) must supply light to the plants during the Moon's dark period.

Funding various agricultural programs in the late 20th century, NASA researchers discovered that a certain blend of LED lights could replace hot and heavy incandescent grow lights. Today, installing smart LED lights with precise controls that will not overheat plants is a wise choice.

A combination of red and blue lights generates more light than green LEDs by design, because plants could photosynthesize using red LEDs and avoid becoming too tall and spindly using blue LEDs. Many of today's indoor farms offer plants a similar diet of red and blue photons, appearing bathed in purple light. Similarly, NASA's Expedition 44 crew members have attempted to grow plants under the purple pinkish hue created by the red and blue lights and have successfully grown plants under the Veggie plant growth system [12].

3.4. Fertilizer

Many plants are also heavy feeders of nutrients, quickly depleting the nutrient-rich soil, and thus requiring a constant, steady supply of water and nutrients throughout

its growth. If plants become nutrient deficient, they may show symptoms such as yellow discoloration and deformation of leaves.

Worms are essential for the health of the soil and plants, for they feed on organic waste such as the non-eaten remains of the crops. Their excrements are further decomposed by bacteria, releasing important nutrients such as nitrogen and phosphorus into the soil. Worms also enhance soil structure and decrease the density of the hydrophobic lunar soil by excavating burrows, making it easier for water to penetrate the soil. Thousands of worms have already been launched into space for different experiments. Second, bacteria such as Rhizobium binds nitrogen from the air turning it into nitrate and improves soil quality. In fact, Wieger Wamelink, a Mars and Moon soil research expert at Netherlands' Wageningen University, has already tested earthworms and nitrogen fixing bacteria in space-like environments and discovered that they had thrived in the given environments [13]. Potato peels and coffee grounds, both examples of organic matter rich with nutrients inside, improve soil quality by improving water drainage, retention, and aeration in the soil. Coffee grounds can be transported from Earth, and potato peels can be extracted from leftover peels after harvesting them on the Moon. Peat moss and vermiculite are other additives that improve soil health [14]. These additives, which ensure healthy plant growth and a self-sustaining ecosystem, are applicable to various plants such as cabbage plants, radish plants, wheat, tomato plants, and potatoes.

Plants need to grow in fertile, well-drained, and healthy soil. Hard or compacted soil, a defining characteristic of lunar soil, may lead to misshapen tubers and unhealthy lateral stems and buds in potato plants. Lunar soil is also extremely poor in carbon, nitrogen (specifically, NO3 and Nh4), and phosphorus, which are necessary nutrients for almost all plant growth.

Although data from several Earth-lunar regolith experiments (such as the Plant the Moon Challenge) show that combining Earth and Moon soil will provide missing nutrients for plants, it is unrealistic to bring Earth soil to the Moon because of monetary reasons and transportation difficulties. Meanwhile, the recycling of human urine and poop as manure is essential for self-sustaining space agriculture, for resources are heavily limited, and everything humans use and produce must be recycled for efficiency reasons. The nutrient solution in human feces and urine are as follows: ammonium ion (NH_4), Nitrate (NO3). Phosphorus (P), Potassium (K), Calcium (Ca), Magnesium (Mg), and Sulfate (SO_4). Sawdust may also help materials in the feces decompose and break down into less complicated components, resulting in simpler, nutrient-rich compost [15].

Different plants prefer different amounts of fertilizer for efficient growth. For example, while many plants thrive on nitrogen-rich fertilizer such as sterilized human feces or urine compost, some plants such as the radish plant do not prefer fresh manure or fertilizers high in nitrogen.

Radish plants are sensitive to excess nitrogen in soil, and it may slow the growth of the plants, resulting in small, unhealthy root bulbs with heavy top growth. In these cases, applying phosphorus-rich organic compost such as worm castings or rock phosphates to the soil will encourage plant growth.

4. Construction of Dome

The average temperature on the Moon ranges from -298 degrees Fahrenheit (-183 degrees Celsius) at night to 224 degrees Fahrenheit (106 degrees Celsius) during the day. Unlike Earth, the Moon does not have a significant atmosphere or magnetic shield to deflect solar wind or trap heat at night, so its temperature fluctuates in its extremes [16]. Therefore, it is impossible to grow plants directly on the Moon's surface with full, unprotected exposure to its natural surroundings.

In order to successfully germinate and grow the seeds she has safely brought to the Moon, a separate dome must be constructed that can withstand cosmic radiation due to the absence of a magnetic field on the Moon. Starting underground will be a wise choice, for underground habitats will protect living organisms from radiation, temperature variation, and other above-ground damages.

Additionally, the ISS frequently uses titanium, kevlar, and high-grade steel (an alloy of iron and carbon). These materials were required by engineers to create a construction that was both light and impenetrable to damage. Minimizing weight is essential since each of the Station's can-shaped metal components must be lifted into orbit. The majority of the modules' outer shell is made of lightweight aluminum rather than heavy steel, and this shell must offer defense against incoming small meteorites and man-made debris. Even grains the size of dust pose a serious threat to the ISS since it travels through space at a speed of around 27,000 km/h. In fact, to ensure the safety of the crew, the Space Station wears a "bullet-proof vest" [17]. Layers of Kevlar, ceramic fabrics, and other advanced materials form a blanket up to 10 cm thick around each module's aluminum shell. (Kevlar is the material used in the bullet-proof vests used by police officers.)

Titanium on the moon is primarily found in the mineral ilmenite, a compound that contains iron, titanium and oxygen. If humans one day mine on the moon, they could break down ilmenite to separate these elements. Furthermore, Apollo data showed that minerals rich in titanium are better at capturing solar wind constituents like helium and hydrogen. [18]. These gases would likely be vital resources in the construction of lunar colonies and for exploration of the moon.

High-grade steel, an alloy of iron and carbon, can be found from extracting hematite. Hematite, a mineral composed of ferric oxide (Fe2O3), has also been found on the moon [19]. This mineral is a product of a reaction between iron, oxygen, and liquid water. Iron can be extracted from hematite (Fe2O3) in a blast furnace.

5. Conclusion

Science has made significant progress to prepare for long-term settlements in space, not only for further space exploration but also for solutions to food insecurity and prevention of the destruction of humanity. For future research, scientists must consider these questions: Can understanding the genes and their alterations in plants help us discover potential solutions to reduce the stress plants receive from lunar soil? Are materials from different areas of the Moon more conducive to plant growth than others? Could studying lunar regolith help us understand more about the Mars regolith and potentially growing plants in that material as well? In essence, people, as a collective group of scientists, astronomers, researchers, companies, and governments, must work together to advance discoveries in this nascent research field.

References

[1] Keeter, Bill. "Scientists Grow Plants in Lunar Soil." NASA, NASA, 12 May 2022, www.nasa.gov/feature/biological-physical/scientists-grow-plants-in-soil-

from-the-moon.

[2] Wong, Sam. "First Moon Plants Sprout in China's Chang'e 4 Biosphere Experiment." New Scientist, New Scientist, 16 Jan. 2019, www.newscientist.com/article/2190704 -first-moon-plants-sprout-in-chinas-change-4-biosphere-experiment/.

[3] Paul, Anna-Lisa, et al. "Plants Grown in Apollo Lunar Regolith Present Stress-Associated Transcriptomes That Inform Prospects for Lunar Exploration." Nature News, Nature Publishing Group, 12 May 2022, www.nature.com/articles/s42003-022-03334-8.

[4] Niederwieser, Tobias, et al. "FRIDGE – The next Generation Freezer/Refrigerator/Incubator for Food and Experiment Conditioning Onboard the ISS." Journal of Space Safety Engineering, Elsevier, 12 June 2022, www.sciencedirect.com/science/article/abs/ pii/S2468896722000635.

[5] "Ask an Astronomer." Cool Cosmos, coolcosmos.ipac.caltech.edu/ask/168-What-is-the -temperature-on-the-Moon-.

[6] "Active Thermal Control System (ATCS) Overview." NASA,www.nasa.gov/pdf/473486main iss_atcs_overview.pdf.

[7] Chappell, Bill. "Water On The Moon: NASA Confirms Water Molecules On Our Neighbor's Sunny Surface." NPR, NPR, 26 Oct. 2020, www.npr.org/2020/10/26/927869069/water-on-the -moon-nasa-confirms-water-molecules-on-our -neighbors-sunny-surface.

[8] Potter, Sean. "NASA's SOFIA Discovers Water on Sunlit Surface of Moon." NASA, 26 Oct. 2020, www.nasa.gov/press-release/nasa-s-sofia-discovers -water-on-sunlit-surface-of-moon.

[9] Newsource, CNN. "These Robots Could Search for Life in Our Solar System's OceanWorlds." Local News 8, 14 July 2022,localnews8.com/news/national-world/cnn -world/2022/07/14/the-next-gen-robots-that-could-expl ore-ocean-worlds/.

[10] "Nasa Project Investigates - How Do You Water a Plant in Space?" BBC News, BBC, www.bbc.co.uk/newsround/57157873.

[11] "GMS: 100 Lunar Days - Parts I and II." NASA, svs.gsfc.nasa.gov/12739.

[12] Rainey, Kristine. "Crew Members Sample Leafy Greens Grown on Space Station." NASA, NASA, 7 Aug. 2015, www.nasa.gov/mission_pages/ station/research/news/meals_ready_to_eat/.

[13] Wamelink, Wieger. "Earthworms Can Reproduce in Mars Soil Simulant." WUR, Wageningen Environmental Research, 27 Nov. 2017, www.wur.nl/en/newsarticle/earthworms-can-reproduce-in-mars-soil-simulant.htm.

[14] "Plant the Moon Challenge." Help NASA Return to the Moon to Stay!,plantthemoon.com/best-in-show-fall21/.

[15] Zeldovich, Lina. "A History of Human Waste as Fertilizer." JSTOR Daily, 18 Nov. 2019, https://daily.jstor.org/a -history-of-human-waste-as-fertilizer/.

[16] "UCLA Research Discovers That Full Moon May Not Be Protected by Earth's Magnetic Field after All." UCLA Physical Sciences,www.physicalsciences.ucla.edu/ucla -research-discovers-that-full-moon-may-not-be -protected-by-earths-magnetic-field-after-all/.

[17] "One Giant Leap for Steel." – Official POSCO Newsroom, 3 Nov. 2016, newsroom.posco.com/en/one-giant-leap -steel/.

[18] "Moon Packed with Precious Titanium, NASA Probe Finds." Space.com, Space, 11 Oct. 2011, www.space.com/13247-moon-map-lunar-titanium.html.

[19] "The Moon Is Rusting, and Researchers Want to Know Why." NASA, NASA, www.jpl.nasa.gov/news/the-moon -is-rusting-and-researchers-want-to-know-why.

The Physics in Science Fiction Movies , Batman, The Dark Knight

Anisa Kaviani Maram [a], Shoshana Buchler [b] ;

a)North Toronto C.I, anisakaviani@gmail.com , b) North Toronto C.I, shoshanabuchler@gmail.com

ARTICLE INFO

a) participant in IYPT 2023 and

Gold medalist in ISAC Olympiad 2023

Awarded by Ariaian Young Innovative

Minds Institute , AYIMI

http://www.ayimi.org ,info@ayimi.org

ABSTRACT

The movie "The Dark Knight" offers a thrilling platform for the application of physics in famous movies. With numerous action sequences like intense chases, violent crashes, gravity-defying leaps, and explosive interactions, the movie offers a diverse take on physics in science fiction and superhero movies. This in-depth investigation of these sequences offers insight into the artistic view that the filmmakers take with the laws of physics. Bad physics is often used as a device to improve the entire cinematic experience. Therefore, this analysis seeks to identify both good and bad examples of physics in "The Dark Knight." By doing so, we seek to analyze the effects of inaccurate physics on the movie and how they shape the narrative and spectacle of this film.

1. Introduction

The second movie in the batman trilogy is set a year after the events in Batman Begins (2005) where Gotham city is experiencing an unusual peace as Batman, Lieutenant James Gordon, and newly appointed District Attorney Harvey Dent collaborate successfully to put criminals behind bars. However, they all face a new and dangerous challenge as a mysterious and sadistic mastermind called "The Joker" appears and creates a new wave of mayhem. The Joker during an intense bank robbery, steals all of the Gotham's mob money. He uses this money to stage a series of horrific and strategic attacks against the city and its people, each one carefully planned and aimed at Dent and Batman. Batman's battle with the Joker rapidly intensifies and becomes deeply personal which forces him to "confront everything he believes". Additionally, a love triangle between Bruce Wayne, Harvey Dent and Rachel Dawes. The joker next plan causes results in a tragic turn of events as the Batman and Commissioner Gordon are forced to choose between saving Rachel or Harvey. This eventually results in Rachel's death and Dent's severe disfigurement. The Joker strategically uses Harvey's damaged emotions to transform him to the vengeful two-faced.

While batman eventually manages to catch the joker after one of his massacres, he realizes the Joker's intentions: the turning of Harvey Dent. Commissioner Gordan and Batman are forced confront Harvey who is consumed by rage and blames Gordon for Rachel's death. The confrontation tragically results in Dent's demise. Gordan and Batman are faced with the difficult decision of uncovering Dent's recent actions and risk losing the city's hope and justice. Batman takes responsibility for Dent's crimes. His sacrifice saves Dent's reputation as the city's savior. The film concludes with Batman on the run, facing the consequences of his decisions and leaving the city in a state of uncertainty.

The movie "The Dark Knight" offers a thrilling platform for the application of physics in famous movies. With numerous action sequences like intense chases, violent crashes, gravity-defying leaps, and explosive interactions, the movie offers a diverse take on physics in science fiction and superhero movies. This in-depth investigation of these sequences offers insight into the artistic view that the filmmakers take with the laws of physics. Bad physics is often used as a device to improve the entire cinematic experience. Therefore, this analysis seeks to identify both good and bad examples of physics in "The Dark Knight." By doing so, we seek to analyze the effects of inaccurate physics on the movie and how they shape the narrative and spectacle of this film.

2. Good Physics

2.1. Scene 1: Bullet Denting the Truck

In car chase scene under the bridge, the Joker (Heath Ledger) shoots at the SWAT truck which contains Harvey Dent (Aaron Eckhart). Using the first gun (Glock 17), the Joker shoots at the SWAT Truck. In the next scene inside the car, it can be observed that the Joker has managed to make indents in the walls of the armored steal truck. Afterwards, the Joker uses his second (Remington 870 sawed-off) and third (Bazooka) gun to shoot at the truck after finishing his ammo.

Harvey Dent then asks the officer in the SWAT truck "These things are made for that right?" and the officer replies "He'll need something a lot bigger to get through this" The real question is whether the Joker's gun would actually have enough energy to dent the SWAT truck?

To prove that this scene included good and correct physics, the gun range and its energy right before hitting the truck is calculated.

While in the scene that is being analyzed, the Joker is standing and shooting, the picture bellow can be used to estimate the trucks distance from the ground and later using that information, the bullet's distance to the ground when shooting the bullet can be estimated. Using Logger Pro, the scale was set using the truck's height (excluding the wheels) which is around 2.7 m. The height between the ground and the layer which the Joker is standing on is around 0.91m.

It is assumed that the Joker holds the gun straight in his hands and his hand makes a 90° angle with his body, as observed in the picture bellow. Using Heath Ledger's height, 1.85m, the height of the gun in the Joker's hand from the truck's ground was estimated to be around 1.56m. Therefore, this and the previous information can be used to calculate the bullet's total distance from the ground.

$$\Delta d_{y_{bullet}} = \Delta d_{Truck\ floor-Ground} + \Delta d_{Gun-Ground}$$

$$\Delta d_{y_{bullet}} = 0.91 + 1.56$$

$$\Delta d_{y_{bullet}} = 2.47m$$

Vertical and Horizontal analysis to calculate the horizontal range of the bullet:

Vertical ↑ +	Horizontal → +
$\vec{v_{1_y}} = 0\frac{m}{s}$ [up] Assuming that the Glock 17 was shot horizontally $\Delta\vec{d_y} = -2.47\ m\ [up]$ Since the bullet's velocity was far too great to be able to calculate the gravitational potential energy, the value is estimated. $\vec{a} = -9.8\ \frac{m}{s^2}\ [up]$ $t = ?$	The average muzzle velocity of a Glock 17 gun is approximately $375\frac{m}{s}$ $\vec{v_{1_x}} = 375\frac{m}{s}$ [left] $t = 0.71\ s$ $\Delta\vec{d_x} = ?$
$\Delta\vec{d} = \frac{1}{2}\vec{a}\Delta t^2 + \vec{v_i}\Delta t$ $-2.47 = \frac{1}{2}(-9.8)t^2$ $t = \sqrt{\frac{(-2.47)(2)}{(-9.8)}}$ $\mathbf{t = 0.71s}$	$\vec{v} = \frac{\Delta\vec{d}}{\Delta\vec{t}}$ $375 = \frac{\Delta\vec{d_x}}{0.71}$ $\mathbf{\Delta\vec{d_x} = 266.25m\ [right]}$

The distance between Joker's truck and the SWAT truck is approximately 10m. Therefore, the bullet's range was calculated to be 270m which can easily reach the SWAT

truck. The range calculated for the Glock 17 is also similar to its real "effective" range which is roughly around 60m. The difference between these two values is due to the fact that air resistance was seen as negligible in the calculations and the range is from the moment the gun is shot to the moment it hits the ground while the real value is only the effective range. This also conclude that the bullets velocity when hitting the SWAT truck is greater than it would be if it was farther away from the other truck.

The second part of the calculations is to prove whether the bullet will be able to dent the SWAT truck's wall. This is done by calculating the muzzle energy of the gun to see if it can damage the steel walls of the truck. But first, the bullets velocity when hitting the SWAT truck is calculated using the kinematic equations.

The bullet's mass (m bullet) estimated by using the mass of the bullet typically used for the Glock 17. The distance between the SWAT truck and Joker's Truck was also estimated using values found online. The time it took for the bullets to hit the truck was calculated using Adobe Premiere and the time interval between the two bullets making contact with the SWAT truck were calculated. Next the time it took for the joker to pull the triger was calculated and this value was subtracted from the other value. The Δt calculated is the true time it took for the bullet to hit the SWAT truck after being released.

$$m_{bullet} \approx 90\ gr = 0.09kg$$

$$\vec{v_1} = 375\frac{m}{s}\ [left]$$

$$\Delta\vec{d} \approx 10\ m$$

$$\Delta t = 0.04s$$

$$\vec{v_2} = ?$$

$$\Delta\vec{d} = \left(\frac{\vec{v_1}+\vec{v_2}}{2}\right)\Delta t$$

$$10 = \left(\frac{375+\vec{v_2}}{2}\right)(0.04)$$

$$v_2 = 125\frac{m}{s}$$

Next, using the velocity, the bullet's kinetic energy is calculated.

$$E_k = \frac{1}{2}m.v_2^2$$

$$E_k = \frac{1}{2}(0.09)(125^2)$$

$$\underline{\mathbf{E_k = 703.125\ J}}$$

Therefore, the kinetic energy also known as the "muzzle energy" of the Glock 17 is approximately 700 J, assuming that the mass of each bullet is 0.09kg.

The SWAT truck's material is hardened steel with thicknesses varying from 3.17 mm to greater than 6.35 mm depending on the level of resistance required to build most of the body. For this specific scene, it is assumed that the wall's thickness is around 4.5mm. According to MyArmoury.com, it takes around 400J to dent a 3.00mm truck made of steel. And by further calculations it can be estimated that 600J (400×4.5÷3.00) of energy is needed to dent the 4.5mm thick SWAT truck. This value is very close to the bullet's kinetic energy (700 J). In conclusion, this physics is a good explanation of how the Joker's bullet was able to reach the SWAT truck from his own truck and make an indent inside the SWAT truck's walls in a way that it can be visible from inside.

2.2. Scene 2: Maroni's Legs Breaking from a Fall

During one of the scenes, Batman (Christian Bale) interrogates Maroni (portrayed by Eric Roberts), demanding information about the Joker's whereabouts and hold Maroni over the edge of a balcony. The exchange is intense, and Maroni mocks Batman, saying that the vigilante won't kill him because of his moral code. He also says that "A fall from this height won't kill me" and the Batman replies, "I'm counting on it" and drops Maroni. The scene concludes with Maroni falling and hitting the ground with a slight angle and breaking his legs.

The batman believed that the fall from that height would only injure Maroni and won't kill him. Therefore, this analysis will prove whether his statement was true and if the force from the ground acting upon Maroni's feet were enough to break his legs.

Falling from different heights result in minor or severe injuries, they can cause fractures in certain situations. For example, if a person falls directly on a hard surface, such as concrete or pavement, that can easily cause a Tibia fracture. This also seems to be the case for Maroni's injury.

The comprehensive force per area necessary to break the tibia in the lower leg is estimated to be around 1.6×108 N/m^2 . Additionally, the smallest cross-sectional area of the tibia is around 3.2×10−4 m^2 which is slightly above the ankle.

To simplify the calculations, the person is considered a point located at his center of mass which is located slightly below the belly-button. It is also assumed that the acceleration during this time is negative and constant. To analyze the problem, it will be divided into different parts.

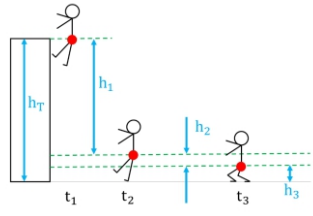

First, the average force of the ground on Maroni's legs during the impact will be calculated. For the time interval between t1 and t2, the final velocity can be calculated using Kinematic 2D and the Work-Energy Theorem. However, due to the moving camera angle, this value cannot be analyzed using applications such as Logger Pro. Therefore, we will use the Work-Energy approach. According to the law of conservation of energy, assuming that the force of friction is negligible, we have:

$$E_{T_1} = E_{T_2}$$

$$E_{g_1} + E_{k_1} = E_{g_2} + E_{k_2}$$

E_{k1}= 0 (The initial velocity is zero because the batman was holding Maroni over the edge of the balcony and simply dropped him).
Knowing that $h_T = h_1 + h_2 + h_3$ the equation above can be simplified into this equation:

$$mgh_1 = \frac{1}{2}mv_2^2 \qquad (a)$$

Next, the time interval between t_2 and t_3 is considered. This time, there is work being done, which is a contact force from the floor on the person. Its direction is the opposite direction to the displacement which is why the contact force does negative work. This negative work is:

$$W_{ground,\ person} = -F_{floor}h_2$$

Using the Work-Energy Theorem we get:

$$W = \Delta E$$

$$F_{floor}h_2 = E_{k_2} + E_{g_2}$$

$$F_{floor}h_2 = \frac{1}{2}mv_2^2 + mgh_2$$

h_2 refers to the time right before and after impact. The change in potential energy is mgh_2
Now this equation is rearranged using equation (a)

$$F_{floor}h_2 = mgh_1 + mgh_2$$

$$F_{floor} = \frac{mg\,(h_1 + h_2)}{h_2}$$

$$F_{floor} = mg\left(\frac{h_1}{h_2} + 1\right) \qquad (b)$$

Using this formula, the value of F_{floor} is calculated.

$$m_{Maroni} = 75\ kg$$

$$g = 9.8\ \frac{m}{s^2}$$

h_1= Maroni's height from waist up subtracted from the average height of a second-floor balcony above ground (=15 ft) which was calculated using Logger Pro using the same method from "Scene 1: Bullet denting the truck"

$$h_1 = 4.57\ m$$

$$h_2 = 0.06\ m$$

$$F_{floor} = (75)(9.8)\left(\frac{4.57}{0.06} + 1\right)$$

$$F_{floor} = 5.7 \times 10^4 N$$

5.7×10^4N is the force acting on Maroni's legs

2.2.1. Calculating the Real Force Needed to Break a Person's Legs

The maximum force that the tibia can withstand: 1.6×10^8 N/m^2
Smallest cross-sectional area of the tibia: 3.2×10^{-2} m^2
The value is multiplied by 2 because the force is acting on both legs :

$$F_{max} = (1.6 \times 10^8)(3.2 \times 10^{-4}\ m^2)(2)$$

$$F_{max} = 5.12 \times 10^4\ N$$

Since the force acting on Maroni's legs in the movie is larger than the minimum force needed to break the leg's tibia ($F_{max} < F_{floor}$). In conclusion, using the Work-Energy Theorem, it can be proven that this scene from the movie portrays accurate physics. Maroni would most likely break his legs as a result of that fall and would not suffer other life-threatening injuries based on the way he landed n his feet with his bent at a very slight angle. This slight angle evidently decreased his chances of getting more injuries which was proven during the analysis above.

2.3. Scene 3: Truck Knocked Out of Its Path

In this scene, the Joker tries to capture Harvey Dent to create disorder and mayhem in Gotham City. Many police and SWAT cars are driving around the area. The Joker and his thugs are trying to control the region and eliminate the police. The Joker's truck hits one of the SWAT cars. The force exerted by the truck on the SWAT car is displayed accurately. The SWAT car changes directions and falls into a body of water. This scene demonstrates good physics.

After the Joker's truck hits the SWAT car, it ventures off to the side of the road and ultimately lands in a body of water. The scene shows an accurate representation of a projectile following a parabolic trajectory. The force of gravity is displayed as the object falls into the water at a reasonable time. The following data is from a portion of the fall, starting from the initial fall.

	VideoAnalysis									
	Time (s)	X (m)	Y (m)	X Velocity (m/s)	Y Velocity (m/s)					
12	6.133	16.61	13.17	5.001	0.134	29	6.700	22.74	11.71	14.161	-7.485
13	6.167	16.45	13.28	6.476	-0.068	30	6.733	23.17	11.41	12.959	-6.645
14	6.200	16.93	13.19	10.806	-0.893	31	6.767	23.70	11.20	9.388	-3.999
15	6.233	17.35	13.14	10.420	-0.508	32	6.800	23.75	11.17	7.157	-2.103
16	6.267	17.73	13.17	7.469	-0.444	33	6.833	24.04	11.12	8.457	-1.834
17	6.300	17.75	13.17	6.893	-1.711	34	6.867	24.34	11.07	9.540	-2.229
18	6.333	18.07	13.03	9.473	-2.582	35	6.900	24.71	10.94	10.082	-1.929
19	6.367	18.42	12.95	11.239	-2.365	36	6.933	25.05	10.96	9.123	-2.056
20	6.400	18.89	12.90	11.088	-2.712	37	6.967	25.29	10.83	8.858	-2.845
21	6.433	19.27	12.74	8.045	-2.211	38	7.000	25.61	10.70	9.302	-1.708
22	6.467	19.29	12.79	8.820	-2.783	39	7.033	25.93	10.72	9.117	-0.663
23	6.500	19.69	12.56	14.017	-3.489	40	7.067	26.30	10.67	6.915	0.000
24	6.533	20.33	12.53	16.383	-3.250	41	7.100	26.35	10.72	5.456	0.557
25	6.567	20.88	12.40	15.942	-4.391	42	7.133	26.62	10.72	5.121	0.597
26	6.600	21.47	12.16	13.266	-3.703	43	7.167	26.75	10.75	3.714	0.905
27	6.633	21.68	12.18	12.571	-4.046	44	7.200	26.80	10.80	3.971	0.645
28	6.667	22.21	11.97	14.527	-6.424	45	7.233	26.99	10.80	4.834	0.155
						46	7.267	27.18	10.80	4.655	-0.052
						47	7.300	27.28	10.78	4.959	0.323
						48	7.333	27.49	10.83	5.667	0.983

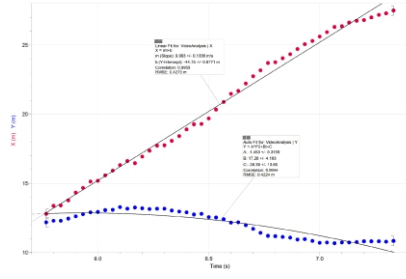

The mass of the SWAT truck was estimated to be 4,985 lbs. or 2261.158 kg.

2.3.1. Horizontal Analysis of Logger Pro Calculations (→+)

$$\vec{a} = \frac{\vec{v_2} - \vec{v_1}}{\Delta t}$$

$$\vec{a} = \frac{23.17 - 12.79}{0.966}$$

$$\vec{a} = 11 \frac{m}{s^2} [\rightarrow]$$

$$m = 2261.158 \text{ kg}$$

$$a = 11 \frac{m}{s^2} [\rightarrow]$$

$$F_{net} = ma$$

$$F_{net} = (2261.158)(11)$$

$$F_{net} = 2.5 \times 10^4 \text{N} [\rightarrow]$$

The force the Joker's truck applied to the SWAT car was approximately 2.5×10^4 N [→].
According to Newton's 3rd law, the action force of the truck acting on the car is equal in magnitude and opposite in direction to the force of the car acting on the truck.

$$F_{net} = ma$$

$$-24{,}872.738 = (15{,}875.733)a$$

$$a = -1.6 \frac{m}{s^2} [\rightarrow]$$

The truck will experience an acceleration of -1.6 m/s^2 [→] due to the crash.
This scene follows Newton's first law of motion. The SWAT car appears to be moving at a uniform velocity and would continue to do so unless acted upon by an external force: Joker's truck car pushing on the SWAT car. The Joker's truck travels at high velocity, visually higher than the SWAT car's velocity. The Joker's truck also has a larger mass than the SWAT car. That means its kinetic energy is much higher and has the ability to cause more destruction to the SWAT car than it would receive, as shown in the scene. The driver's reaction to this force is shown. The driver is wearing a seatbelt to restrain the full effect of the force. The driver still jolts to the side in the direction of the push.

The scene also follows Newton's second law of motion. The Joker's truck causes the SWAT car to accelerate as it exerts a force on the SWAT car. The acceleration of the SWAT car is directly proportional to the force exerted on it and inversely proportional to its mass. The scene demonstrates the law accurately. The SWAT car's velocity increases and changes direction after being pushed by the Joker. This push and ultimate land in the water demonstrates Newton's third law of motion. For every action, there is an equal and opposite reaction. The Joker applies force on the SWAT car and receives that same force back, accelerating both vehicles.

3. Poor Physics

3.1. Scene 1: Rachel and Batman Falling off a Building

In this scene, Rachel and Batman fall out of a high building. The Joker crashes Harvey Dent's fund raiser event at the penthouse of the building below. The Joker threatens Rachel and holds her over the ledge of the building. The Joker lets go of Rachel, and Batman quickly follows her. They both, holding on to each other, slide on the incline of the building, then free fall and land on a car uninjured.
There are two main problems with the scene.
1. Batman and Rachel survive and acquire no injury after enduring a significant fall. The car also appears to have no damage.
2. The calculated free fall time is 11 seconds. This time is very long for Rachel and Batman to land with gravity acting on them.

In this analysis, Batman's protection is neglected, as falling from such height will undermine any influence of such little protection.

In this scene, Rachel and Batman fall out of a high building. The Joker crashes Harvey Dent's fund raiser event at the penthouse of the building below. The Joker threatens Rachel and holds her over the ledge of the building. The Joker lets go of Rachel, and Batman quickly follows her. They both, holding on to each other, slide on the incline of the building, then free fall and land on a car uninjured.

Illinois Center Building (111 East Wacker Drive)
Film Location of Batman's penthouse in free fall scene

$m_b = 86$ kg (Batman's weight)

$m_r = 60$ kg (Rachel's weight)

$$F_{net} = F_g$$

$$F_g = mg$$

$$F_g = (m_b + m_r) \cdot g$$

$$F_g = (86 + 60) \cdot 9.8$$

$$F_g = 1430.8 \text{ N}$$

$$F_g = 1.43 \times 10^3 \text{N}$$

This scene breaks the rule of Newton's 3rd law of motion. When Rachel and Batman exert a force of 1430.8 N downwards on the car, an equal force is exerted upwards on Rachel and Batman. A significant and abrupt force on their bodies like this would result in death or severe injury. Rachel and Batman, however, appear fine after the crash. Also, the force applied by Rachel and Batman on the car would likely cause some damage to it. Newton's first law of motion states that an object in motion will stay in motion unless acted upon by another force. Rachel and Batman are falling at a very high velocity to stop their movement; the characters will experience extreme force and acceleration.

3.1.1. Calculations for Real Estimated Time

To solve for time, the initial velocity should be calculated. The initial velocity of this free fall is not zero. Before Rachel and Batman free fall, they slide down the building's incline and gain kinetic energy.

To estimate vertical displacement the Batman and Rachel had, the angle of the slope on which they were sliding was estimated to be around 30° and using this information, the initial velocity was calculated. The initial velocity of the free fall is the final velocity from when Rachel and Batman are sliding. The Joker let's Rachel go, and she slides onto the roof; Batman follows. It is assumed that initial velocity of the sliding part is 0 m/s.

Batman's height: 1.83 m

Rachel's height: 1.75 m

Rachel and Batman slid on the incline roof, holding each other with their arms stretched out. We can see Rachel slide alone on her own before Batman joins her. It appears Rachel slides alone twice her height. Batman comes along and slides a little less than double their height. Batman and Rachel's height were added twice to account for the distance of their arms spread out. These values were added together to find the length of the inclined roof. (Let h represent the length of the hypotenuse)

$$h = 2(1.83 + 1.75 + 1.75)$$
$$= 10.66\ m$$
$$= 11.0\ m$$

$$sin\ 30° = \frac{1}{2}$$

$$\frac{1}{2} = \frac{y}{11}$$

$$11 = 2y$$

$$\frac{11}{2} = y$$

$$y = 5.50\ m$$

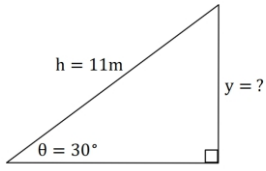

Vertical Analysis: [↓] +

$\Delta\vec{d_y} = 5.5\ m\ [\downarrow]$

$\vec{v_{y_1}} = 0\ \frac{m}{s}\ [\downarrow]$

$\vec{a} = 9.8\ \frac{m}{s^2}\ [\downarrow]$

$\vec{v_{y_2}} = ?$

$2\vec{a}\Delta\vec{d} = v_2^2 - v_1^2$

$2(9.8)(5.5) = v_2^2 - 0$

$v_2^2 = 107.8$

$\mathbf{\vec{v_{y_2}} = 10.4\ \frac{m}{s}\ [\downarrow]}$

3.1.2. Free Fall Calculations

Vertical Analysis: [↓] +

$\vec{v_{y_2}} = 10.4\ \frac{m}{s}\ [\downarrow]$ (From the previous calculation)

$\vec{a} = 9.8\ \frac{m}{s^2}\ [\downarrow]$

$\Delta\vec{d_y} = 110.3 - 5.5$

$\Delta\vec{d_y} = 5.5\ m\ [\downarrow]$

$\Delta t = ?$

$\Delta\vec{d} = \frac{1}{2}\vec{a}\Delta t^2 + \vec{v_i}\Delta t$

$104.8 = \frac{1}{2}(9.8)t + 10.4t$

$0 = \frac{1}{2}(9.8)t + 10.4t - 104.8$

$t = 3.68504\ ,\ t \neq -5.80395$

$t = 3.69\ s$

The correct time Rachel and Batman took to free fall is approximately 3.69 seconds.

3.1.3. Rachel and Batman's velocity when hitting the ground

$2\vec{a}\Delta\vec{d} = v_2^2 - v_1^2$

$2(9.8)(104.8) = v_2^2 - 10.4^2$

$v_2^2 = 2161.87999996$

$\mathbf{\vec{v_{y_2}} = 46\ \frac{m}{s}\ [\downarrow]}$

Gravitational potential energy at top of the building, relative to the ground:

$$E_g = mg\Delta h$$
$$= (86 + 60) \cdot 9.8 \cdot 110.3$$
$$= 157{,}817.24\ J$$
$$= 1.6 \times 10^5\ J$$

Gravitational potential energy at free fall, relative to the ground:

$$E_g = mg\Delta h$$
$$= (86 + 60) \cdot 9.8 \cdot 104.8$$
$$= 1.50 \times 10^5\ J$$

Gravitational potential energy at landing (relative to the car's height):

$$E_g = mg\Delta h$$
$$= (86 + 60) \cdot 9.8 \cdot 0$$
$$= 0.00\ J$$

Kinetic energy when hitting the ground:

$$E_k = \frac{1}{2}mv^2$$
$$= \frac{1}{2}(86 + 60)46^2$$
$$= 154{,}468\ J$$
$$= 1.50 \times 10^5\ J$$

Kinetic energy at start of free fall:

$$E_k = \frac{1}{2}mv^2$$
$$= \frac{1}{2}(86 + 60)10.4^2$$
$$= 7.9 \times 10^3\ J$$

Kinetic energy at top of the building (before joker lets go of Rachel):

$$E_k = \frac{1}{2}mv^2$$
$$= \frac{1}{2}(86+60)\ (0)$$
$$= 0\ J$$

At the top of the building, the gravitational potential energy of Rachel and Batman is very high. As they free fall, their gravitational potential energy decreases and their kinetic energy increases. Their kinetic energy is highest when they land and lowest at the very top of the building. This sudden landing is dangerous, and landing with such high kinetic energy will result in injury as your body will take in the impact forces, leading to death or severe injuries. Rachel and Batman experience nothing realistic.

The use of poor physics in this scene creates suspense. Throughout the exaggerated time Rachel and Batman free fall, the audience anticipates their harm. The suspense of their survival adds thrill to the scene. Furthermore, when they survive the audience is relieved and witnesses Batman's strength and abilities. And the impression is

given that Batman saved Rachel. Overcoming the impossible and using poor physics allows Batman to execute his superpowers. Using poor physics allowed the directors to add more thrill and action to the movie. If Rachel and Batman were to fall from a much smaller distance or at a smaller time, the suspense and anticipation would be less. Using poor physics shows Batman's true capabilities.

3.2. Scene 2: Joker and the Batman Crashing Head-on

In this scene, the Joker tries to hijack the police vehicle to capture Harvey Dent. The Joker is in the trailer area of the truck, shooting missiles. Joker's thugs are also in the truck. One of the thugs is driving the vehicle. Driving on the highway, they face Batman head-on. Batman, driving the Batmobile, is trying to stop the Joker. He crashes into him from the opposite direction at what looks to be a similar speed.

Batmobile facing Joker's truck before the crash
Dark Knight, Batman Rises (2008)

When the cars crash, the Batmobile drives the truck up and over the Batmobile, causing the truck to accelerate backwards. The Joker appears to have no injuries or any impact from the crash. Batman and the Batmobile also experienced no injury after the collision. The Batmobile experiences much less, if any, of an impact from this collision.

This scene displays the use of poor physics. First, the Joker and Batman experience no injury or impact from the collision. Second, the Batmobile experiences far less of an impact and is able to bring the truck above itself, then backwards.

(a) (b)
a) Batmobile after the crash Joker's truck after the crash; b)Dark Knight, Batman Rises (2008)

The use of poor physics makes for a thrilling scene. The poor physics in this scene is necessary to show that Batman has special powers. (And within his Batmobile gadgets/tools to overcome the impossible). This scene shows Batman and his Batmobile to have functions that defy the laws of physics. These capabilities, of course, do not exist in real life. But this is what makes Batman a superhero, and this scene helps emphasize Batman's superpowers. Additionally, intense crashes create a fast-paced film that keeps the audience hooked. When Batman and the Joker survive these crashes, the action can continue for longer.

3.2.1. Kinetic Energy of the Vehicles

The Joker's truck and the Batmobile collided head-on. The vehicle that has less kinetic energy should experience the most destruction. In this case, the Batmobile has less kinetic energy; it should experience more damage than the Joker's truck. The kinetic energy of a vehicle depends on its velocity and mass, as $E_k = \frac{1}{2}mv^2$. The truck and the batmobile appear to be travelling around the same speed. The kinetic energies of both vehicles is calculated using the same estimated velocity. The velocity of the car and truck look nearly the same. If there is a slight difference, the demonstration will still prove the inaccuracy of the scene because their masses significantly differ.

The Joker's truck is an ordinary semi-truck with an empty trailer attachment. Semi-trucks attached to an empty trailer have a mass of 35,000 pounds or 15,875.733 kg. The Batmobile weighs 5500 pounds or 2494.758 kg.

In this scene, Batman and the Joker are driving on the highway. Most highways have a speed limit of 100-110 km /hr. Given the intensity of this scene and the probable fact the Joker and Batman were not following the speed limit, it is estimated that the truck and the Batmobile were going 130 km/hr (36.1 m/s).

3.2.2. Kinetic Energy of Joker's Truck: →+

$v = 36.1\ \frac{\mathrm{m}}{\mathrm{s}}[\rightarrow]$

$m = 15{,}875.733\ kg$

$E_k = \frac{1}{2}mv^2$

$= \frac{1}{2}(15{,}875.733) \cdot 36.1^2$

$= 10{,}351{,}069.54\ J$

$= 10 \times 10^7 J$

3.2.3. Kinetic Energy of Batmobile: ←+

$v = 36.1\ \frac{\mathrm{m}}{\mathrm{s}}[\leftarrow]$

$m = 2494.758\ kg$

$E_k = \frac{1}{2}mv^2$

$= \frac{1}{2}(2494.758) \cdot 36.1^2$

$= 1{,}625{,}596.787\ J$

$= 1.6 \times 10^6 J$

∴The kinetic energy of the Joker's truck is approximately 10×10^7j and the kinetic energy of the Batmobile is approximately 1.6×10^6 j.

Since the kinetic energy of the Batmobile is lower, it should take the most destruction. The Batmobile should encounter immense damage, more than the truck, accelerating significantly. The collision should cause the truck and car to accelerate in the opposite direction the Batmobile was initially moving or the same direction the truck was initially moving. The Batmobile does not have enough kinetic energy to cause the truck to move above it.
In addition, this scene breaks Newton's 2nd law of motion: objects with a larger mass require more force to accelerate. The truck holds the larger mass but appears to accelerate more than the Batmobile. The smaller vehicle, the Batmobile, should experience greater acceleration.

Newton's third law states for every action, there is an equal and opposite reaction. The car exerts a force on the truck, and the truck exerts an equal and opposite force on the car. This law is unrepresented in this scene. The Batmobile appears to move forward as it moves the truck

over itself. Batman, with control, accelerates his car backwards. The Batmobile would endure immense destruction and uncontrollably accelerate backwards from the force exerted by the truck.

Momentum is the product of the mass and velocity. In the car/truck collision, the vehicles collide inelastically. Momentum is conserved in the system of the car and truck, and the kinetic energy is lost. Kinetic energy is lost in such crashes as it transforms into something else, like destruction in the car/truck or heat. To solve for the final velocity after the objects collide, the law of conservation of momentum. The momentum before the crash is equal to the momentum after the crash. (Directions: →+)

m_t=15,875.733 kg

m_c=2494.758 kg

Momentum before crash = Momentum after crash

$$P_{car} + P_{truck} = P_{ct}$$
$$m_c \cdot \overrightarrow{v_{c_1}} + m_t\overrightarrow{v_{t_1}} = (m_c + m_t)\overrightarrow{v_2}$$
$$v_2 = 26.303147058$$
$$v_2 = 26.3\ \frac{m}{s}\ [\rightarrow]$$

In a car collision, many forces come into play. It is difficult to identify all of these forces and to apply them. For that reason, the calculations for the action and reaction forces of the collision will be provided and other horizontal forces will be ignored. The impulse formula is used to solve for this force exerted on the car and truck.

$$F_{c,t} = F_{t,c}$$
$$\Delta v_t = v_{t2} - v_{t1}$$
$$= 26.303147058 - 36.1111$$
$$= -9.8\ \frac{m}{s}$$
$$F = \frac{\Delta p}{\Delta t}$$
$$F_{c,t} = \frac{m\Delta v}{\Delta t}$$
$$= \frac{15{,}875.733 \cdot (-9.8)}{0.2}$$
$$= \frac{-155{,}708.4}{0.2}$$
$$= -778{,}542\ \text{N}\ [\rightarrow]$$
$$F_{c,t} = 7.8 \times 10^5 \text{N}\ [\leftarrow]$$

$$\Delta v_c = v_{c2} - v_{c1}$$
$$= 26.303147058 - (-36.1111)$$
$$= 62.41424705\ m/s$$
$$= 62\ m/s$$

$$\Delta p = F\Delta t$$
$$F = \frac{\Delta p}{\Delta t}$$
$$F_{t,c} = \frac{m\Delta v}{\Delta t}$$
$$= \frac{(2494.758)(62.41424705)}{0.2}$$
$$= 778{,}542\ N\ [\rightarrow]$$
$$F_{t,c} = 7.8 \times 10^5 N\ [\rightarrow]$$

The force of the truck acting on the car is 7.8×10^5 N[→] and the force of the car acting on the truck is 7.8×10^5 N [→]

Newton's first law states that an object will remain at rest or at constant velocity unless acted on by an external force. The joker before the crash was standing in the middle of the trailer. The Joker moves at the same velocity as the truck. At the crash, there was a sudden acceleration as the car moved backwards. The joker, because of his inertia and Newton's first law, will continue to move forward within the trailer at the same velocity. The Joker will be introduced to an external force, the front wall of the trailer, and collide with it. A head on collision with such speed would have the Joker experiencing significant force. Following the crash, the Joker appears to have endured no trauma. Head-on collisions, like the one in this scene, are the most dangerous type of car accidents, often accounting for the highest death toll of all types of car accidents. For the Joker to appear completely unharmed, as if nothing has happened, is beyond unrealistic and demonstrates poor physics.

In addition, Batman, just like Joker, should feel the force from this head on collision. The force of impact doubles because the truck and Batmobiles velocity is combined. According to the estimated velocity, each car was traveling at 130 km/h or 36.1 m/s. That means, the impact force would be that of a collision where the velocity was 260 km/h or 72.2 m/s. And with the kinetic energy of the truck being higher than the Batmobile, the Batmobile would acquire more damage. Therefore, for Batman to endure no life-threatening injury, let alone come out of this crash alive, is virtually impossible.

3.3. Scene 3: Batmobile Jumping Over Another Car

The scene involves the Batmobile (also known as the Tumbler) in a high-speed chase with the Joker's truck. As the pursuit intensifies, there's a moment where the Batmobile executes its boost thrusters and manages to jump over a car while landing safely and continuing the chase. This scene demonstrates the agility and advanced technology behind the Batmobile's design. During this time, the joker aims a Bazooka towards a SWAT truck and fires. However, the Batmobile manages to get in between the SWAT truck and the incoming rocket. A great explosion occurs when the rocket makes contact with the Batmobile but the Batmobile does not alter its course and its armor does not seem to take much damage from the impact. Eventually the Batmobile lands in front of the car it was jumping over safely. Remarkably, as the smoke clears, the Batmobile reaches the ground unscathed, having not only absorbed the rocket but also landed safely in front of the car it initially soared over. To analyze the Batmobile's stunt, the motion is divided into its projectile motion when jumping over the car and the impact it suffers from the rocket.

The following graph represents the projectile motion of the Batmobile while jumping over the car. The graph was made using Logger Pro and the Batmobile was considered a point located at its center of mass. However, the Batmobile's movement can only be partially tracked since multiple camera angles are used to capture the scene. As a result, there are gaps in the graph before and amidst the projectile motion, and thus can only be used to analyze the movement.

First, the projectile motion of the car will be analyzed. It is assumed that the boosters stop working after giving the Batmobile its initial velocity as the flames of the boost thrusters were not visible in later scenes.

The Batmobile's starting angle was calculated with a

protractor using a shot showcasing the side of the vehicle while jumping ($\theta \approx 13°$).

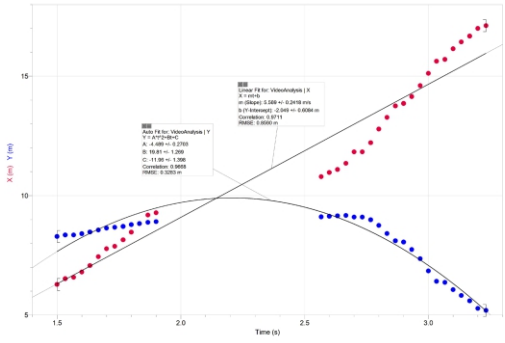

The Batmobile can reach the velocity of 102 m/s with its boost thrusters and by assuming this was its velocity during the motion, the vertical and horizontal velocity can be calculated.

Vertical ↑ +	Horizontal →+
$\vec{v_{1y}} = 102\sin 13$ $\vec{v_{1y}} = 22.945 \frac{m}{s}$ [up] $\vec{a} = -9.8 \frac{m}{s^2}$ [up] $\Delta \vec{d_{y_{max}}} = ?$ [up] $\Delta \vec{d_y} = 0$m [up] $t = ?$	$\vec{v_{1x}} = 102\cos 13$ $\vec{v_{1x}} = 99.386 \frac{m}{s}$ [right] $t = 4.682s$ $\Delta \vec{d_x} = ?$ m [right]
$2\vec{a}\Delta\vec{d} = v_2^2 - v_1^2$ $2(-9.8)\Delta\vec{d} = 0 - 22.945^2$ $\Delta \vec{d_{y_{max}}} = 26.86$m The maximum height of the Batmobile from the ground. Movement from the start until ($v = 0 \frac{m}{s}$)	$\vec{v} = \frac{\Delta\vec{d}}{\Delta\vec{t}}$ $99.386 = \frac{\Delta\vec{d}}{4.682}$ $\Delta \vec{d_x} = 21.22$m [right] The horizontal distance that the Batmobile can take according to its initial velocity and time.
$\Delta\vec{d} = \frac{1}{2}\vec{a}\Delta t^2 + \vec{v_1}\Delta t$ $0 = \frac{1}{2}(-9.8)t^2 + 22.945t$ $0 = t(-4.9t + 22.945)$ $t = 0s$ $t \approx 4.682s$ The time it takes for the Batmobile to finish the projectile motion	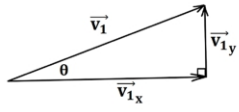

The car that the Batmobile jumped over is a Touareg SUV 2008 with the height of 1.726m, and the maximum height that the Batmobile could jump over was well over that range. It can be concluded that the Batmobile would be able to jump over the car using its boost thrusters. The time needed to complete the movement was calculated to be around 4.7s. However, the time it took from the moment the car left the ground until it made contact with the ground was 6.61s in the movie. This scene was lengthened for exaggeration and a few explosions were added to make the scene exciting for viewers. Next, the horizontal range for the car was calculated to be around 21.22m with the time of 4.7s. Since the horizontal displacement of the Batmobile in the movie was less than 10m, the time and horizontal displacement in the movie is illogical and it can be said without a doubt that this scene included poor physics.

While the Batmobile was in mid-air, the Joker shot a rocket at it with a bazooka. A bazooka rocket could penetrate as much as 0.127 m of armour plate. The rocket contains approximately 6.65 megajoules of explosive energy. However advanced Batman's technology seems, it is very unlikely that he would be able to survive that blast without a scratch. Additionally, the Batmobile's armour did not suffer much damage from the explosion and the only real damage that was done was to the back wheels. In later scenes, the Batmobile easily transformed into a motorbike which did not look slightly damaged. Even if the Batmobile's armour was strong enough to withstand the explosion, the force of the rocket should have changed its direction which is another instance of poor physics in this scene.

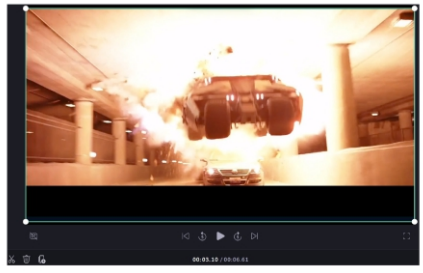

Although this scene is visually pleasing and exciting for viewers, it does not follow the laws of physics. The use of poor physics in movies, particularly in action sequences such as this one, is often intentional. The directors add impossible effects to adrenaline-filled scenes for cinematic purposes. In this case, the use of boost thrusters and the jump over a car contributes to the overall spectacle. By exaggerating the capabilities of the Batmobile, viewers subconsciously engage with the narrative as they try to accept the exaggerated reality presented on screen. The longer some exciting scenes last, the more people will become immersed in the scene. Additionally, the Batmobile is a fictional vehicle designed by Bruce Wayne (Batman) which showcases advanced technology. By finishing impossible tasks such as surviving a direct hit from a rocket without significant damage, the filmmakers highlight the indestructible nature of Batman's technology which also reinforces the idea that Batman is a powerful superhero. It is also implied that although the Batman might suffer a few losses along the way, he is overall indestructible and cannot be beaten easily.

While the scene may follow the laws of physics, its main focus is to entertain and immerse the audience in the world of Gotham City and Batman. The use of poor physics is for creating a thrilling cinematic experience rather than aiming for strict realism.

4. Conclusion

Poor physics creates a dramatic and suspenseful effect. Using good physics may not be as engaging for the audience as it can look less exciting. Using poor physics allows the directors and writers of the film to be more creative and explore scenes beyond reality. Superhero movies are a great example of this.

This movie showcases many incidents of good and poor physics. Poor physics can enhance movies to make a simple action scene look more phenomenal than it actually is. Due to this it is normal to see strange sequences and can be easily identified as not following simple physics laws. Christopher Nolan loves to exaggerate his movies,

especially in The Dark Knight, by adding extra explosions, high technology and insanely high free fall scenes to blow the audience's mind. However, some accurate physics is also included to ensure that the movie is not too unrealistic for the audience. A balance between the two parts is what makes an action movie worth watching. After all, some of the best scenes in the film industry are those that greatly defy every day physics.

References

[1] IMDb.com. (2008, July 18). The dark knight. IMDb. https://www.imdb.com/title/tt0468569/

[2] Weiner, A. (2008, August 16). The physics of batman. Popular Science. https://www.popsci.com/entertainment-gaming/article/2008-08/physics-batman/

[3] The dark knight. The Dark Knight - Internet Movie Firearms Database - Guns in Movies, TV and Video Games. (n.d.).https://www.imfdb.org/wiki/The_Dark_Knight#:~:text=Glock%2017%20(Two%2Dtone%20Converted%20to%20full%2Dauto),-The%20Joker%20

[4] Glock 17 vs 19. Diffen. (n.d.).https://www.diffen.com/difference/Glock_17_vs_Glock_19

[5] Armored truck. How Products Are Made. (n.d.). http://www.madehow.com/Volume-4/Armored-Truck.html

[6] myArmoury.com. (n.d.). Featured content and articles. http://myarmoury.com/features.html

[7] Physics of the dark knight. Physics of the dark knight - Home. (n.d.). https://batmanphysics.weebly.com/

[8] The Johns Hopkins University, The Johns Hopkins Hospital, and Johns Hopkins Health System. (2021, April 28). Tibia and fibula fractures. Johns Hopkins Medicine. https://www.hopkinsmedicine.org/health/conditions-and-diseases/tibia-and-fibula-fractures

[9] Jason A. Lowe, MD, Stuart J. Fischer, MD. (n.d.). Tibia (shinbone) shaft fractures - orthoinfo - aaos. OrthoInfo. https://orthoinfo.aaos.org/en/diseases--conditions/tibia-shinbone-shaft-fractures/ (2002). (tech.). JUMPING FROM A HEIGHT. https://ocw.mit.edu/courses/8-01x-physics-i-classical-mechanics-with-an-experimental-focus-fall 2002/28cad245e198f1513b93728c05ea5c41_jumping.pdf

[10] Colucci, B. (2023, July 29). How fast batman's Batmobile is at top speed. ScreenRant. https://screenrant.com/how-fast-batman-batmobile-top-speed-dc-comics/

[11] 2008 Volkswagen Touareg Reviews. CarsGuide. (n.d.). https://www.carsguide.com.au/volkswagen/touareg/2008

[12] Encyclopædia Britannica, inc. (n.d.). Bazooka. Encyclopædia Britannica. https://www.britannica.com/technology/bazooka

[13] Cargo Van Rental. (n.d.). : Uhaul. https://www.uhaul.com/Truck-Rentals/Cargo,

[14] The Dark Knight. (2023). https://movie-locations.com/movies/d/Dark-Knight.php#17th

[15] One Illinois Center. (n.d.). https://www.skyscrapercenter.com/building/one-illinois-center/13136

[16] Tyler, A. (2023). How Much Weight Christian Bale Has Gained & Lost For Movie Roles.: Screen Rant. https://screenrant.com/christian-bale-movies-weight-gained-lost-how-much/

[17] Maggie Gyllenhaal Height, Weight, Age, Body Statistics. (n.d.).: Healthy Celeb. https://healthyceleb.com/maggie-gyllenhaal/

[18] 6 Common Types of Serious Car Accidents That Have Occurred on California Roads. (n.d.).: West Coast Trial Lawyers. https://westcoasttriallawyers.com/california-car-accident-lawyer/most-common-type-of-serious-auto-accidents

[19] Czernia, PhD, D. (2023). Car Crash Calculator. : omni calculator. https://www.omnicalculator.com/physics/car-crash-force

[20] M. Robertson, Ph.D, J. (n.d.). 9.2 Impulse and Collisions. : Lumen Learning. https://courses.lumenlearning.com/suny/osuniversityphysics/chapter/9-2-impulse-and-collisions/

[21] Henderson, T. (n.d.). Car and Truck in Head-on Collision.: The Physics Classroom. https://www.physicsclassroom.com/mmedia/momentum/cthoe.cfm

[22] AUTOMOBILE ACCIDENTS PRACTICE AREA Head on Collisions. (n.d.).: The Cochran Firm. https://cochranfirm.com/new-orleans/head-on-collisions/#:~:text=

[23] What are elastic and inelastic collisions? (n.d.).: Kahn Academy. https://www.khanacademy.org/science/physics/linear-momentum/elastic-and-inelastic-collisions/a/what-are-elastic-and-inelastic-collisions

[24] What Happens to Your Body in a 40 Mph Car Crash? (2023).: The Solomon Law Group. https://solomonlawsc.com/what-happens-to-your-body-in-a-40-mph-car-crash/#

[25] Enrera, R. (2023). Elastic vs Inelastic Collision | Definition, Equation & Examples.: study.com. https://study.com/learn/lesson/elastic-vs-inelastic-collision-theories -examples.html#

[26] Inelastic Collision Formula. (n.d.).: Soft Schools. https://www.softschools.com /formulas/physics/inelastic_collision_formula/91/

[27] All images: Copyright: TM & © DC Comics. © 2008 Warner Bros. Entertainment Inc.

Colored Line

José Antônio Eleutério[1], joseeleuterio999@gmail.com

Instituto Federal de Ciência Educação e Tecnologia do Ceará – Campus Juazeiro do Norte (Brazil)

ARTICLE INFO

Gold medalist in ISAC Olympiad 2023 and participant in IYPT 2023

Awarded by Ariaian Young Innovative Minds Institute , AYIMI

http://www.ayimi.org ,info@ayimi.org

ABSTRACT

This problem states that when a compact disc or DVD is illuminated with light from a filament lamp in such a way that only rays with large angles of incidence are selected, a clear green line can be observed. The color of the line varies slightly when the angle of incidence is changed. The solution presented in this paper is based on analyzing the diffraction effects caused by the disc's structure and developing the geometrical characteristics of the colored line formed, as well as its dependencies on relevant parameters.

Keywords : *: Colored line, Diffraction, filament lamp, Compact Disc*

1. Introduction

1.1. Problem Statement

Based on the problem statement, it is evident that the lighting angle, the color of the line formed, and the disc inclination are crucial parameters. Additionally, the use of a filament lamp for illumination is recommended since the light spectrum it emits (Fig.1) covers the entire visible spectrum more uniformly than the spectrum produced by other light sources like LEDs.

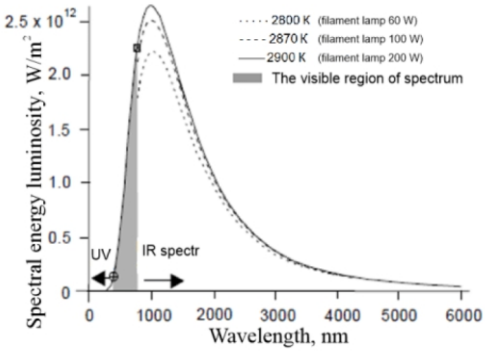

Fig. 1: Radiation spectrum of incandescent lamps with different power. Sidorenko, Alexey & Tupikina, Nadezhda & Sergey, Lisakov & Kin, Isa & Sypin, Eugene. (2019)

1.2. Disc Structure

The structure of optical media is based on storing binary information through pits carved in a radial track on one of the disc's layers (track layer). The size of the pits and the distance between the tracks of pits are from the order of one micrometer. A laser reads the alternation between the pits and the plain of the disc and returns binary values (Fig.2).

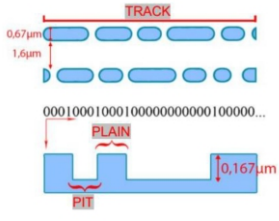

Fig. 2: Structure and reading of information stored on optical media (Author)

2. Theoretical Analysis

2.1. Light-Disc Interface

We can define a model for the interface between the incoming light rays hitting the disc as parallel wavefronts hitting an obstacle (Figs. 3 , 4).

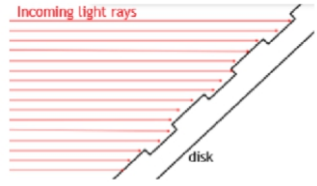

Fig.3: Incoming parallel light rays (Author)

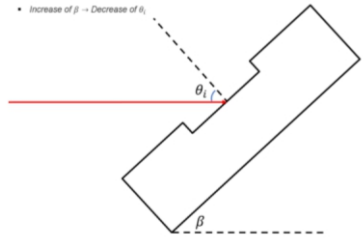

Fig.4: Behavior of angle of incidence with inclination of the disc (Author)

The length of the pits is of the same order of magnitude as the wavelength of light rays. This means that diffraction has a significant effect on the phenomenon of the colored line (Fig. 5).

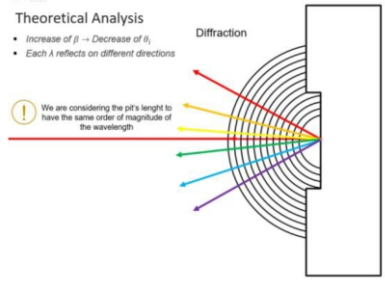

Fig.5: Diffraction effects caused by the pits (Author)

The organization of the pits in tracks leads to the creation of a line through constructive interference between diffracted and reflected light rays. Multiple angles, which are integer multiples of the angle between the light rays and the disc (θ), make different orders of magnitude for this constructive interference and result in the formation of the line (Figs. 6, 7).

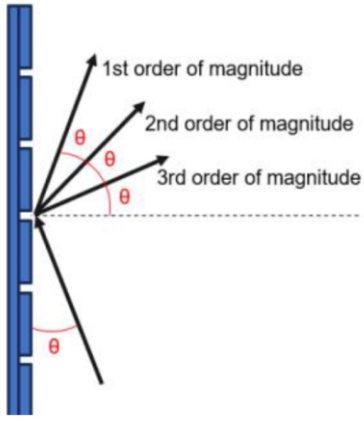

Fig. 6: Different orders of magnitude for an oncoming light ray being diffracted (author)

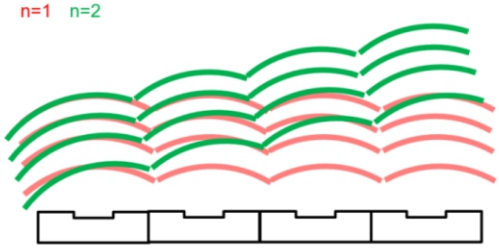

Fig. 7: Different colors (wavelengths) for each order of magnitude n (author)

Since for a single wavefront there may be many orders of magnitude that define constructive interference, for different angles of observation, the color of the colored line may change (Fig. 8).

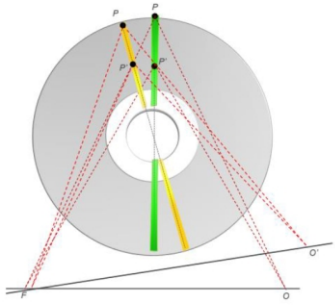

Fig. 8: Different observers obtain different colors for the colored line for the same wavefront (author)

2.2. Geometrical Description

We will initially define some essential characteristics of the discs in relation to the formation of the colored line, such as radius parameters and observational distances (Fig.9).

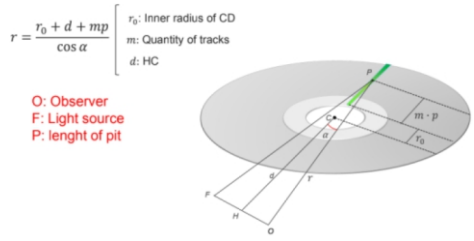

Fig.9: Radius parameters and observational distances (R. De Luca , M. Di Mauro , O. Fiore , and A. Naddeo , Am. J. Phys. 86(3), 169 (2018))

2.3. Physical Description

With the geometrical characteristics of the disc already defined, it is possible to calculate the interference between the electrical fields emitted to the disc and their points of maxima interference (where the colored line is formed) and solve the sets of equations using the vector of Poynting. Electrical fields on CD radius and sum of electrical fields are as written in Eqs. (1, 2).

$$\vec{E}_m = \vec{E}_m \exp(ikr) = \vec{E}_m \exp(ik\frac{r_0 + d + mp}{\cos\alpha}) \quad (1)$$

$$\vec{E} = \vec{E}_0 \exp\left(ik\left(\frac{r_0 + d}{\cos\alpha}\right)\right)\exp(\frac{iNkp}{2\cos\alpha})\frac{\text{sen}\left(\frac{(N+1)kp}{2\cos\alpha}\right)}{\text{sen}\left(\frac{kp}{2\cos\alpha}\right)} \quad (2)$$

The points of maxima interference (intensity of wavefronts) is calculated using the vector of Poynting (Eq. 3).

$$I = S_m = \frac{|E|^2}{\mu c}$$

$$I = \frac{1}{\mu c}|E_0|^2 = \frac{1}{\mu c}\exp\left(2ik\left(\frac{r_0 + d}{\cos\alpha}\right)\right)\exp(\frac{iNkp}{\cos\alpha})\frac{\text{sen}^2\left(\frac{(N+1)kp}{2\cos\alpha}\right)}{\text{sen}^2\left(\frac{kp}{2\cos\alpha}\right)} \quad \text{(Maximize; Does not depend on r)} \quad (3)$$

The wavelength of the constructive interference observed at a certain angle will be given by the equation (4). Wavelength of observed colored line (λ) is in function to the number of tracks on the disc (P) and angle (α).

$$\frac{kp}{2\cos\alpha} = n\pi \Rightarrow \quad \lambda_n = \frac{p}{n\ \cos\alpha} \quad (4)$$

2.4. Geometrical Description – New Parameter

For the inclination of the disc a new parameter will be added (β) (Fig. 10).

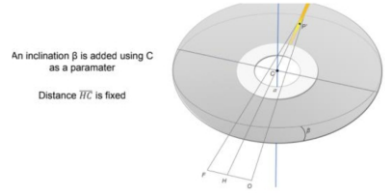

Fig. 10: New parameter added (angle of inclination of disc) (R. De Luca , M. Di Mauro , O. Fiore , and A. Naddeo , Am. J. Phys. 86(3), 169 (2018))

With this new parameter there must be a correction in our previous geometrical model as exemplified in Figure (11).

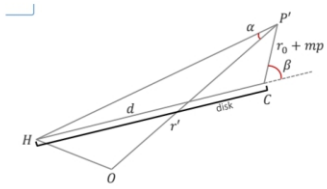

Fig. 11: Geometrical corrections (author)

With this new angle we can add to the (Eq. 4) the correction, where the colored line will suffer an interference in its wavelength according to the angle of inclination of the disc. Correction of wavelength of observed colored line at a certain angle of inclination will give (Eq. 5).

$$\lambda'_n = \frac{p\cos(\beta)}{n\cos(\alpha)} \quad (5)$$

3. Experimental Methodology

3.1. Verifying Assumptions

To verify the assumption that the discs behave as a diffraction grating we used a Scanning Electron Microscope in a collaboration with the Universidade Federal do Cariri laboratories of Materials Engineering (Fig. 12).

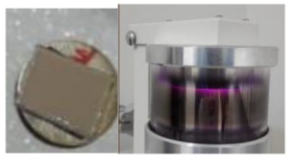

Fig. 12: Preparation of disc sample for analysis in SEM, the sample had to be covered in a thin gold layer using atom transference by plasma (author)

Fig. 13: Sample being inserted inside SEM (Author)

The images obtained show that the distance between the tracks of the disc is in fact from the same order of magnitude as observable light (Fig. 14).

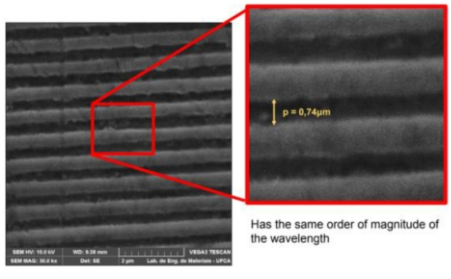

Fig. 14: Results from the SEM analysis (author)

3.2. Experimental Setup

To minimize human error and possible inaccuracies, stands and supports were utilized to provide accuracy in results. For the analysis of the images obtained, computer software Tracker was used (Fig. 15).

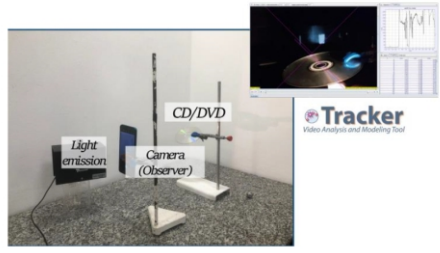

Fig. 15: Experimental setup and software tracker being used in the experimental methodology (author)

4. Experimental Results

4.1. Inaccurate and Unstable Results

Due systemic errors, the images we obtained were too noisy and the colors observed suffered many interference from other light sources (Fig. 16).

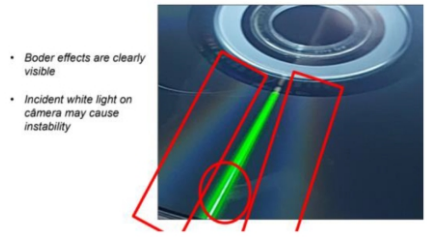

Fig.16: Border effects are seen as well as incident white light (author)

To reduce experimental flaws we isolated the light emitter and used a convex lens to make the incoming light rays parallel (Fig. 17).

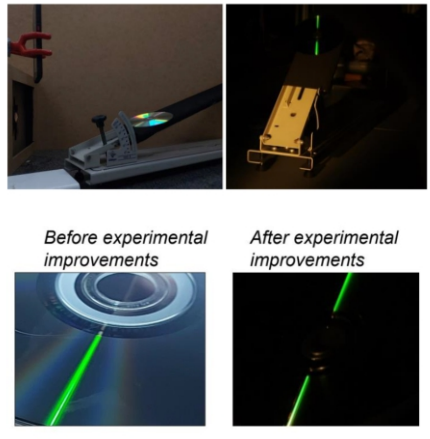

Fig. 17: Experimental setup with improvements (author)

4.2. Wavelength Measurement

The analysis of the wavelength of the colored line was made using a diffraction grating as a spectrometer. By positioning the grating in front of the camera, pointing to lasers with known wavelengths and measuring the distance in pixels of the next point of interference of the lasers we can draw a linear profile between the distance of the interference and the wavelength of the light observed by the camera (Fig. 18).

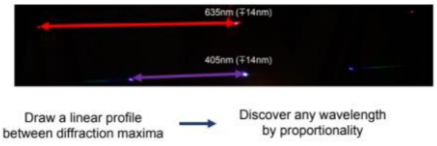

Fig.18: Experimental method for measuring wavelength of observed light (author)

4.3. Observed Results

By changing the angle of inclination of the disc we obtain different wavelengths for the colored line. In the same angle, the diffracted rays will compose a colored line at the points of maxima interference (n) (Fig. 19).

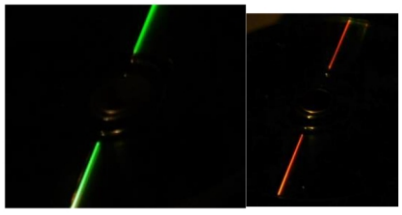

Fig. 19: Colored lines for different angles of inclination (author)

The relation between the wavelength of the colored line and the inclination of the disc fitted our theoretical explanation as shown in Figure (20).

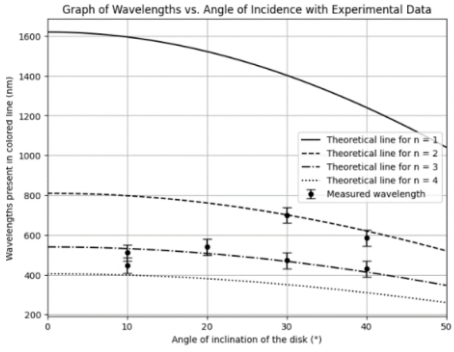

Fig. 20: Angle of inclination of the disc changing the wavelength observed (author) (CDs, p = 1600nm).

Since CDs and DVDs have different distance between tracks, the colored line will have differences in their wavelength at same angle of inclination (Fig. 21).

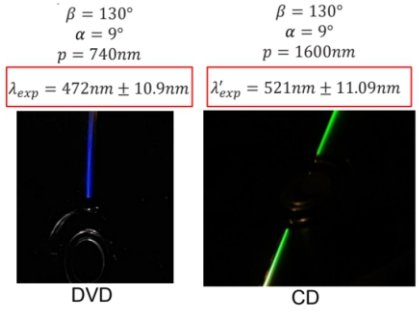

Fig. 21: Different wavelenghts in CD and DVD at same conditions of observation (author)

4.4. Observed Results

At certain angles of inclination, more than one order of magnitude may fit within the observable range. Forming an effect of "false colors". Using a diffraction grating we can separate the wavelengths and measure each one of them individually (Fig. 22).

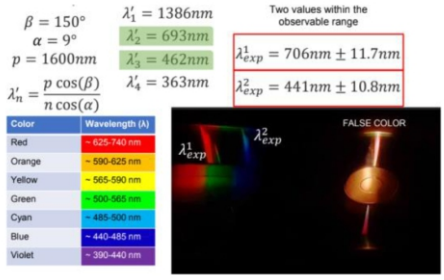

Fig.22: Observed false color of magenta decomposed using a diffraction grating. (author)

5. Conclusions

The problem statement proposes an analysis of the colored line formed on optical media discs and the changing of their colors as the angle of inclination is altered.

This paper proposed such analysis by using theoretical models to predict the behavior of the colored line and followed a rigorous experimental methodology to verify and test assumptions.

We initially assumed the disc to behave as a diffraction grating and later used a Scanning Electron Microscope to verify such an assumption. The white light emitted to the disc suffers diffraction and the diffracted light rays will interfere constructively to compose the colored line stated in the problem.

References

[1] Sidorenko, Alexey & Tupikina, Nadezhda & Sergey, Lisakov & Kin, Isa & Sypin, Eugene. (2019).

[2] R. De Luca , M. Di Mauro , O. Fiore , and A. Naddeo , Am. J. Phys. 86(3), 169 (2018))

Short Length Wire as an Electrical Fuse

Mahan Fallahpour , Sharif University, fallahpourmahan@gmail.com

ARTICLE INFO

Former participant in IYPT

New Edition of the published paper in No 1, 2023

Accepted by Ariaian Young Innovative

Minds Institute , AYIMI

http://www.ayimi.org ,info@ayimi.org

ABSTRACT

This study focuses on the phenomenon of a compact wire segment's functionality as an electrical fuse. Fuses are pivotal for electrical safety, designed to melt and disconnect when excessive current flows. The primary objective is to analyze the factors affecting the time until fuse disruption. Two key parameters are examined: the current magnitude and the wire's melting point. The study also investigates the impact of resistance, an indirect factor, and physical wire attributes like length and width, assuming a constant current. This research enhances our understanding of fuse behavior, advancing electrical safety and engineering practices for reliable operation.

Keywords : *: Compact Wire Segment, Fuse, Constant Current , Electrical Engineering*

1. Introduction

The conducted study represents a rigorous scientific investigation aimed at addressing a complex problem posed by the 35th International Young Physicists' Tournament (IYPT). The focal point of this research revolves around a fundamental inquiry, stated as follows: "Under what conditions and to what extent does a concise segment of wire function as an electrical fuse? Elucidate the intricate interplay between different parameters and their influence on the temporal characteristics of fuse disruption." The pivotal terminology encompassing this research comprises "the fuse," signifying the wire segment with potential electrical fuse properties, "the time taken," indicative of the temporal interval leading to fuse disruption, and "blow," denoting the critical juncture at which the fuse's functionality is compromised. In the realm of electrical engineering and physics, the phenomenon of a short length of wire acting as a fuse holds profound implications. By meticulously examining the intricate dynamics at play, the study endeavors to unravel the underlying principles that dictate the fuse's behavior. This involves a comprehensive exploration of variables encompassing wire material composition, wire gauge, current magnitude, and ambient temperature, all of which distinctly contribute to the intricate mechanism leading to the fuse's eventual disruption. The research methodology employed entails a meticulous combination of theoretical analysis, empirical experimentation, and computational modeling. Theoretical insights gleaned from fundamental principles of electrical conductivity, Joule heating, and material science provide a robust foundation for understanding the underlying processes that govern the fuse's behavior. Empirical experiments, carried out under controlled conditions, scrutinize the effects of varying parameters on fuse disruption time, elucidating the nuanced relationships between these variables. Furthermore, computational simulations using advanced numerical methods serve to validate and extend the experimental findings, offering a predictive framework to extrapolate the behavior of the fuse under a broader spectrum of conditions. The synergy between theoretical analysis, empirical experimentation, and computational simulations fosters a comprehensive understanding of the intricate interactions at the heart of the fuse's behavior. In conclusion, this research endeavor stands as a testament to the dedication of scientific inquiry.

2. Theory

In accordance with the scientific method, the investigation centers on the critical process of fuse disruption. A central prerequisite for fuse blowing is the fusion of the conducting element, a transformation driven by the heat generated within the wire due to current flow. This pivotal heat generation underscores the significance of the produced current in this context. Leveraging the reasonable presumption that the wire functions as an ohmic conductor, the heat evolved within the wire during the passage of a current (I) is represented by RI^2t, with t denoting the elapsed time since the current's initiation.

The velocity of fuse disruption is intricately tied to both the magnitude of current coursing through it and the material constituting the fuse. Distinct materials exhibit diverse melting points, even when possessing equivalent resistance. This variation in melting points underscores the importance of material selection, as it profoundly influences the threshold at which the wire succumbs to fusion. The fusion mechanism pivots on the synergy between current, the wire's resistive properties, and the material's specific heat characteristics. Through this systematic analysis, the study enhances our understanding of the intricate amalgamation of current, resistance, and material properties, unraveling the nuanced phenomenon of fuse disruption.

2.1. Effect of Current

The impact of current on this phenomenon is pivotal, as elucidated by the Ri^2 formula governing heat generation. The magnitude of current directly influences the heat produced within the wire, amplifying the chances of fuse disruption.

A fundamental insight lies in the RI^2t formula, underscoring the current's quadratic effect on heat generation. This signifies that even small increments in current lead to disproportionately higher heat output, rendering current a dominant factor in determining the fuse disruption time.

To illustrate, consider a copper wire with a resistance of 0.1 ohms and a melting point suitable for this analysis.

When subjected to a higher current of 20 amperes, the RI^2t demonstrates that the heat generated is proportional to (0.1 *20^2*t), resulting in a significant increase in heat production. Conversely, at a lower current of 5 amperes, the heat generation is governed by (0.1*5^2* t), yielding notably less heat. This divergence in heat accumulation between the two scenarios leads to a substantially shorter fuse disruption time for the higher current case, exemplifying the exponential relationship between current and heat generation in determining the temporal aspects of the phenomenon.

$$V = RI \tag{1}$$

$$P = \frac{W}{t} = \frac{q.\Delta V}{t} = I\Delta V = IV = \frac{V^2}{t} \tag{2}$$

2.2. Physical Parameters: Length, Width

The distinct roughness and length of a wire significantly impact the phenomenon's duration. Increased roughness elevates wire resistance due to augmented surface area, leading to intensified heat generation for a given current, hastening the fuse's disruption. Conversely, greater wire length escalates overall resistance, extending the time needed to accumulate sufficient heat for disruption. These effects arise from the intricate interplay of resistance, current, and surface characteristics, influencing the delicate balance between heat production and dissipation, ultimately dictating the temporal evolution of the phenomenon.

2.3. Melting Point

The time frame of the phenomenon is intricately influenced by variations in wire material and their corresponding melting points. Altered wire materials with diverse melting points distinctly affect the thermal characteristics of the system. Materials with higher melting points necessitate more substantial thermal energy accumulation to achieve the critical threshold for disruption, thus prolonging the phenomenon's duration. Conversely, materials with lower melting points require comparatively lesser energy accumulation, resulting in a shorter temporal span for disruption. This temporal modulation arises from the interaction between specific heat capacities, melting point temperatures, and the heat generation mechanism, underscoring the pivotal role of material selection in shaping the phenomenon's time course.

2.4. Other Parameters

Beyond the discussed parameters, ambient temperature and wire cross-sectional area exert substantial influence on the phenomenon's duration. Elevated ambient temperatures expedite heat transfer and reduce the time needed for heat accumulation, thus shortening the phenomenon's duration. On the other hand, a larger cross-sectional area lowers wire resistance, augmenting the heat generation rate and promoting faster disruption. Additionally, the wire's purity level and crystal structure influence its electrical and thermal conductivities, which directly affect heat generation and dissipation dynamics. Altogether, these unexplored parameters further underscore the intricate interplay between various factors in governing the temporal characteristics of the phenomenon.

3. Basic Theory

When an electric current traverses the wire, it engenders a conversion of electrical energy into heat, denoted as electrical power (P_{elec}). This generated heat is subject to intricate dissipative mechanisms. A portion of this thermal energy is transferred to the surrounding environment through convective processes, constituting convective power loss.

$$p_{convection} = hA\,(T-T_{amb}) \tag{3}$$

Simultaneously, another fraction of the heat dissipates through conduction, a process governed by the transfer of thermal energy within the wire's material itself. The comprehensive theoretical framework underlying these heat transfer dynamics provides insights into the complex interplay of convection, conduction, and electrical power, illuminating the mechanisms shaping the wire's thermal behavior during the phenomenon (Fig. 1).

$$P_{elec} - P_{conv} = \text{mc}.\frac{dT}{dt} \tag{4}$$

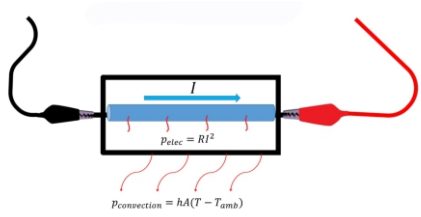

Fig. 1: Current in Fuse

3.1. The Conditions for the Creation and Non-creation of the Phenomenon

As the temperature elevation ensues consequent to the traversal of electric current through the wire, a concomitant augmentation in the convective current materializes. In cases where this thermal process unfolds gradually, a state of thermal equilibrium ($P_{elec}=P_{conv}$) is attained within the wire, characterizing a consistent temperature profile.

$$(T_F=T_{amb}+\text{RI}^2/hA) \tag{5}$$

Should this resultant equilibrium temperature remain below the material's melting point, the phenomenon remains quiescent. Conversely, if the attained equilibrium temperature surpasses the material's melting point, the stage is set for the observable manifestation of the phenomenon.

3.2. Instantaneous Temperature and Time

When examining the phenomenon through a temporal lens, the temperature of the wire experiences incremental increases (RI^2dt) at each successive instant. Simultaneously, the convective heat transfer mechanism precipitates a continuous temperature loss ($hA(T- T_{amb})dt$) during each time increment. This complex interaction leads to the formulation of a differential equation that includes the dynamic relationship between temperature rise and convective heat loss.

$$(Ri^2dt - hA(T- T_{amb})dt = mcdt) \tag{6}$$

Separation of this differential equation leads to the extraction of an analytical expression that provides the possibility of determining the final thermal state obtained by the wire in that second:

$$T = \frac{RI^2}{hA} \cdot e^{-\frac{\alpha}{m \times c} t} + \frac{RI^2}{hA} + \mathrm{T_{amb}} \quad (7)$$

By assigning the ultimate temperature as the melting temperature within the context of this differential equation, we can discern the temporal duration requisite for the phenomenon's manifestation:

$$t_{blow} = \frac{mc}{hA} \times \ln\left(\frac{RI^2}{RI^2 - hA(T_l - T_{amb})}\right) \quad (8)$$

3.3. Place of Melting

Due to the observed conduction phenomenon, it may initially appear that the temperature of a designated region, denoted as "part 3," surpasses that of an alternate segment. This implication leads to the presumption that the point of melting should correspond to "part 3." However, this inference is misleading and lacks accuracy. Contrary to imagination, this phenomenon happens in episode 4.

The elevated heat generation within "part 4" is attributed to impurities present in the wire. Despite its proximity to the reference point represented by the "crocodile wire," conduction's impact is relatively mitigated. Consequently, within the theoretical framework, conduction is ascribed a diminished influence.

For enhanced elucidation of this phenomenon, a partition of the wire into three discrete segments is undertaken. The premise of the wire's intrinsic impurity necessitates an assumption wherein $R'' > R' > R$. Within this framework, a uniform current distribution is postulated across the entire wire over a defined temporal interval. Consequently, the segment characterized by heightened impurities manifests augmented heat generation. Empirical validation accentuates the observation of heat loss due to conduction. However, the efficacy of this heat transfer mechanism is notably curtailed owing to suboptimal propagation, consequently warranting its exclusion from the theoretical construct(Fig. 2).

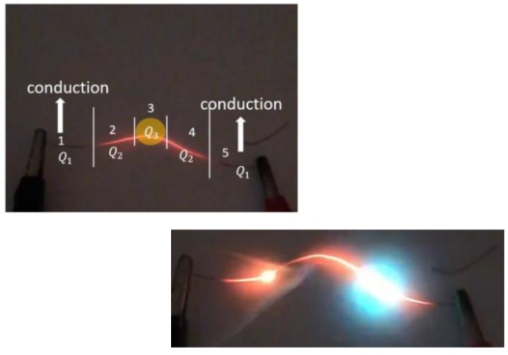

Conductin 1 ≈ Conductin 5 > *Conductin* 2 ≈ *Conductin* 4 > *Conductin* 3

Fig. 2: Melting point

4. Experiment setup

1.Amperemeter
2.Voltmeter
3.Short length of wire
4.power supply (Fig. 3)

4.1. Finding Convection Coefficient (*h*):

The determination of the convective coefficient is derived through the manipulation of Equation (2):

$$h = \frac{V^2}{\frac{(T_{max} - T_{amb})R}{A}} \quad (9)$$

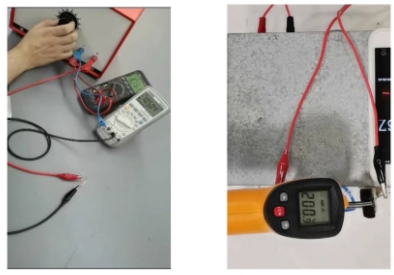

Fig. 3: Experimental setup

The acquisition of the convective coefficient (h) necessitated the selection of an elemental unit characterized by readily determinable cross-sectional area ($A \approx 0.001$) and resistance. Subsequently, the temperature differential of this chosen unit was ascertained through the implementation of a meticulously devised experimental procedure. This procedure involved the utilization of a laser thermometer to capture instantaneous temperature variations. The ensuing dataset was graphically portrayed, enabling the subsequent deduction of the convective coefficient (h): $h \approx 28$ (Fig. 4).

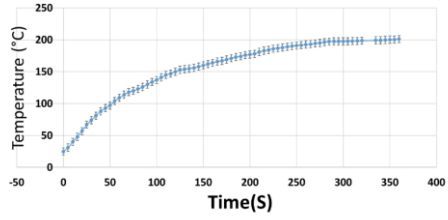

Fig. 4: Temperature vs time

4.2. Make a Fuse

Within this specific section, the primary objective is to establish an operative range for voltage and current values, beyond which the fuse is anticipated to undergo combustion. By employing Equation (2) and under the premise of equating the ultimate temperature to the melting temperature, the upper bounds for both voltage and current are deduced :

$$I < \sqrt{\frac{29680\, A_{(WIRE)}}{R}}\ ,\ V < \sqrt{29680\, A_{(WIRE)}\, R} \quad (10)$$

4.3. Time of Blow vs. Length

In this designated section, a meticulous examination was conducted to scrutinize the proportionality between alterations in length and the corresponding temporal adjustments. This investigation involved subjecting wires of varying lengths to controlled testing conditions. Evidently, a noteworthy correlation emerged, revealing that an escalation in wire length correlated with an elongation in the temporal persistence of the wire under investigation (Fig. 5).

4.4. Voltage vs. Time

In this dedicated section, a systematic exploration was undertaken to assess the proportional relationship between alterations in voltage and the associated temporal variations. This analysis was conducted using wires of

identical composition yet varying in length. The results unveiled a discernible pattern wherein an escalation in voltage was inversely correlated with the duration of wire persistence, leading to a reduction in the time interval over which the wire endured (Fig. 6).

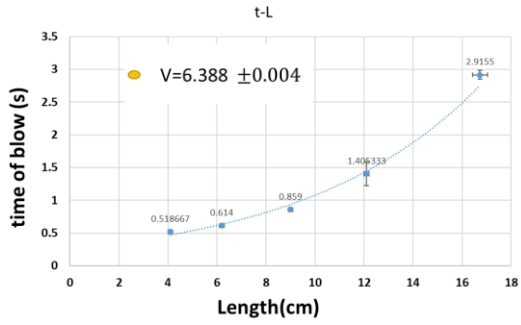

Fig. 5: Time of blow vs. Length of wire

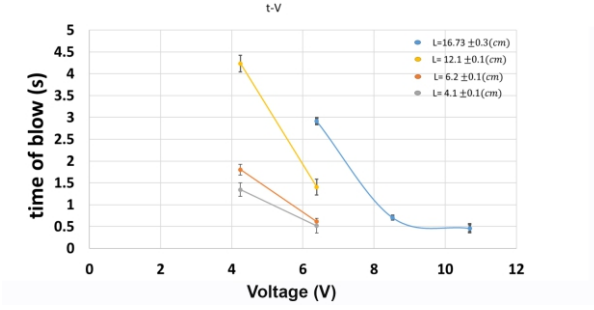

Fig. 6: Time of blow vs. voltage

5. Conclusion

Section 3.2 encompassed the utilization of Equation (7) to ascertain the ultimate temperature, while Equation (8) enabled the determination of the temporal interval necessary for wire disruption. The subsequent Section 3.3 elucidated the significant interrelation linking wire termination locations with the inherent impurity content at specific points. Moving forward, Section 4.2 engendered the establishment of a standard range for fuse voltage and current parameters through systematic analysis. Section 4.3 substantiated a direct correlation between wire length and the temporal duration of its functionality. Lastly, Section 4.4 rigorously evidenced an inverse relationship between voltage magnitudes and the temporal span of wire endurance.

References

[1] Holiday Edition 10, pages753-761.

[2] Frank P. Incropera and David P. Dewitt, Introduction to heat transfer

Teaching Material for Environmental Literacy: Exhibiting Fish and Arthropods with Epoxy Resin Method, Introducing them with DataMatrix

Ceren Çayan[a], Müşerref Şeyma Şahin[b] ; Giresun Science School, Turkey
a) cerenchayan@gmail.com, b) mseymasah@gmail.com

ARTICLE INFO

Gold medalist in ISAC Olympiad 2023

Awarded by Ariaian Young Innovative

Minds Institute , AYIMI

http://www.ayimi.org ,info@ayimi.org

ABSTRACT

The protection of biodiversity is important for our future and the increase in environmental problems shows the importance of raising environmental awareness. Within the scope of the rich biodiversity of our country, the importance of active learning of arthropods and fish in biology lessons is increasing. In addition, the distance of students from arthropods for various reasons poses a problem in raising an environmentally conscious individual.

Keywords : *: Biodiversity, Epoxy Resin, Teaching Material, Fish, Arthropod*

1. Main Abstract

The protection of biodiversity is important for our future and the increase in environmental problems shows the importance of raising environmental awareness. Within the scope of the rich biodiversity of our country, the importance of active learning of arthropods and fish in biology lessons is increasing. In addition, the distance of students from arthropods for various reasons poses a problem in raising an environmentally conscious individual. The lack of importance given to laboratory activities in schools and the difficulties in preparing the materials related to the classification of 9th grade living things make it difficult to teach the concepts. When the textbooks are examined, it is seen that the examples related to the animal kingdom are insufficient and make it difficult to learn the concepts. Exhibiting fish and arthropod specimens in epoxy resin in biology laboratories instead of storing them in ethanol or formalin provides more usage areas. In this method, the color loss in stuffed animals is less than those stored in liquid. Our aim of the project is to prepare permanent and useful teaching materials by embedding arthropods from Giresun region and fish samples from our region, obtained from fishermen's stalls, in epoxy resin. Preferred fish species for epoxy resin application for our project, Carassius gibelio (Israeli Carp), Salmo trutta (Stream trout), Leuciscus cephalus (Pulleyfish), Diplodus annularis (Sparring), Chelidonichthys lucernus (Swallow), Hippocampus guttulatus (Sea squid) fish) was. In addition, the arthropod specimens treated with epoxy resin were Carcinus spp. (Freshwater crab), Pachygrapsus spp. (Saltwater crab), Scorpiones spp. (scorpion), Araneae spp. (spider), Lepidoptera spp. (Scaly-winged), Mantodea spp. (Mantis), Odonata spp. (Daughter beetle), and Coleoptera spp. A website called https://bio.giresunfenlisesi.com/ containing information on epoxy samples was prepared and mobile phones were directed to the relevant section of the website with the QR code application.

2. Introduction

Conservation of biodiversity is important for our future and it shows the importance of environmental experiences in raising people's environmental awareness [1].

It will be very useful to provide active learning in biology lessons about the fish diversity of our country surrounded by seas on all four sides and to raise awareness about their importance in the ecosystem. In the same context, students' distance from invertebrates to arthropods causes negative attitudes. The teaching material to be prepared will be used in the biology laboratory environment of our school and will contribute positively to the active learning process. In addition, the prepared materials will give the opportunity to get to know and examine the fish diversity and arthropods of our country.

The lack of importance given to laboratory activities in schools and the difficulties in preparing the materials related to the classification of 9th grade living things make it difficult to teach the concepts. When the textbooks are examined, it is seen that the examples related to the animal kingdom are insufficient and make it difficult to learn the concepts.

The tools used in biology laboratories in secondary education provide permanent learning and active learning [2]. For this purpose, it is important to prepare and exhibit auxiliary materials for biology lesson laboratory applications by using fish belonging to our region, which are sold at the fishermen's stall by Giresun fishermen, and arthropods living in our region caught by us.

Our aim of the project is to prepare permanent and useful teaching materials by embedding arthropods of Giresun region and fish samples obtained from fishermen's stalls in epoxy resin medium. In addition, it is to prepare a website containing information on arthropod-fish samples with epoxy application and to direct mobile phones to the relevant website section with data matrix application.

Our project differs from the studies mentioned in the literature on the following issues.

1. Epoxy resin application for Fish and Arthropods
2. Exhibition of epoxy resin samples in the biology laboratory
3. Establishment of a website where epoxy resin samples are promoted
4. Creating and routing data matrix for each sample

Students' distance from insects causes negative attitudes.

Conservation of biodiversity is important for our future. It is important to raise awareness for arthropods from invertebrates and to prevent their destruction.Providing active learning about the fish diversity of our country

surrounded by seas on all four sides and raising awareness about their importance in the ecosystem will be very useful for the biology course. In our project, permanent and useful teaching materials were prepared by embedding the arthropods of the Giresun region and the fish samples obtained from the fishermen's stalls in the epoxy environment.

The prepared teaching material will be used in the biology laboratory environment of our school and will contribute positively to the active learning process. In addition, the prepared materials will give an opportunity to recognize and examine for students who have fear of arthropods such as insects and scorpions.

The collections of invertebrates and fish from vertebrates are an important source for studies on biodiversity for the purpose of course material in secondary education biology laboratories. There are many methods for preservation in the preparation, preparation, archiving, display and educational use of materials in school laboratories. Among the methods used for the preservation of these materials; drying method by drawing the tissue fluid of the animal, the method of storing the tissue in ethanol or form aldehyde solution, and the method of freezing the whole body in the refrigerator [3].

If there is too much material, it will be technically difficult to store whole samples in ethanol or formaldehyde solution or to freeze them. Therefore, the most appropriate storage method for future genetic activities is to store skin and skull samples [4]. In fish, a similar structure can be prepared from gills and fins and covered with skin [5]. It also provides DNA analysis thanks to the tissue samples obtained from the materials [6].

Taksidermi has been translated into Turkish as embalming. The foundations of the embalming method are based on mummification in ancient Egypt. In the 19th century, some taxidermists began to remove the bones completely and add them to separate collections [7]. In addition, specimens are preferred more in museums for systematic and paleontological studies because they are preserved with their spines [8].

2.1. Material Development and Model Teaching Method

With the developing and changing conditions, educators and those who need other presentation technologies can easily find the teaching tools and materials they need in the market. In these cases, teachers can prepare some of the tools and materials they need themselves, or they can have students prepare by guiding them [9]. What makes the use of materials in education so valuable is the linear relationship between learning and sense organs. Students learn 83% of their learning by sight, 11% by hearing, 3.5% by smell, 1.5% by touch and 1% by taste. In addition, people remember 10% of what they read, 20% of what they hear, 30% of what they see, 50% of what they see and hear, 70% of what they say and 90% of what they do and say [10]. The effect of seeing and hearing on learning at this rate makes the design of visual materials extremely important.

Model Teaching Method; It is a teaching method applied with the help of examples of real objects made of the same or other material, and objects brought to the classroom from their natural environment. Models may be larger or smaller than the original object, or may be exactly the same size and structure as the actual object it replaces [11].

In the field of science, it is important for students to acquire concepts that are difficult to reach, dangerous, inaccessible even though they are abstract or concrete, both visually, audibly and descriptively by using models in the classroom environment and by making use of today's technology [12].

2.2. EPOXY Method and Material Development

Epoxy is any of the main components or cured end products of 'epoxy resins' and also the name of the epoxide functional group [13]. Epoxy has a wide range of applications for structural and other purposes, including use in metal coatings, electronic/electrical components/LEDs, high voltage electrical insulators, paint brush fabrication, fiber-reinforced plastic materials and adhesive. Epoxy is an adhesive chemical resin from the thermosets group. Its resistance to water, acid and alkali is very good, it does not lose its resistance feature over time. The epoxy adhesive filled in the crack transforms the discontinuity environment created by the crack into a continuous state, continuously bonds both sides of the crack along the crack and prevents stress accumulations. Generally, two-component epoxies, like other thermoset plastics, go from liquid to solid after a certain period of time and reach their final hardness by maturing within a week or two. The word epoxy is derived from two Greek prefixes: “epi” meaning “over” and “oxy” meaning “sharp/acidic”. Epoxy resin mixed with pigment can be poured in layers to create a painting medium. It is also used in the form of dome resin for jewelry, embellishments and labels, and in decoupage applications for art, countertops and tables [14]. Epoxy resin was first synthesized in 1930 and used for many industrial applications. These application areas are; building materials, coatings, composite materials, aerospace, laminates, adhesives [15].

3. Method and Experimental Details

3.1. Tools Used

Materials used for epoxy treatment for arthropods and fish:

- 4 units ARC brand Ultra Transparent Cast Type Glossy Epoxy Resin Transparent Set
- 1 unit of ARC brand Hardener
- Plastic Silicone Gun
- Silicone Sealant 500 ml for the production of 2 molds
- Container and wooden stick for mixing Epoxy Resin and Hardener
- Pin for fastening
- Electronic balance
- A 5 lt basin provided for use in making silicone molds
- Liquid soap

3.2. Epoxy Application Stages

I. Silicone Mold Design: 4 liters of tap water and liquid soap were put into the basin provided to be used in mold making and mixed.

II. With the help of 500 ml Plastic Silicone Gun, Silicone Sealant is poured into the basin and shaped with the help of hand, silicone molds are obtained (Fig.1).

Fig. 1: Silicone Mold Making

III. 4 parts of Transparent Epoxy Resin and 1 part

part of Hardener were mixed with the help of an electronic balance in a suitable container with the help of a wooden stick for 10 minutes (Fig. 2).

Fig.2: Mixing Epoxy Resin and Hardener

IV. After pouring some of the Epoxy Resin and Hardener mixture into the molds, arthropod and fish samples were placed in epoxy. The remaining part of the epoxy mixture is poured on the sample (Fig. 3& Fig. 4).

Fig. 3: Placing invertebrate specimens in epoxy

Fig.4: Placing fish samples in epoxy

3.3. Arthropod and Fish Samples Treated with Epoxy

The arthropod specimens caught by us and the local names of the fish species offered for sale by the fishermen are the species names.

- Carassius gibelio (Israeli Carp)
- Salmo trutta (Stream trout)
- Carcinus aestuarii (Freshwater crab)
- Pachygrapsus marmoratus (Saltwater crab - Marmara hermit crab)
- Leuciscus cephalus (Freshwater mullet, Pulley fish)
- Diplodus annularis (Sparse fish)
- Chelidonichthys lucernus (Swallow)
- Hippocampus guttulatus (Sea Horse Fish)
- Arthropod collection in bulk: Arachnida (scorpion-spider), Lepidoptera (Scaly-winged), Mantodea (Mantis), Odonata (Girl beetles) and Coleoptera (Beetle-wings)

3.4. Website Preparation

A website containing information on arthropod and fish species on which epoxy application is made has been prepared on the website whose link is given below, with the facilities of our school.

For each arthropod or fish species in each epoxy application, a section containing information has been prepared on the website (Fig.5).

- Website address: https://bio.giresunfenlisesi.com/

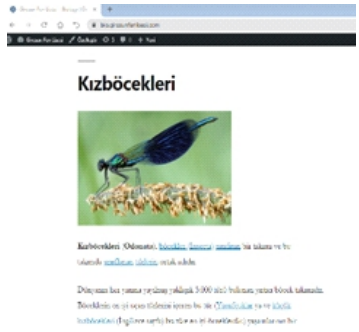

Fig.5: Snapshot of our website

3.5. QR Code Application

With the help of the new free add-on of the Google chrome application used for browser purposes, a QR code has been created for each epoxy. The student, who examines the epoxy material in the laboratory environment, will be directed to the website:
https://bio.giresunfenlisesi.com/
with the help of the data matrix application on the epoxy with the help of a mobile phone and have information about the related species. As seen in Figure 2.6, it is directed to the website with the data matrix created for the seahorse placed in epoxy.

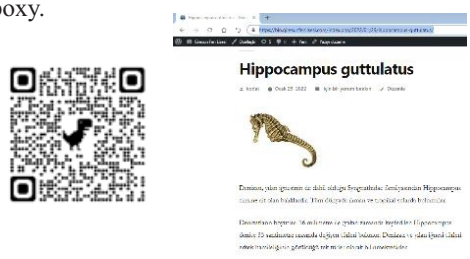

Fig.6. : The relevant section on the website directed by QR code

4. Result

Epoxy samples made by us for Carcinus aestuarii (Freshwater crab) samples for course material in the laboratory environment are shown in Figure(7) and Pachygrapsus marmoratus in Figure(8).

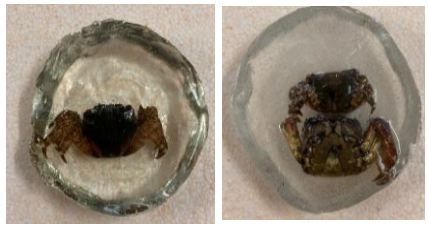

Fig.7: Carcinus aestuarii

Fig. 8: Pachygrapsus marmoratus

Other samples are in Figures (9-15).

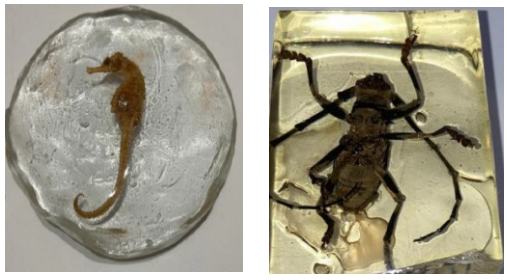

a b

Fig. 9: a) Hippocampus guttulatus; b) Hylotrupes spp. (Coleoptera)

Fig. 10: Examples of Arthropoda (Arachnida, Lepidoptera (Scaly-winged), Mantodea (Mantis), Odonata (Dragon beetle) and Coleoptera (Beetle)

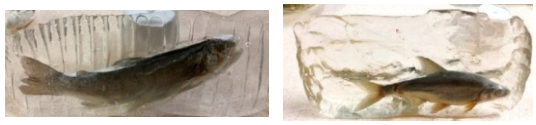

a b

Fig. 11: a) Salmo trutta (Stream trout); b) Carassius gibelio (Israeli Carp)

a b

Fig. 12: a) Leuciscus cephalus (Pulleyfish); b) Diplodus annularis (Sparrow) and Chelidonichthys lucernus (Swallow)

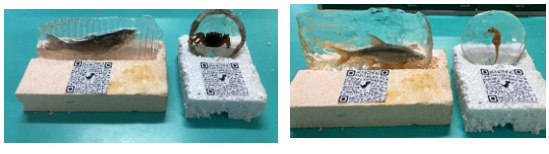

a b

Fig. 13: a) Biology laboratory exhibition material-1; material 2

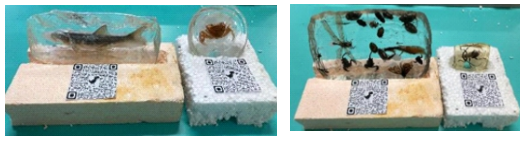

a b

Fig. 14: a) Biology laboratory exhibition material-3; material 4

5. Conclusion

It will be very useful to provide active learning in biology lessons about the fish diversity of our country surrounded by seas on all four sides and to raise awareness about their importance in the ecosystem. In the same context, students' distance from invertebrates to arthropods causes negative attitudes. The teaching material to be prepared will be used in the biology laboratory environment of our school and will contribute positively to the active learning process. In addition, the prepared materials will give the opportunity to get to know and examine the fish diversity and arthropods of our country.

The lack of importance given to laboratory activities in schools and the difficulties in preparing the materials related to the classification of 9th grade living things make it difficult to teach the concepts. When the textbooks are examined, it is seen that the examples related to the animal kingdom are insufficient and make it difficult to learn the concepts. For this purpose, it is important to prepare and exhibit auxiliary materials for biology lesson laboratory applications by using the fish belonging to our region, which are sold at the fishermen's stall by Giresun fishermen, and the arthropods living in our region caught by us.

Permanent and useful teaching materials were prepared by embedding the arthropods of the Giresun region and the fish samples obtained from the fishermen's stalls in the epoxy environment. In addition, a website named containing information about the Arthropod-Fish samples, on which epoxy was applied, was prepared. With the QR code application, mobile phones were directed to the relevant website section. In school laboratories and field studies, difficulties are faced in terms of fluid transport protocols. Therefore, materials in alcohol or formalin solution limit studies. Color loss in animals stuffed with this method is less than those stored in liquid. Since the samples are prevented from getting air, it will protect against the effect of moth in school laboratories. Thus, the maintenance cost of the samples has been reduced compared to the formaldehyde-alcohol mixture that needs to be renewed. It provides convenience for the storage of samples.

This method minimizes possible risks and side effects and makes it possible for people with odor sensitivity and chemical respiration problems to be less affected if they work in this field. With this method, while working with materials prepared for educational purposes, it is possible to perform a healthier laboratory work by being exposed to the least chemical vapor and active substance. In particular, the preparation of course materials with this method will be more useful in terms of health and visuality. In biology teaching, both educational situations and the abstract and complex nature of biology concepts cause students to have difficulty in understanding some subjects and to learn by memorizing without understanding. In order to solve this problem, well-prepared three-dimensional models in biology lessons provide easier comprehension of information [17]. In studies on new curricula in Turkey, it is frequently encountered that there are teachers' opinions that "significant disruptions are experienced in the implementation of the curricula due to the lack of structures, tools, materials and materials" [18]. Model teaching method; It is a teaching method applied with the help of examples of real objects made of the same or other material, and objects brought to the classroom from their natural environment [11].

Acknowledgements

We participated in this organization with the support of

BUCA-IMSEF. We would like to thank our school Giresun Science High School for their support during the project process.

References

[1] Coyle, K. (2005). Environmental literacy in America: What ten years of NEETF/Roper research and related studies say about environmental literacy in the US. National Environmental Education & Training Foundation

[2] ENSARİ, S., & Rıdvan, K. E. T. E. (2010). Lise 1. Sinif biyoloji derslerinde ders materyali kullanimina ait öğrenci tutumlari. Kastamonu Eğitim Dergisi, 18(1), 131-146

[3] Rhinehart, J. R. (1983). Taxidermy Fish Body Insert Piece and Method of Marking It

[4] De Moraes-Barros, N., Morgante, J. S. (2007). A simple protocol for the extraction and sequence analysis of DNA from study skin of museum collections. Genetics and Molecular Biology, 30(4), 1181–1185. https://doi.org/10.1590/s1415-47572007000600024

[5] Pequignot, A. (2006a). The History of Taxidermy: Clues for Preservation. Collections, 2(3), 245–255. https://doi.org/10.1177/ 155019060600200306

[6] Muhammad, H. (2016). An Efficient Method for Dna Isolation From Fish Fin. Pakistan Journal of Agricultural Sciences, 53(04), 843–850. https://doi.org/10.21162/ PAKJAS/16.3998

[7] Bahuguna, A. (2018). Forensically informative nucleotide sequencing (FINS) for species and subspecies of genus Prionailurus (Mammalia: Carnivora: Felidae) through mitochondrial genes (12SrRNA and cytochrome b) by using old taxidermy samples. Mitochondrial DNA Part B, 3(2), 615–619. https://doi.org/10.1080/ 23802359.2018.1462115

[8] Pavia, M., Boano, G. (2018). Recovery of skeletal elements and extended wing from a mounted specimen of the nearly extinct Slender-billed Curlew (Numenius tenuirostris). Rivista Italiana Di Ornitologia, 88(1), 9–14. https://doi.org /10.4081/rio.2018.340

[9] Şahin Yanpar, T. ve Yıldırım, S. (1999). Öğretim Teknolojileri ve Materyal Geliştirme. Anı Yayıncılık, Ankara.

[10] Ergin, A. (1995). Öğretim Teknolojisi ve İletişim. Pegem Yayınları, Ankara.

[11] Çilenti, K. (1985). Fen Eğitimi Teknolojisi. Kadıoğlu Matbaası, Ankara

[12] Gülen, S. (2018). Using volume of concept in the class environment. Journal of Technology and Science Education, 8(4), 205-213. https://doi.org/ 10.3926/ jotse.362

[13] May, C. (Ed.). (2018). Epoxy resins: chemistry and technology. Routledge.

[14] McCreight, T., & Bsullak, N. (2001). Color on Metal: 50 Artists Share Insights and Techniques. Guild.

[15] Vaia, R., Jandt, K., Kramer, E. ve Giannelis, E., 1995. Kinetics of Melt İntercalation, Macromelecules, 28: 8080 -8085

[16] Karamustafaoğlu, O. (2006). Fen ve teknoloji öğretmenlerinin öğretim materyallerini kullanma düzeyleri: Amasya ili örneği. Bayburt Eğitim Fakültesi Dergisi, 1(1), 90-101.

[17] Çömlekçioğlu, U. ve Bayraktaroğlu, E. (2001). Biyoloji ve Bilişim Teknolojileri. Kahramanmaraş Sütçü İmam Üniversitesi Fen ve Mühendislik Dergisi 4

[18] Şahin, M., & Akbaba, s. (2010). Ilköğretim okullarinda zorbaci davranişlarin azaltilmasina yönelik empati eğitim programinin etkisinin araştirilmasi1. Kastamonu Eğitim Dergisi, 18(1), 331-342

Oscillating Screw

Nita Jafarzadeh , Alghadir School , Kish Island, Iran, nitaj1385@gmail.com

ARTICLE INFO

Participant in IYPT2023

Gold Medalist in ISAC Olympiad 2023

Awarded by Ariaian Young Innovative

Minds Institute , AYIMI

http://www.ayimi.org ,info@ayimi.org

ABSTRACT

This research is about the behavior of a screw when placed on its side on a ramp and released. It may experience growing oscillations and travels down the ramp. To Investigate how the motion of the screw, as well as the growth of these oscillations depend on the relevant parameters some different experiments have been done. As it is observed, the screw has two different types of motions. One of these motions is related to the rolling of the screw; and the other to its slipping, sliding and oscillations .The angle of releasing , different sizes and other parameters of the screw are studied to solve this problem.

Keywords : *: Screw, Oscillation, Motion, Slipping, Sliding, Angle*

1. Introduction

To illustrate a phenomenon different experiments are performed to help in finding suitable analysis. The conducted study represents a scientific investigation aimed at solving a complex problem in IYPT2023. The focal point of this research revolves around a fundamental inquiry, stated as follows:

When placed on its side on a ramp and released, a screw may experience growing oscillations it travels down the ramp. Investigate how the motion of the screw, as well as the growth of these oscillations depend on the relevant parameters.

As it is observed, the screw has two different types of motions. One of these motions is related to the rolling of the screw; and the other to the slipping, sliding and oscillations of it.

2. Observation and Theory

Applied forces on the screw are shown in (Fig. 1). As it is observed, the screw has two different types of motions. One of these motions is related to the rolling of the screw; and the other to its slipping, sliding and oscillations. The growing oscillation happens in y axis and there is an acceleration in x axis.

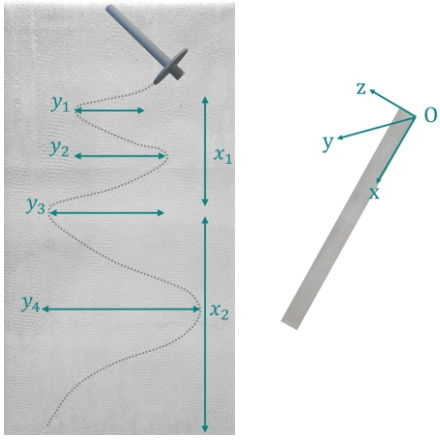

Fig. 1: Motion of the screw

The force analysis has been shown here; there is a gravity force that has been divided into two parts. Parallel force to ramp and perpendicular weight force to ramp in origin system in point A and A'. There are also incline forces and friction forces for both of the points in y and x axes (Fig. 2).

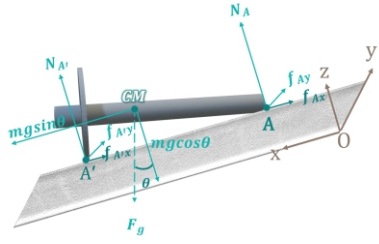

Fig. 2: Applied forces on screw

where;

- F_g = Gravity force
- $mgsin\theta$ = Parallel force to ramp
- $mgcos\theta$ = Perpendicular weight force to ramp
- $N_{A'}$ = Normal force of incline of point A'
- N_A = Normal force of incline of point A
- $f_{A'x}$ = x-axis friction of point A'
- f_{Ax} = x-axis friction of point A
- $f_{A'y}$ = y-axis friction of point A'
- f_{Ay} = y-axis friction of point A

These are some of the data that have been extracted for the further equations. The data has been divided into two individual parts for the head and the body of the screw. An important consideration is that there are three centers of mass. First the body's center of mass, second the head's and third, the whole screw's center of mass.

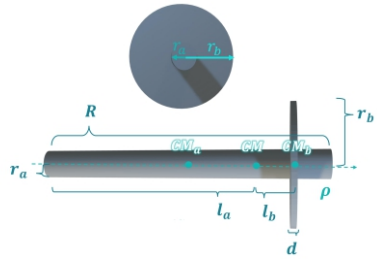

Fig. 3: Different parts divisions in screw

where;

- CM_a =The center of the body mass
- CM =The center of mass
- CM_b =The center of the head mass
- r_a =Body radius
- R =Body length
- r_b =Head radius
- d =Head thickness
- ρ =Density
- l_b = Distance between the and the CM and the head of the screw
- l_a =Distance between the CM and the bottom of the screw

For the friction magnitude of A and A' calculation, the following formula can be used (Eqs. 1, 2) (Fig. 4).

$$(N_{A'}\mu_K)^2 = {f_{A'x}}^2 + {f_{A'y}}^2 \quad (1)$$

$$(N_A\mu_K)^2 = {f_{Ax}}^2 + {f_{Ay}}^2 \quad (2)$$

where;

- $N_{A',A}$ = Normal forces
- μ_K = Coefficient of kinetic friction
- $f_{A',Ax}$ = x-axis frictions
- $f_{A',Ay}$ = y-axis frictions

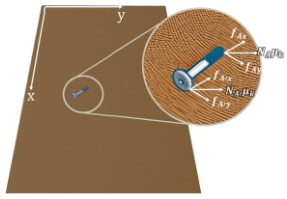

Fig. 4: Frictions applied on X-Y axes

In a perfect rolling when the screw rotates, the distance between the center of the circle that has been created from the screw's rotation and the end of the screw is constant in the whole rotation time. We call this distance x. In this phenomenon, there is a motion close to perfect rolling (Fig. 5).

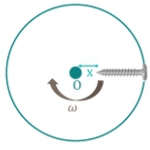

Fig. 5: Perfect rolling

The data are collected and some of the forces acting on the screw on the horizontal plane are shown in (Fig. 6).

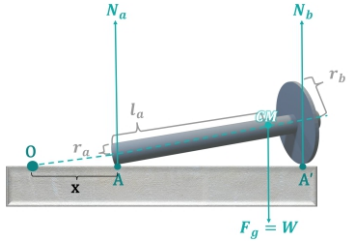

Fig. 6: Screw on horizontal plane

By placing the screw on a horizontal surface, if we continue the symmetry axis until it meets the horizontal surface, a cone is created.

Now, the screw is placed on a ramp with Theta angle. As the screw moves down and slides, a torque applies to it, which equals to the weight of the screw multiplied by the angle that the symmetry axis makes with the surface of the ramp. Actually, x is a way to reach the torque (Fig. 7).

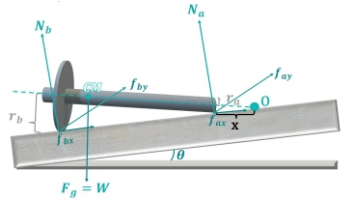

Fig. 7: Screw on a plane with Theta angle

For calculation it is simplified as a cone (Fig. 8).

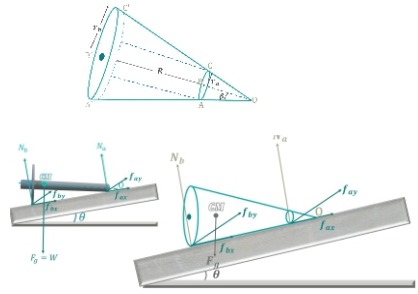

Fig. 8: Screw is considered as a cone

Frictional forces apply on 2 points on our cone. If the screw rolls on two wheels AC and A'C without slipping, the screw rotates around the point O (Fig. 9).

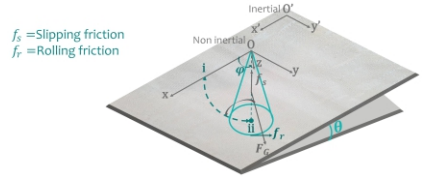

Fig. 9: Frictional forces

One time it is considered the as rolling without slipping and another time rolling with slipping. So the torque is used for the first situation and the dynamic system is studied for the second part.

The cone is of polar system type that centered around O. Because we want to investigate the situation of the symmetry axis toward the x axis, the screw has been considered in a non-inertial origin system so it can be studied as O sliding as a particle in the x' direction from O'(Figs. 10, 11)(Eq.3) .

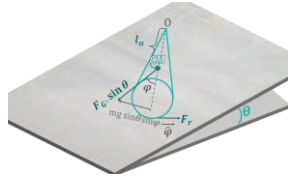

Fig. 10: Torque in the first situation

$$\begin{cases} \tau_\varphi = -F_G \sin\theta \sin\varphi\, l_a + f_r R \\ \tau_\varphi = I_\circ \ddot{\varphi} \end{cases} \Rightarrow -F_G \sin\theta \sin\varphi\, l_a + f_2 R = I_\circ \ddot{\varphi} \quad (3)$$

In rolling with sliding (Eqs. 4-6).

When the sliding is perpendicular to the x axis and k isn't constant by the rotational motion based on rolling friction and torque", coefficient of friction as a function of tangential velocity is calculated and If the φ in differential equation becomes small enough the Equations (4-8) are given (Fig. 11).

$$\vec{f_r} = kN_r\hat{\varphi} \tag{4}$$

$$k \simeq k_o + k_1 v \quad v = \text{Tangential velocity} \Rightarrow \quad v = l\dot{\varphi}$$

$$-F_G \sin\theta \sin\varphi\, l_a + f_2 R = I_\circ \ddot{\varphi} \tag{5}$$

$$\ddot{\varphi} = -A\sin\varphi + B\dot{\varphi} + C \tag{6}$$

$$-F_G \sin\theta \sin\varphi\, l_a + k_o R + k_1 R l\dot{\varphi} = I_\circ \ddot{\varphi} \tag{7}$$

$$\ddot{\varphi} \approx -A\varphi + B\dot{\varphi} + C$$
$$\Longrightarrow \varphi \approx C_1 e^{\alpha t}\sin t + C_2 \tag{8}$$

In this formula C1 and C2 are the constants and according to the screw's specific characteristics for a small angle of φ, the chart is given in Figure (11) and it happens when the oscillation angle around the x axis is between 12 and 90 degrees.

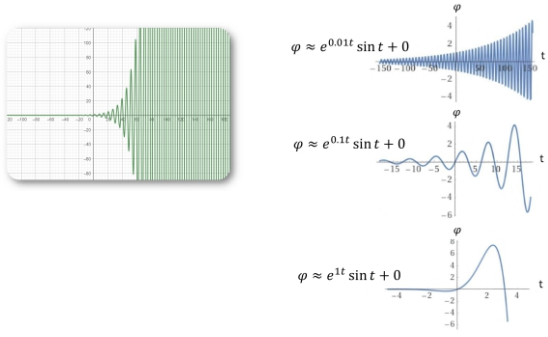

Fig. 11: the diagram of oscillation If the φ in differential equation becomes small enough

These are a part of the charts that have been obtained from the theory. This is for a case where the screw deviates to the left and right, and then when the screw becomes horizontal, it moves like an axle with two unequal wheels.

The related parameters include the friction coefficient of the ramp, the angle of the ramp(α), The angle at which we release the screw(β), The body's length(d), The mass of the head of the screw and the Radius of the washer (r).

If the φ gets bigger (Eq. 9):

$$\sin\varphi \not\approx \varphi$$
$$\ddot{\varphi} = -A\sin\varphi + B\dot{\varphi} + C \tag{9}$$
$$12° < \varphi < 90°$$

3. Experiments

Different size of the screws, the washers with different radiuses, and the holes with different sizes are the main parts of the experimental setup (Fig. 12).

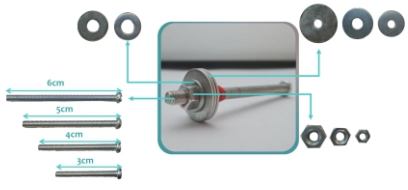

Fig. 12: Experimental setup

By increasing the friction coefficient of the ramp while the number of oscillations increases, the oscillations amplitude decreases.

When the angle of the ramp decreases, the number of oscillations increases, but the oscillations amplitude decreases.

The angle of releasing the screw is one of the other parameters. By increasing this angle, it has been observed that the number of oscillations decreases, but the oscillations amplitude increases (Figs. 13a and b).

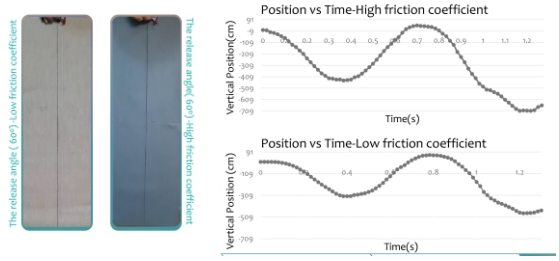

(a)

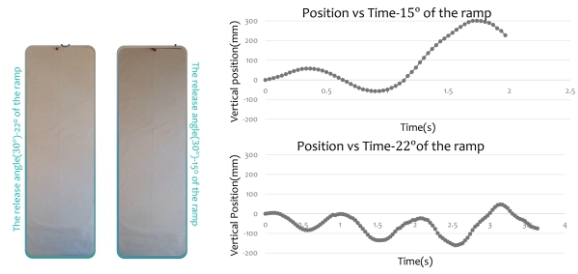

(b)

Fig. 13: a) the role of friction , b) the angle of ramp

The angle of releasing the screw is one of the other parameters. By increasing this angle, it has been observed that the number of oscillations decreases, but the oscillations amplitude increases (Fig. 14).

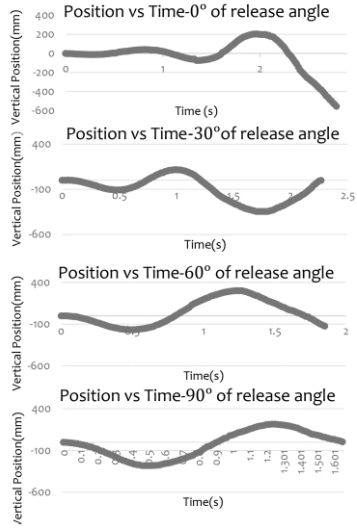

Fig. 14: The angle of releasing the screw

Changes in the screw's body's length have been investigated as well. By decreasing the body's length, the number of oscillations increases (Fig. 15).

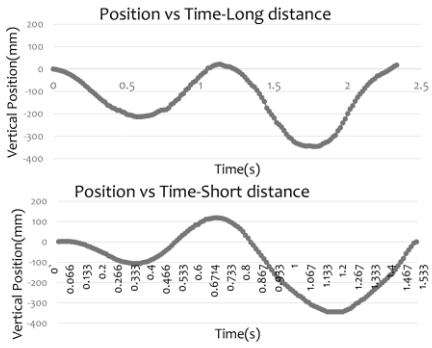

Fig. 15: The effect of body length

We've done experiments with different sizes of radius. As it can be observed , the oscillation amplitude in the screw with a smaller radius is higher than the oscillation amplitude in the screw with a bigger radius (Fig. 16).

Also by changing the mass of the head of the screw, the number of oscillations decreases, but the oscillations amplitude increases (Fig. 17).

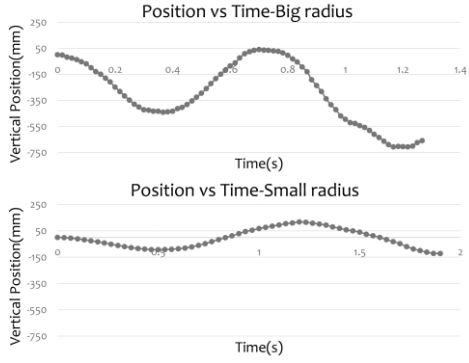

Fig. 16: Different radiuses of the washers

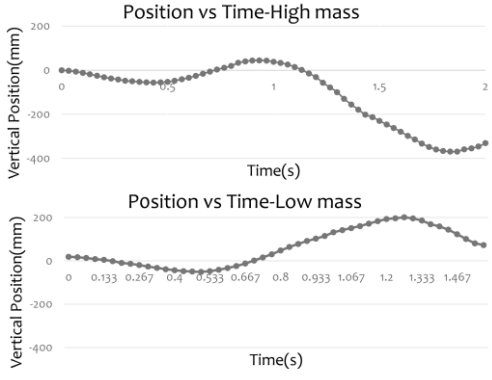

Fig. 17: Different masses of the head

4. Results

By comparing the charts obtained from the experiment and theory, it can be seen that they fit well together. If some part of it doesn't fit the chart obtained from the theory means various reasons may cause errors, including surface friction that occurs due to the non-uniformity of the surface.

Different parameters have been investigated in our theory and experiment to find the main reason of the screw oscillation in a plane in different angles.

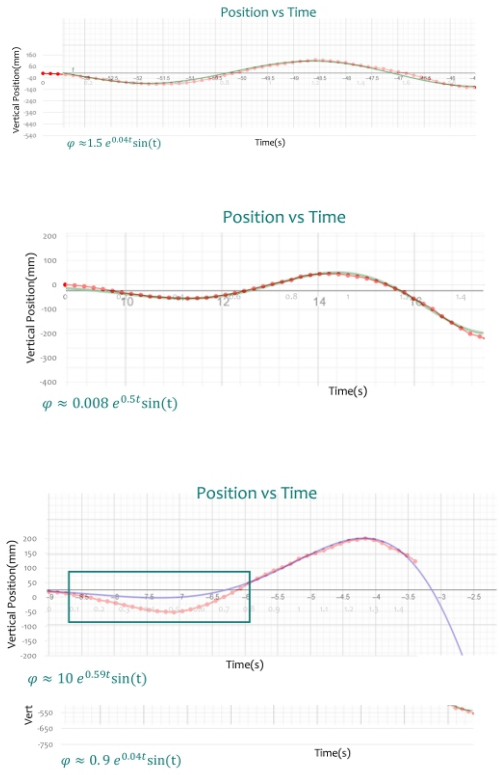

Fig. 18: Comparison between Theory and Experiments

5. Conclusions

1. By decreasing the friction coefficient of the ramp while the number of oscillations decreases, the oscillation amplitude increases.
2. By increasing the angle of the ramp, the number of oscillations decreases, but the oscillations amplitude increases.
3. By decreasing the release angle, the number of oscillations increases, but the oscillations amplitude decreases.
4. By increasing the body's length, the number of oscillations decreases, but the oscillations amplitude increases.
5. By decreasing the mass of the head, the oscillation amplitude decreases.
6. By increasing the radius of washer, the oscillation amplitude increases.

References

[1] Cross R 2022 Pendulum motion on an inclined plane Phys. Educ. 57 055012

[2] https://physics.stackexchange.com/questions/753918/back-and-forth-oscillation-of-a-screw

The Effect of Ammonia on Flowers with Anthocyanin Pigment

Niki Abtahi ; Valeh cultural and educational institute , nikabt2007@gmail.com

ARTICLE INFO

Gold medalist in ISAC Olympiad 2023 (Junior)

Awarded by Ariaian Young Innovative

Minds Institute , AYIMI

http://www.ayimi.org ,info@ayimi.org

ABSTRACT

Anthocyanins are a group of pigments found in flowers, fruits and vegetables, and it is an unstable combination which changes color under the influence of factors such as pH, temperature and other parameters. In this research the tests were designed based on the hypothesis and the results show the change in color of flowers with anthocyanin pigment due to alkaline environment which is more than acidic environment and their color are wither when placed in ammonia gas environment.

Keywords : *: Anthocyanin, Alkaline, Environment, Color*

1. Introduction

Anthocyanins are secondary metabolites and water-soluble pigments belonging to the phenolic group, with important functions in nature such as seed dispersal, pollination and development of plant organs. In addition to these important roles in plant life, anthocyanins are also used as natural pigments in various industries, due to the color palette they can produce from red to blue and purple. In addition, recent research has reported that anthocyanins have important antioxidant, anticancer, anti-inflammatory and antimicrobial properties, which can be used in the chemoprevention of various diseases such as diabetes, obesity and even cancer. However, anthocyanins have a major disadvantage, namely their low stability. Thus, their stability is influenced by a number of factors such as pH, light, temperature, co-pigmentation, sulfites, ascorbic acid, oxygen and enzymes. It is very important to be precisely aware of the impact that each parameter has on the stability of anthocyanins, in order to minimize their negative action and subsequently potentiate their beneficial health effects.

Anthocyanins are a class of natural water-soluble pigments that are part of the flavonoid family. They are very widespread in nature, found not only in the colored petals of flowers but also in the roots, stems, tubers, leaves, fruits and seeds . This type of pigment has a strong absorption in the UV-visible region of the electromagnetic spectrum and is the main determinant of red-blue colors and their derivatives in the plant kingdom. These characteristics place them second in importance, immediately following chlorophyll pigments. Anthocyanins play an important role in seed dispersal, pollination, development of plant organs, but also in their adaptation to various changes in biotic (pathogenic attacks) and abiotic (drought, lack of nutrients, high intensity light) factors. Due to their chemical structure, with a central core in the form of 2-phenylbenzopyrylium or flavylium cation, anthocyanins can be classified as polyphenols and secondary metabolites .

When the viola flower is exposed to ammonia, it changes color and withers, during this phenomenon, chemical and biological reactions occur, which are fully explained in this issue . It was assumed that this phenomenon occurs duo to osmotic swelling and cell tissue destruction as a biological process and PH changing as a chemical change . pH, of the acidity or basicity of aqueous or other liquid solutions, was investigated as one of the cases in this experiment. Denaturation involves the breaking of many of the weak linkages, or bonds (e.g., hydrogen bonds), within a protein molecule that are responsible for the highly ordered structure of the protein in its natural state. It is one of the biological processes that happened in this experiment for flowers due to the ammonia gas. Deprotonation is the removal of a proton (hydrogen ion) from a molecule to form a conjugate base and in biological molecule means the loss of its three-dimensional structure. It happens in the process of changing the color of anthocyanins. There are three type of denaturation :

1. Denaturation by changing pH
2. Chemical Denaturation
3. Denaturation with heat or radiation

Denaturation by changing pH

Changes in the pH of the environment affect the total molecular charge, the interaction of amino acids with each other and the three-dimensional structure of the protein which happens in this experiment (Fig. 1).

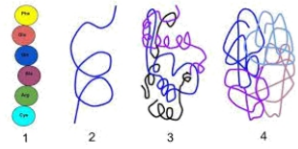

Fig .1 : Denaturation- biology dictionary, https://biologydictionary.net/denature/

Cell swelling can have several effects: Organelles in the cell may become compressed if cell swelling becomes severe. Changes in cell pH can lead to the degradation of internal cellular organs. In this experiment, it happens due to the exposure to ammonia gas for the flower and causes the flower to be wither which changes the PH .

2. Materials and Methods

To test different viola flower – carnation flower – rose flower – miniature rose flower – petunia -ammonia(NH3) – vinegar – beaker – graduated cylinder- test chamber are used.

Test 1 and 2 were designed and conducted to investigate the effect of pH change on anthocyanins. Test 3 and 4 were designed and carried out to investigate the effect of ammonia on viola flower and its effect on other plant species.

3. Experiments

Test 1 :

1. Two types of flowers that have anthocyanin pigment (miniature rose and petunia) were exposed to 20 ml of vinegar with pH :3.
2. Observations were made to check the color change.
3. The final results were recorded (Fig. 2).

Fig. 2: The result of Test 1

Test 2 :

1. Two types of flowers that have anthocyanin pigment (miniature rose and petunia) were exposed to 20 ml of ammonia with pH: 3.
2. Observations were made to check the color change.
3. The final results were recorded (Fig. 3).

Fig. 3: The result of Test 2

Test 3 :

1. 15 ml of ammonia was poured into the beaker.
2. Then it was placed under the test chamber.
3. Viola flower was exposed to ammonia gas for 2.5 hours.
4. Then the results were recorded.

Test 4 :

1. 15 ml of ammonia was poured into the beaker.
2. Then it was placed under the test chamber.
3. Roses and carnations were exposed to ammonia gas for 7 and 5 hours, respectively.
4. Then the results were recorded.

4. Results

Test 1 : Investigating the effect of acidic substances on anthocyanins by exposing miniature petunia and rose to vinegar (Fig. 4).

The procedure:

1) Exposure to vinegar
2) Start of changing in color
3)Fading and changing in color happen

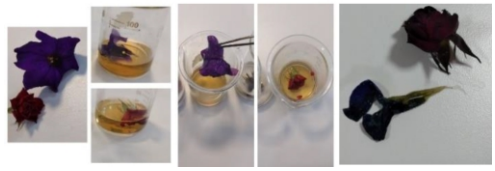

(1) (2) (3)

Fig. 4 : Data from Test 1

Test 2: 1 Investigating the effect of alkaline substances on anthocyanin by exposing petunias and miniature roses to ammonia.

The procedure:

1) Exposure to ammonia
2) Start of changing in color
3)Fading and changing in color happen (Fig. 5)

(1) (2) (3)

Fig. 5 : Data from Test 2

Test 3: Investigating the effect of ammonia on viola flowers by exposing viola flowers to ammonia gas.

The Procedure:

1) Exposure to ammonia
2) Start of changing in color
Change from purple to yellow
3)Fading and changing color to dark yellow and brown (Fig. 6).

(1) (2) (3)

Fig. 6 : Data from Test 3

Test 4 : Investigating the effect of ammonia on other plant species by exposing roses and cloves to ammonia gas.

The procedure

1) Exposure to ammonia
2) Changing the color of carnation and rose to dark brown and black respectively
3) Final color , withering of rose and carnation and changing the color of rose to black and carnation to dark yellow (Fig. 7).

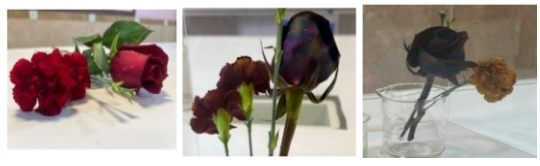

Fig. 7 : Data from Test 4

5. Data Analysis

The color changes observed in the experiments are shown as follows:

Anthocyanin color changes in alkaline environment faster than in acidic environment.

About 80% of the cell space is the vacuole of the cell

has an acidic atmosphere.

Ammonia is an alkaline substance; ammonia gas molecules are the same size as air molecules, they can easily penetrate the cell and when combined with the acidic atmosphere of the cell, it changes the pH of the cell.

The change in pH of the cell due to exposure to ammonia gas, the anthocyanin present in the flower changes color and causes the color of the flower to change. As mentioned in the theories, denaturation is a process during which the proteins of the cell were changed and various reasons such as changing the pH of the cell are among the reasons for this phenomenon. In this test, due to the change in the pH of the cell, denaturation occurs in the cell and affects the proteins and nucleic acids, causing the plant cells to no longer have the ability to perform their activities.

When ammonia gas enters the cell and combines with the water inside the vacuole, it causes the production of ammonium ions and hydroxide, and the production of these ions causes the destruction of cellular tissue and disrupts cellular respiration, causing the flower to wither and lose its freshness.

6. Results and Discussion

Ammonia has chemical and biological effects on flowers, causing discoloration and wilting of flowers.

A) Chemical :

1- PH changes in cell

2- Ammonium and hydroxide production by ammonia and water reaction

B) Biological : as a result of chemical process

1- Osmotic swelling

2- Disrupting the basic hydrogen bonding of DNA (denaturation) that cause Blocking oxygen transmission and breathing

Ammonia is one of the gases in air pollution.

The largest amount of ammonia is produced by agriculture globally and nationally from sources such as animal manure, but vehicles with internal combustion engines also contribute to ammonia emissions because their catalytic converters reduce nitrogen oxides and create ammonia.

This ammonia gas can cause the problems mentioned in the laboratory simulation test and in the long run it can cause the loss of vegetation.

Acknowledgments

I would like to thank Mr. Mohammad Arjamand and Mr. Homan Gharibzadeh for their valuable guidance and support in this project.

References

[1] Bianca Enaru, Georgiana Drețcanu, Teodora Daria Pop, Andreea Stănilă, and Zorița Diaconeasa, "Anthocyanins: Factors Affecting Their Stability and Degradation", Antioxidants (Basel). 2021 Dec; 10(12):1967 Published online 2021 Dec 9. doi: 10.3390/antiox10121967

[2] Britannica, The Editors of Encyclopaedia. "pH". Encyclopedia Britannica, 3 Jul. 2023, https://www.britannica.com/science/pH. Accessed 5 October 2023

.

[3] Britannica, The Editors of Encyclopaedia. "denaturation". Encyclopedia Britannica, 28 Feb. 2023, https://www.britannica.com/science/denaturation. Accessed 5 October 2023.

[4] Annual Record of Science and Industry, Volume 6 -page 356

[5] Popular Science - Jun 1875- page 256

[6] Biologydictionary.net Editors. "Denature." Biology Dictionary, Biologydictionary.net, 18 Dec. 2016, https://biologydictionary.net/denature/.

[7] J. Chem. Educ. 2019, 96, 9, 1982–1987,Publication Date:June 19, 2019, https://doi.org/10.1021/acs.jchemed.9b00001

[8] LOYD, D. The pH Stability Region of Proteins and Osmotic Swelling. Nature 130, 24–25 (1932). https://doi.org/10.1038/130024c0

[9] Study.com ,Hydropic Degeneration and Cell Swelling https://study.com/learn/lesson/hydropic-degeneration-causessignificance.html#:~:text=Cell%20swelling%20can%20have%20several,degradation%20of%20internal%20cellular%20organs.

The Effect of Different Jumping Techniques with Starting Positions on Its Maximum Height

Sarina Nosrati ; Valeh cultural and educational institute , sarina.n1386@gmail.com

ARTICLE INFO

Gold medalist in ISAC Olympiad 2023 (Junior)

Awarded by Ariaian Young Innovative

Minds Institute , AYIMI

http://www.ayimi.org ,info@ayimi.org

ABSTRACT

Today there are many types of jumping in the world. The main reason for jumping is the conversion of potential energy stored in the legs into kinetic energy, which are the main theories of this problem.The test that was considered for this problem was different jumping techniques in different starting points which states if a person uses more forces in both hands and feet will have the highest height, and the position that causes more potential energy to be stored in the legs, causes more height in the jump because more potential energy is converted into kinetic energy.

Keywords : *: Jumping, Kinetic Energy, Height, Techniques*

1. Introduction

A person can jump with straight legs, which is called vertical jump. Actually vertical jump or vertical leap is the act of jumping upwards into the air. The types of vertical jump have different heights and the amount of differences may be small or large.

In general, what happens in this movement is related to the elastic potential energy. When a person wants to jump, he/she first sits on his knees. When a person sits, the muscles are contracted or compressed. This can happen in some objects or even body parts, which are examples of compression. When the legs contract, energy is stored in the legs, which is called elastic potential energy and is effective in the strength and height of a person's jump.

In the next stage, when the person's knees are straightened then jumps up, the stored elastic potential energy in the legs is converted into kinetic energy. The more a person sits on his knees, the more muscles and legs are compressed, as a result, more elastic potential energy is stored in the legs and more energy is converted into kinetic energy which makes jumping higher.

This is like a spring that when it is compressed, elastic potential energy is stored in it. After the spring is released, the spring intends to return to its previous state, so it jumps. The higher the compression, the higher the spring jump.

2. Categories and Characteristics in Different Jumps

The jump height depends on factors that are generally divided into two categories :

- Characteristics of the person such as a person's height, BMI , physical strength, weight ,etc.

-Type of the jump and the starting position which this category itself is divided into two groups as follows:

2-1. The Technique of Jumping

Different techniques are basically the types of jumps that are known in the world, such as :

2-1-1. Countermovement Jump

The vertical jump test is usually performed with a countermovement, where the knees are bent immediately before the jump . Taking help from the arms can help the height of jumping

2-1-2. Squat Jump

It is a body weight exercise characterized by jumping straight up at the top of the movement. It is basically adding a jump to the squat.

2-1-3. Triple Jump

A jumping which a participant leaps on one foot from a take off point, lands on the same foot, steps forward on the other foot .

2-1-4. Long jump

A jump in which a person jumps forward and focuses on length.

2-2. Starting Position

The position of a person in start point of a movement is called the starting position. In this factor, the technique does not make any difference and the starting position is different. Jumps are associated with sitting, and the starting position of the sitting position is the angle of the knee.

Knee's angle is generally divided into 3 angles :

1. Sharp that is less than 90 degree
2. Right that is 90 degree
3. Open that is more than 90 degree

In this issue, the effect of different jumping techniques and different starting positions on the maximum jump height will be investigated. It means that the influence of individual characteristics is not involved and the best method and situation for the highest height should be determined.

3. Materials and Methods

Materials :

1. Meter
2. Sport mat
3. Jogging suit

Method :

Investigating the influence of starting postures and jumping techniques on the maximum height of the jump

Test A) Based on the technique

For this test 4 experiments have been conducted.

1. Testing countermovement jump

2. Testing squat jump
3. Testing triple jump
4. Testing long jump

Test B) Based on the starting positions

For this test 2 techniques with 3 position (6 experiment) have been conducted to confirm correctness.

1. Testing countemovement jump by sitting at a sharp degree
2. Testing countermovement jump by sitting at a right degree
3. Testing countermovement jump by sitting at a open degree
4. Testing squat jump by sitting at a sharp degree
5. Testing squat jump by sitting at a right degree
6. Testing squat jump by sitting at a open degree

3. Experiments

Test A part 1 (Fig. 1) :

Fig. 1: Countermovement jump and measuring the height

Test A part 2 (Fig. 2):

Fig. 2: Squat jump and measuring the height

Test A part 3 (Fig. 3) :

Fig. 3: Triple jump and measuring the height

Test A part 4 (Fig. 4):

Fig. 4: Long jump and measuring the height

The heights in different techniques in test A are compared in Figure (5).

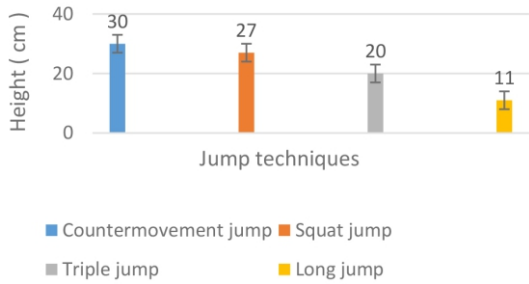

Fig. 5: Heights in different techniques in Test A

Test B part 1 (Fig. 6):

Fig. 6: countermovement jump by sitting at a sharp degree and measuring the height

Test B part 2 (Fig. 7) :

(Fig. 7): Countermovement jump by sitting at a right degree and measuring the height

Test B part 3 (Fig. 8):

Fig. 8: Countermovement jump by sitting at a open degree and measuring the height

Test B part 4 (Fig. 9):

Fig. 9: Squat jump by sitting at a sharp degree and measuring the height

Test B part 5 (Fig. 10):

Fig. 10: Squat jump by sitting at a right degree and measuring the height

Test B part 6 (Fig. 11) :

Fig. 11: Squat jump by sitting at a open degree and measuring the height

The heights in different techniques in test B are compared in Figure (12).

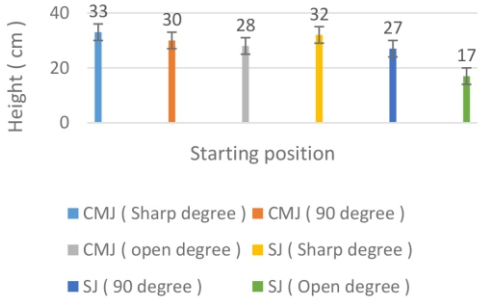

Fig. 12: Heights in different techniques in Test B

4. Results and Discussion

The height of jumps based on techniques in two test are compared as follows:

CMJ > SJ > Triple jump > Long jump

In countermovement jump, the person bends the knees before jumping to receive energy. It also takes help from the hands for more power, for this reason, the highest jump height belongs to the countermovement jump.

In the squat jump, there is an initial bending of the knees, but the hands are facing the face when the knee is sitting, and when the person jumps, the hands are at the side of the body. That is, the strength of the hands does not contribute much to the height of the jump. For this reason, it has a lower height than the countermovement jump.

In the triple jump and long jump, the focus is on the length of the jump and not on the height of the jump. For this reason, these two jumps have a lower height than countermovement jump and squat jump.

The difference between the triple jump and the long jump:

In the triple jump, as the name suggests, it has three steps, the steps before the jump increases to the person's jumping power. (A participant leaps on one foot from a takeoff point, lands on the same foot, steps forward on the other foot).But in long jump, a person does not take a step to receive power and jumps with two feet. For this reason, the jump height is three steps higher than the long jump.

Comparison of the height of jumps based on starting positions :

Countermovement jump :

Sharp degree > Right degree > Open degree

Squat jump :

Sharp degree > Right degree > Open degree

More sitting on knees = More height on jump

As mentioned, one of the effective factors in jumping height is the amount of initial sitting on the knees so that the more a person sits, the more kinetic energy increases and the jumping height increases.

Test B was investigated by two techniques and in three modes. In the test where the amount of sitting was higher, more potential energy was stored in the legs and the person performed the jump with more strength to be able to jump higher.

But in the other two tests, when the amount of sitting decreased gradually, the stored energy and the height of the person's jump also decreased gradually.

This result was the same for both types of jumps (countermovement jump, squat jump).

The highest jump height is related to countermovement jump with the highest sitting on the knee. Because in this technique, in addition to sitting on the knees, the energy of the hand is also used, and with more sitting, the person will have more energy.

References

[1] Topend sports , counter movement jump https://www.topendsports.com/testing/vertical-jump-technique.htm

[2] Garage Strength youtube channel , Vertical jump https://youtu.be/GozaG81Fquk

[3] MasterClass | Articles , Squat jump https://www.masterclass.com/articles/jump-squats-guide

[4] BYJU'S , Elastic potential energy https://byjus.com/elastic-potential-energy-formula/#:~:text=Elastic%20potential%20energy%20is%20the,k%20and%20the%20distance%20stretched.

[5] Third Space London , Counter movement jump https://youtu.be/09yR5a4u-6A

[6] Track football consortium, counter movement jump photo https://www.google.com/url?sa=i&url=https%3A%2F%2Ftrackfootballconsortium.com%2Fcountermovement-and-squat-jump

[7] Front . Physiol ., 17 march 2020, countermovement jump https://doi.org/10.3389/fphys.2020.00231

[8] Science for sport , Article , Owen Walker , August 25th , 2023 , squat jump https://www.scienceforsport.com/squat-jump/

[9] The evolution of high jumping technique , Article , Jesus Dapena https://ojs.ub.uni-konstanz.de/cpa/article/view/657/580

[10] Researchgate , Article , training methods to improve vertical jump performance , Jorge Perez-Gomez , Jose A Calbet https://www.researchgate.net/profile/Jose-Calbet-

How Does a Magnetic Field Affect the Oscillation of a Suspended Sphere

Sogand Radka , Iran Alghadir School , Tehran / Iran, s.radka8506@gmail.com

ARTICLE INFO

Silver medalist in ISAC Olympiad 2023 and

Bronze medalist in IGO 2023 UK

Awarded by Ariaian Young Innovative

Minds Institute , AYIMI

http://www.ayimi.org ,info@ayimi.org

ABSTRACT

To understand the dynamics of moving objects through the Earth's magnetic field, a light sphere with a conducting surface is suspended from a thin wire which is rotating about its vertical axis in a magnetic field. This work is studying the oscillation of either hollow or solid sphere with a conducting surface when is rotated about its vertical axis (thereby twisting the wire) and then released in the presence of a magnetic field. To investigate how the presence of a magnetic field affects the motion the most detailed and analysis was carried out and the produced drag torque felt by the sphere as a result of the charge redistributions and currents was studied.

Keywords : *: Magnetic Field, Oscillation, Light Sphere, Torque*

1. Introduction

The interaction of a constant magnetic field with a moving extended conductor is an important area of study with applications to linear induction motors, eddy current braking, and levitation. The interaction of a constant magnetic field with a moving conductor sphere makes forces which are exerted on the electrons in the sphere. These electrons generate a non-uniform charge density and electric fields with eddy currents. To find the currents, rotating of a hollow sphere about a perpendicular axis with an applied uniform magnetic field, is studied. By moving the sphere through the magnetic field or when the magnetic field surrounding a stationary conductor is varying, it results in the conductor experiencing a change in the intensity of a magnetic field which produce eddy currents.

2. Materials and Theory

Both solid and hollow sphere will have a radius given by (R) , total mass (M), moment of inertia (I) and angular frequency around the z-axi (ω). The rotation of the sphere in a magnetic field which is produced by Helmholtz coil, makes current around the axis of rotation. The total magnetic field of Helmholtz Coil (Fig.1) is given by (Eq.1).

$$B_t = \frac{\mu_0 NIR^2}{2}\left\{\frac{1}{\left[R^2+\left(z-\frac{R}{2}\right)^2\right]^{3/2}}+\frac{1}{\left[R^2+\left(z+\frac{R}{2}\right)^2\right]^{3/2}}\right\} \quad (1)$$

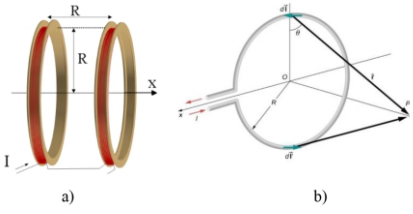

Fig. 1: a) Helmholtz Coil, b) Magnetic field of a loop

Since the sphere is rotating through a magnetic field according to the Lorentz law, it generates forces on the charges in the sphere which is conductive and neutral, the electrons can move and this can result in charge redistribution and possible currents.

The total velocity of the electrons, *Vt,* due to the velocity of sphere, $\acute{V}$, is given by (Eqs. 2, 3).

$$\mathcal{V}_t = \mathcal{V}\, sin(\theta_1.\theta_2) \quad (2)$$

$$\mathcal{V}_t = \frac{L\, sin(\theta_1.\theta_2)\,\acute{\mathcal{V}}}{R} \quad (3)$$

The sphere is a 3D object so we will put it in a spherical coordinate system (Fig. 2), where each of the electrons will have a distance from the source point as L:

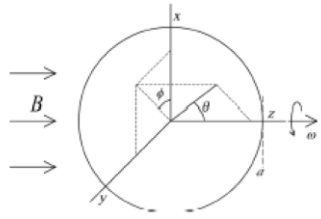

Fig. 2: Modeling of the rotating hollow sphere when the rotation axis is parallel with the uniform magnetic field

$\vec{L}$={$L\sin\theta_1 . \cos\theta_2, L\sin\theta_1 . \sin\theta_2, L\cos\theta_1$}

Then the velocity of any point is (Eq. 4).

$$\mathrm{v} = \vec{\omega} \times \vec{L} \quad (4)$$

Another parameter is the magnetic force which is applied to the sphere from a uniform field parallel to rotation (Eq. 5).

$$\mathrm{F_m} = \omega\overrightarrow{\mathrm{LB}} = \frac{\acute{\mathcal{V}} L\, sin(\theta_1.\theta_2)\mu_0 NIR^2}{2Rl(z^2+R^2)^{3/2}} \quad (5)$$

The eddy current is generated by the applied magnetic field interacting with the rotating conducting sphere, but it is not the total current. This eddy current generates a magnetic field within the sphere that, yields a second eddy current. Then, the second eddy current generates another magnetic field that yields a third eddy current, and, this third eddy current is of the same form as the first eddy current but of opposite sign. So, the third eddy current acts to cancel the eddy current, yielding a negative feedback

loop.

The interaction between the current that generated the applied field and the currents inside of the sphere yields equal and opposite forces, but one acts on the sphere and the other on the coil or the magnet that generated the applied field.

The torque by hanging a hollow conducting sphere by a thin wire and measuring the decay in the amplitude of its torsional oscillations yields (Eq.6).

$$\tau = I\dot{\omega} = -K\theta \tag{6}$$

where $\dot{\omega}$ is the time derivative of the angular velocity, K is the torsion constant of the wire, and θ is the rotation angle of the sphere. There are two resistances, one due to the frictional loss and the other one is magnetic drag, which make the angular velocity of the sphere to be equal as analyses (7).

$$\ddot{\omega} = -\left(\frac{1}{\alpha}+\frac{1}{\gamma}\right)\dot{\omega} - \frac{K}{I}\omega \tag{7}$$

which

α: *Magnetic damping*

γ: *frictional damping*

I: *moment of inertia*

$\dot{\omega}$: *Time derivative of the angular velocity*

K: *Torsion constant of the thread/wire*

ω:*Angular frequency*

While our frictional and magnetic losses are small, equation of sphere oscillation will be (Eqs. 8-9).

$$T=2\pi\sqrt{I/K} \tag{8}$$

$$exp\left[-\frac{t}{2}\left(\frac{1}{\alpha}+\frac{1}{\gamma}\right)\right] = exp\left(-\frac{t}{\delta}\right) \tag{9}$$

where

δ: *Total decay time*

The total decay time can be found by measuring the decay in the oscillation of hanging hollow sphere without a magnetic field, which gives the frictional damping term γ and then by the magnetic field, δ is found.

3. Experiments

We provided two coils with 600 turns per coil and 8.5 Ω and 1200 turns per coil and 35 Ω, power supply, hollow and solid spheres and wire as in Fig. 3. The current through the coils generates a magnetic field measured by a Gauss-meter.We hung hollow and solid aluminum sphere in the center of the coils by a steel wire with a length of about 0.5 m.

Fig. 3: Experimental setup

In our experiments different spheres, hollow and slid, with different mass have been investigated to get relevant parameters by comparing the frequency of their rotations and oscillations. The spheres hang at different distances from the coils and the results are compared with each other.

To track the oscillation of the spheres we used tracker and the plots are recorded in different positions (Figs. 4- 6).

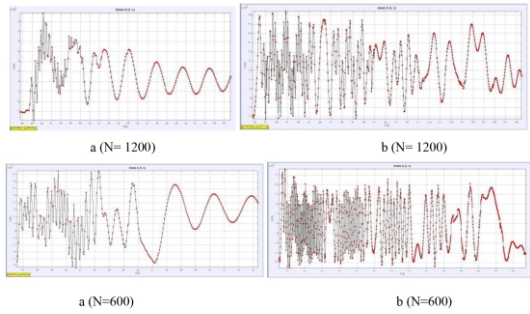

Fig. 4: 9 centimeters distance between the coils, a) hollow sphere, b) solid sphere

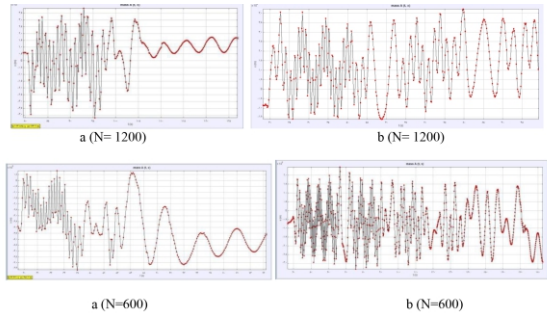

Fig. 5: 13 centimeters distance between the coils, a) hollow sphere; b) solid sphere

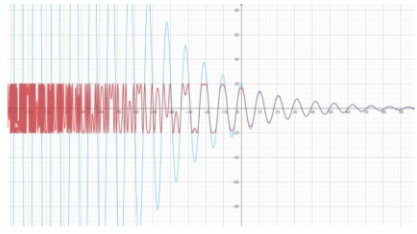

Fig. 6: Comparing the results of solid and hollow spheres

4. Conclusions

Our experiments were performed to examine the forces, torques, and magnetic field interactions with hollow and solid sphere when it starts to slowly oscillate in an applied magnetic field. Finally, the results show in hollow sphere and less distance between coils with more magnetic field and more elasticity of wire the speed of oscillation is more and it stops earlier.

References

[1] Robert C. Youngquist, Mark A. Nurge, and Stanley O. StarrFrederick A. LeveMason Peck. (2016), "A slowly rotating hollow sphere in a magnetic field: First steps to de-spin a space object", Citation: Am. J. Phys. 84, doi: 10.1119/1.4936633

[2] Mark A. Nurge, Robert C. Youngquist, and Stanley O. Starr, (2018), " Drag and lift forces between a rotating conductive sphere and a cylindrical magnet",Citation: American Journal of Physics 86, 443 doi: 10.1119/1.5024220

[3] http://ntrs.nasa.gov/archive/nasa /casi.ntrs.nasa.gov/19630002720.pdf

[4] http://adsabs.harvard.edu/full/1977IrAJ...13....1W

Geometry and Dynamics of the Fractal Fingers

Negar Sharifi, Tehran / Iran, sharifinegar498@gmail.com

ARTICLE INFO

Bronze medalist in IGO 2023UK

Awarded by Ariaian Young Innovative

Minds Institute , AYIMI

http://www.ayimi.org ,info@ayimi.org

ABSTRACT

Fractal fingering is a phenomenon that occurs when a droplet of an ink-alcohol mixture is deposited onto diluted acrylic paint. This effect characterized by the formation of intricate, branching patterns that resemble fractal. The geometry and dynamics of these fingers are influenced by several parameters, including the viscosity and surface tension of the fluids, as well as the concentration and composition of the ink-alcohol mixture. In this paper, we investigate the effect of these parameters on the formation and evolution of fractal fingers in order to gain a better understanding of this fascinating phenomenon.

Keywords : *: Fractal , Acrylic, fluid, , Ink Alcohol mixture*

1. Introduction

Fractal fingering is a phenomenon that can be observed in many different contexts, from the formation of river deltas to the growth of crystals. The geometry and dynamics of the fingers that form during this process are influenced by a number of relevant parameters, including the viscosity and surface tension of the fluids involved, as well as the rate at which they are mixed.

One important factor that affects fractal fingering is the viscosity of the fluids involved. When two fluids with different viscosities come into contact, they tend to mix in a way that creates complex patterns. In the case of fractal fingering, this mixing result in the formation of thin, branching fingers that extend outwards from the droplet.

Another important parameter is surface tension. When two fluids with different surface tension come into contact, they tend to form patterns that reflect relative strengths. In the case of fractal fingering, this can result in complex patterns that resemble tree branches or lightning bolts. The rate at which the fluids are mixed also plays a role in determining the geometry and dynamics of fractal fingers. If one fluid is added slowly to another, for example, it may be possible to observe more intricate patterns than if both fluids are mixed quickly.

Overall, understanding how fractal fingering works requires a deep understanding of fluid dynamics and interfacial phenomenon. By studying these processes in detail, physicist can gain insights into how complex patterns emerge from seemingly simple interactions between fluids. This knowledge has applications in fields ranging from materials science to environmental engineering, and could ultimately help us better understand and control natural phenomena like river deltas or crystal growth.

2. Materials and Methods

Ink as a solvent, soluble alcohol and diluted acrylic are used in this research to investigate the behavior of fractal. Their required properties are listed in Tables 1, 2, and 3.

We considered diluted acrylic as a fluid with a higher viscosity in a glass plate as a base fluid and drop a droplet of ink-alcohol mixture and investigated the behavior of the fractal. No external pressure gradients or injections were applied to drive the flow. All experiments were conducted at ambient temperatures. A camera (Canon EOS 800D) was used to capture fractal behavior directly. They were recorded at 60/50 fps.

Table 1: Ink- Alcohol different concentration viscosity

Alcohol(ml)	4.5(25%)	9(50%)	13.5(75%)	16.2(90%)
Ink(ml)	13.5(75%)	9(50%)	4.5(25%)	1.8(10%)
Viscosity(pa.s)	0.003475	0.002517	0.001885	0.001582

Table 2: Diluted acrylic viscosity

Acrylic(ml)	16.2(90%)	13.5(75%)	9(50%)	4.5(25%)
Water(ml)	1.8(10%)	4.5(25%)	9(50%)	13.5(75%)
Viscosity(pa.s)	0.248936	0.121658	0.06090	0.013591

Table 3: Diluted acrylic surface tension

Acrylic(ml)	16.2(90%)	13.5(75%)	9(50%)	4.5(25%)
Water(ml)	1.8(10%)	4.5(25%)	9(50%)	13.5(75%)
Viscosity(N/m)	-	0.0035	0.02	0.0067

3. Experiments and Results

3.1. Spontaneous Three-Stage Mixing

The results obtained from repeated experiments show that the formation of fractal consists of three separate phases.

After the drop of alcohol-alcohol hits the diluted acrylic surface, the first phase occurs; In this phase, the ink-alcohol begins to diffuse on the diluted acrylic surface and after that the second phase begins; In the second phase, fractal shapes begin to form. Shapes like tree branches, each of which divides into two branches that are half of the previous one, and they compete with each other to divide more. In the third phase, which lasts longer than the

the previous phases, the formed fractal patterns diffuse and dissolve after a long time, and we will not have a fractal pattern anymore.

3.2. Dependence on Ink-Alcohol Composition

The degree of fractal fingering, was found to be related to the composition of the ink-alcohol. By using different compositions of alcohol-ink in our experiments, we found out that when we change the percentage of our mixture, their physical properties change, especially the viscosity (Fig.1), which affects this phenomenon, and finally, the change in viscosity affects the shape and the way fractal are formed. The effect of ink-alcohol viscosity is as follows:

With the increase of alcohol in our mixture, its viscosity also decreases; By testing different percentages of alcohol and ink, we can conclude that the higher the amount of alcohol (at constant surface tension), the finer and narrower the fractal will be. (Figs.2 and 3).

3.3. Dependence on Diluted Acrylic Composition

Almost like the previous part, by changing the composition of diluted acrylic, its physical properties change. The physical properties that affect the phenomenon of diluted acrylic are surface tension and viscosity. As mentioned before, with the increase in viscosity (Fig.4), the fractal becomes smaller and narrower; But when we consider the ink-alcohol mixture constant and work with it on different diluted acrylic compositions, the result will be that with the increase in surface tension (which occurs due to the increase in water), the fractal in a constant percentage of Ink-alcohol becomes wider. (Figs. 5 and 6).

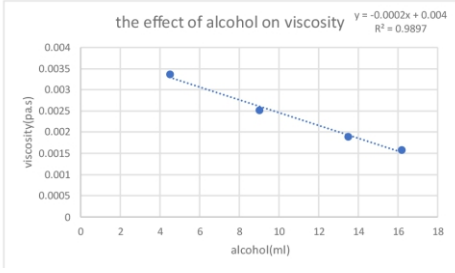

Fig. 1: The effect of alcohol on viscosity

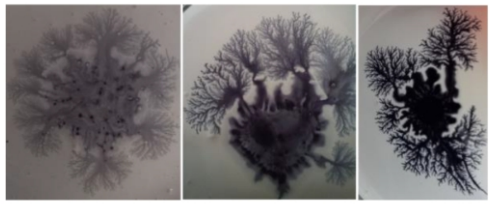

Fig. 2: Different compositions of alcohol on constants surface tension of 25% water

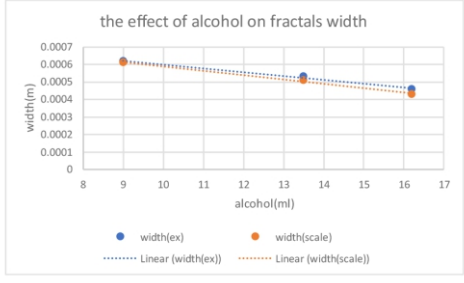

Fig. 3: The effect of alcohol on fractal width

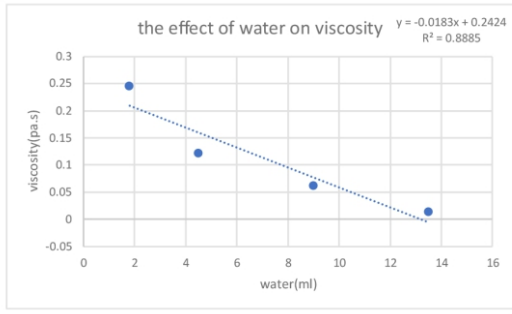

Fig. 4: The effect of water on viscosity

Fig. 5: Considering the constant of ink-alcohol compositions and the increase of surface tension, we see that the width of the fractal has become wider

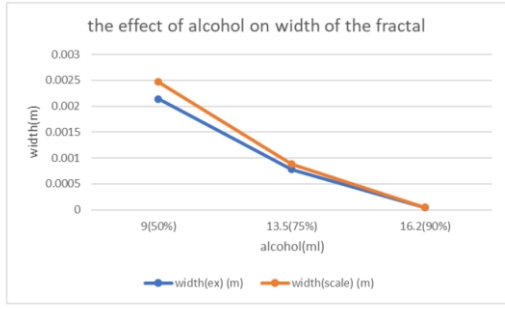

Fig. 6: By increasing the surface tension and testing the same compositions as before, it can be found that the width of the fractals has become wider

3.4. Velocity

The velocity of formation of fractal, as well as how it is formed, depends on parameters such as viscosity and surface tension of mixtures. The result we got from repeated experiments is that by keeping the diluted acrylic concentration constant (keeping the surface tension constant) and changing and increasing the ink-alcohol composition, the velocity of forming fractal increases (Fig. 7).

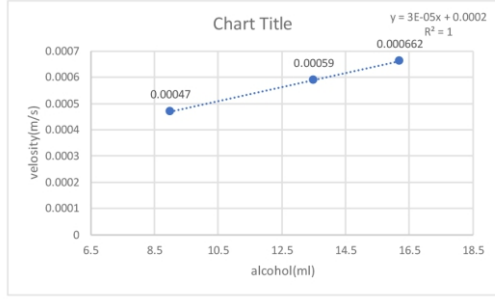

Fig. 7: Constant surface tension with 25% water and different ink-alcohol compositions that led to increased velocity

Also, if we keep the same ink-alcohol compositions and dilute the acrylic (increase the surface tension), the velocity

of forming fractal will increase (Fig. 8).

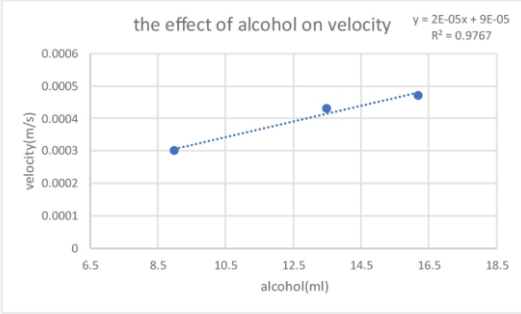

Fig. 8: As the surface tension increases, the speed also increases

4. Discussion

In the previous parts, we observed that without any external pressure, fractal fingers begin to form spontaneously when we drop a droplet of ink-alcohol mixture on diluted acrylic.

Our goal was to investigate the geometry and dynamics of these fractal patterns, which we reached many results after research.

4.1. Three-Stage Spontaneous Fractal Fingering Due to Multicomponent Character of Diluted Acrylic

Under no external pressure gradients, a surprising three-stage diffusive process was observed wherein ink-alcohol appears to finger spontaneously into diluted acrylic.

Acrylic itself is composed of various components such as polymer, pigment, etc.; This is the reason why acrylic has components of different sizes and it can be considered a multi-component solution. In diluted acrylic, small, lighter components are mobile and are susceptible to diffusion. Heavy, branched components, on the other hand, are less mobile in comparison and their self-affinity retains the heavy components in the original diluted acrylic phase. Similarly, lighter components enable the diffusion of other species, such as the ink-alcohol, to diffusive easily, whereas heavier components retard the diffusion of such solvents. As a result, when in contact with a miscible solvent such as ink-alcohol mixture, differential rates of diffusion arise due to molecular size and mobility. The fractal-like fingering process continues until light, mobile components are extracted preferentially by diffusion. Full extraction of the light components marks the conclusion of spontaneous fingering in first stage and the onset of slow diffusion in second stage.

The spontaneous fingers that formed in this phenomenon exhibit self-similarity .

4.2. Existence of Distinct Interfaces

In pressure-driven Saffman-Taylor fingering, instabilities are driven by the most unstable wavelength, λc, given by:

$$\lambda_c = \pi b \sqrt{\frac{\sigma}{\Delta\eta V}}$$

where b is the height of the ink-alcohol mixture, σ is the surface tension, $\Delta\eta$ is the difference in viscosity between diluted acrylic and ink-alcohol, and V is the interfacial velocity. Considering that different compositions were used for the experiments in this article, values should be obtained for each of the above variables with any series of experiments.

The capillary formula mentioned above is for the conditions of Saffman-Taylor fingering experiments, and in order to apply it to our experimental conditions, we must consider b something else.

In the condition of their experiment a liquid was placed between two glass sheets and another liquid injected on it with a syringe attached to it (Fig. 9); in that situation b was the gap between two glasses but in the context of our problem b should be considered as something else. When we drop a droplet of ink-alcohol onto diluted acrylic a new surface is formed on our previous surface (Fig. 10); b should be considered as the height of the new surface (Fig. 11).

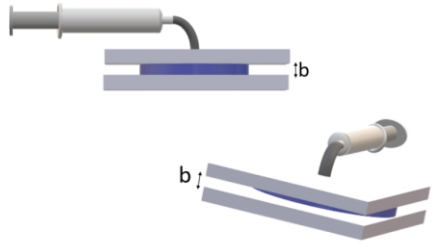

Fig.9: Simplified model of Hele-shaw cell

Fig. 10: ink-alcohol onto diluted acrylic

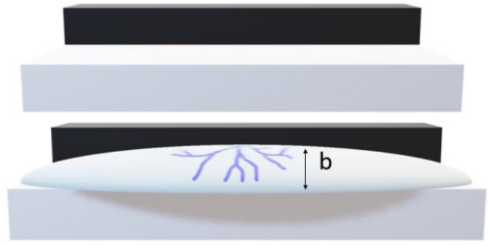

Fig.11: The height of the ink-alcohol mixture

5. Conclusion

The three-stage spontaneous dispersive mechanism observed reveals a surprising mechanism that underlies the Saffman-Taylor instability for miscible, multicomponent fluids. In this work, spontaneous fractal fingering between Ink-alcohol mixture and diluted acrylic were studied.

To be sure of the obtained results and their accuracy, we compared the width of the fractal obtained through our experiments with the widths obtained through the scales taken from the photos of the experiments and converted into real numbers and units (Table 2 and 3).

In this comparison, it can be seen that the obtained data are slightly different from the real data, and this proves to us that the results obtained through these researches and experiments were without problems.

Acknowledgment

This work is supported by the AYIMI/ ADIB institutes. We gratefully acknowledges the support and helps of M.Shariatmadar, N.Hosseini, Dr. M.Khatir.

References

[1] W. Song, N. N. Ramesh, and A. R. Kovscek, “Colloids and

Surfaces A: Physicochemical and Engineering Aspects", 584, 123943 (2020).

[2] C. W. Park and G. M. Homsy, "Physics of Fluids", 28, 1583 (1985).

[3] Canabal, José, et al., "Simulation of Dendritic Painting. Computer Graphics", Forum 39, 2, 597-606 (2020).

[4] Lagrée, Bertrand, et al., "Scaling properties of viscous fingering", (2014).

[5] A. L. Robinson, Science 228, 1077 (1985).

Paper Wrinkles

Yekta Esmail kashi , Tehran / Iran

ARTICLE INFO

Participant in IYNT 2016 (Junior)

Selected by Ariaian Young Innovative Minds Institute , AYIMI

http://www.ayimi.org ,info@ayimi.org

ABSTRACT

Cellulose in the wood, the most important material that is used in the paper, has many links between the fibers of it. After paper was soaked in water and water evaporates a little water is still remained between fibers which causes stress between fibers. Stress will cause deformation and wrinkling . In this study different parameters are investigated by experiments.

Keywords : *: Cellulose, Paper, Wrinkle, Parameters*

1. Introduction

Paper is one of the materials that people have been using in their life to note many important things (for example, the application form to enter an university) all around the history. But, every thing can be loosed even if the paper wrinkles a little. One of the worst accidents that may happen to us is when water pour on the paper and water can impair it. After paper dries, it wrinkles. Hence, it can cause many problems. In this situation knowing that why does paper wrinkle after being wet is really important to remove wrinkles.

Over the centuries, paper has been made from a wide variety of materials (such as wood pulp, rice, water plants, cotton and even old clothes). But, any way for making paper fiber is needed [1]. Paper is manufactured by raw wood, which is made up of fibers called cellulose [2] Wood fiber sources are classified as hardwoods (a.k.a. deciduous, angiosperms) and softwoods (a.k.a. conifers, gymnosperms). While hardwoods form smoother surfaces, softwood fibers give paper more tear strength. The pulp fiber mixture, called the furnish, is carefully controlled to optimize paper properties[3]. Secondary fibers do not bond as well as virgin cellulose fibers. They do not wet to the same degree and the fiber-fiber bond strength is weaker [3]. But studding related phenomena takes very much time and requires expensive tools because fibers of paper are too small and following events happening is hard.

In here, we proved why paper winkles in another way that did not take much time and did not need expensive tools.

2. Experiments

The experiment was with such kind of paper with the qualities as shown in Table (1).

The most common method of testing smoothness or roughness in the paper is by one of three air leakage methods. Bendsten roughness is achieved by clamping the test piece between a flat glass plate and a circular metal head and measuring the rate of airflow in ml/ minute between the paper and head.

The weight of a piece of paper was measured. Then it was soaked in water and was put away to get dried. After drying the weight of the wrinkled paper was measured .

The fibers of paper were studied because if the weight of the paper does not change means that the fibers are changing. A picture of the piece of paper under microscope is taken (Fig.1a and b). The microscope was German Leitz Wetzlar with magnifying of 500.

Table 1. The qualities and properties of the paper used in the most of the experiments [4]

Sl. NO	Particulars	Unit	JKC 75	JKC 80
1	Caliper	Micron	102+/- 2	108+/- 2
2	Breaking length	Meter	4500 ± 500	4500 ± 500
3	Tear factor	--	65 ± 5	65 ± 5
4	Moisture	%	4.0 ± 0.5	4.0 ± 0.5
5	Roughness (Bendsten)	Ml. / Min.	300 Max	300 Max
6	Wax pick (Min)	No.	14A	14A
7	Brightness	% ISO	94 +/- 1	94 +/- 1
8	Opacity (Min)	% ISO	92	92

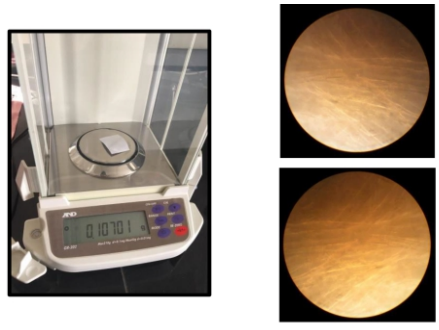

(a) (b)

Fig.1: a) The paper on scale; b)The fibers of the paper under microscope

The paper was soaked in water and it got dried while wrinkling. Then the fibers of the wrinkled paper was seen under microscope and taken pictures of it (Fig. 3).

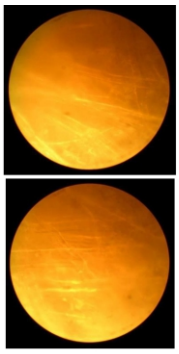

Fig. 3: The fibers of the wrinkled paper under microscope

A strip of paper was made sized 5mm in 10mm and it was soaked in 25ml of water for 3 minutes. It was put on a glass dish for getting dried but because of the hydrogen bonding of water it was stuck to the glass dish so wrinkling would not be the result. After it dried the length of the paper was measured and it was 101mm (Fig.4).

Fig. 4: The paper after getting dried and increasing of the length

Seven strips of paper was made sized 3mm in 70mm and they were soaked in water respectively for 300s, 180s, 60s, 30s, 15s, 10s and 5s. After getting dried and wrinkling the new length of the papers were measured by paint application. Then in the paint application pixels which a line was drawn in a millimeter are shown. That is the way of understanding how many pixels are in a millimeter of the picture (Fig.5).

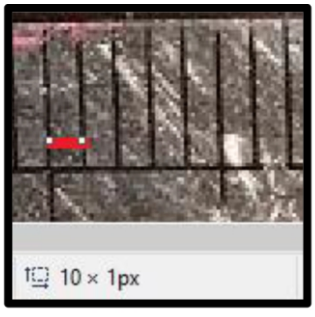

Fig. 5: The pixels of the line from one side to the other side of a millimeter of ruler drawn is shown in paint application

Then lines should be drawn on the length of the paper in the picture to see how many pixels are in a wrinkle of the paper. The pixels of a line of a wrinkle is shown as the length and breadth of a right triangle in paint application (Fig. 6).

Therefore, the line that was drawn on the wrinkle is hypotenuse of the right triangle and the length of hypotenuse can be measured by Pythagoras rule. Then the additional of all hypotenuses is the whole length of paper but unite of it should be changed to millimeter from pixels. "1mm = (A) px, So, L′(mm) = L′(px) / A" can help for finding length of the wrinkled paper.

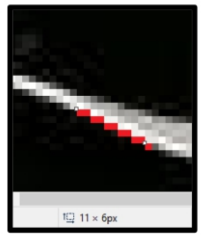

Fig. 6: The line drawn on the wrinkle of 15 seconds soaked paper and the pixels of the right triangle shown

For measuring resistance of wrinkled paper and a smooth paper , six strips of paper were made sized 29.5cm in 0.3cm. Five of them were soaked in water for 2, 10, 30, 60, 300 seconds and the other one was not soaked in water to be smooth. After drying some loops were made by strips that the top of the loop was 23cm. Then 4cm of it was put on surface and the edge of the surface was on the fourth cm of strip that the other piece of paper was hung. Some weights were hung to the loop. If the paper tore with heavier weights means it has more resistance.

For removing wrinkles of a wrinkled paper an iron that worked with humidity was put on some wrinkled strips of paper that were soaked in water for 10 seconds and 30 seconds. Then the new surface of the paper was measured to see if there is any shrinkage with ironing.

3. Results

The weight of the paper before soaking in water and after getting dried was the same (Table 2).

Table 2: The exact weight of paper before soaking in water and after getting dried

Weight of thw paper before soakng in water	Wieght of the paper after getting dried
0.10698 g	0.10701 g

Not changing in the weight of the smooth paper and the wrinkled one, shows that there was not any substances in the paper added or reduced. But, something that is causing wrinkling is the fibers.

When strips of paper were wrinkled, the length of the strips was measured (Table 3).

Table 3 :Average length of the wrinkled paper and the difference between length of the wrinkled paper (L′) and the first length of the paper in different times soaked in water

The time paper The time paper was soaked in water (s)	Average length of the wrinkled papers (mm)	L′ - L
5	66.24063	-3.75937
10	66.22374	-3.77626
15	65.459645	-4.540355
30	63.92412	-6.07588
60	63.525535	-6.474465
180	64.678555	-5.321445
300	66.534525	-3.45475

The length of the paper in the different times of soaking in water differs. Wrinkling has the result of shrinkage. According to the chart if soaking in water is nearer to 60s means that it had the highest length decreasing (Fig. 7). But if paper's length increased when it was stuck to the dish after soaking in water is because of that the fibers could not get as close as they should. Hydrogen bonding between water and glass dish did not allow papers have its shrinkage.

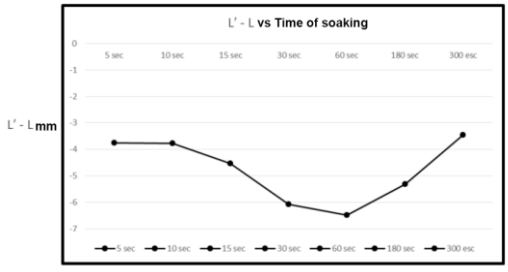

Fig. 7: L′-L in different times of paper soaked in water

When the weights were hung to the strips of papers the weights that paper tore with was measured (Table 4). Paper which has soaked in water nearer to 30s has more resistance and also wrinkled paper has more resistance than a piece of paper that has not soaked in water .

Table 4: Average of the weights which paper tore in different times soaked in water

Time paper was soaked in water (s)	Average of the weights paper tore with (g)
0	222.5
2	302.5
10	330
30	390
60	302.5
300	261

When strips of paper wrinkled after soaking in water , the length of them was measured. For removing wrinkles an steam iron was used. Then the length of the ironed strips of paper were measured (Table 5).

Table 5: Average difference between length of ironed paper and wrinkled paper

The time paper was soaked in water (s)	Average length of the paper after wrinkling (mm)	Average length of the paper after ironing (mm)	L″ - L′	L″ - L
10	67.857	63.107	-4.749	-6.892
30	67.019	63.257	-3.762	-6.742

As it is shown in the table the length of paper was decreased after ironing. Therefore, ironing with steam irons that work with humidity is not helpful for removing wrinkles and shrinkages because humidity can cause wrinkling as water do. For short period of time the iron can remove wrinkles but it would wrinkle after some minutes. Therefore electric irons that humidity does not have effect on their work should be used.

For removing wrinkles and shrinkage of a piece of paper cross-linked fibers should be made. For making cross-linked fibers there is a method that includes heating the treated cellulosic fibers to promote intrafiber cross-linking [5] (Fig. 8).

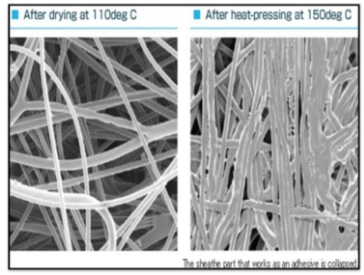

Fig. 8: The difference between heat and heat-pressing for removing wrinkles of paper [6]

Heating and pressing without humidity and water is a good way for removing wrinkles. In the factories, that paper is made, paper is under the pressure of some heavy rollers that make the pulp into sheets (Fig. 9). But when the paper is soaked and not drying with an arrangement, the paper would be wrinkled.

Fig.9: Paper making factory [8]

A sheet of paper that is made up of cellulosic fibers are attracted to each other cross-linking. When paper is soaked in water the fibers get far from each other. When paper got dried a little part of the water is still remained between fibers, water from another sides evaporates. Because of the electronegativity fibers and water are attracted to each other (Fig. 10). Hence, the internal force is not 0. If internal force is not 0, there would be stress between fibers. Stress is the force per unite area [9]. Stress will cause deformation and area of paper would be decreased.

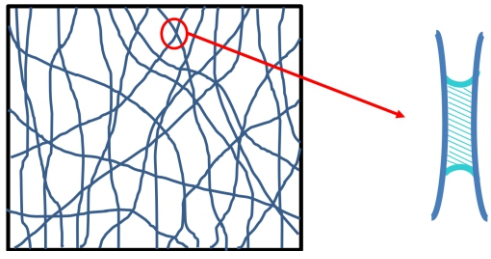

Fig. 10: Cross-linked fibers of paper after water evaporates and the water remaining that is causing stress and deformation

4. Conclusion

From all these information it is concluded that in the factories, wood pulp was converted into thin sheets by some hot rollers, to make water evaporate and make fibers stick together. Hence, there would be more attracting between fibers and because water causes stress and deformation, the result would be wrinkling. Water.

causes stress and deformation and the result would be wrinkling so in factories water should be evaporated. Wrinkled paper has more resistance than a piece of paper that was not soaked in water. Every time with wrinkling, shrinkage would be the result for paper. For converting a wrinkled paper to an smooth paper heat and pressing is needed while there is the least of moisture.

References

[1] http://www.idahoforests.org/paprmake.htm

[2] http://wonderopolis.org/wonder/how-do-you-make-paper-from-a-tree/

[3] D.R. Rothbard, Electron Microscopy for the Pulp and Paper Industry, 2001, page 8

[4] http://www.jkpaper.com/index.php?option=com_content&view=article&id=24&Itemid=25

[5] https://www.google.com/patents/US7074301

[6] http://www.laurelleaffarm.com/item-pages/vintage-Sunbeam-Ironmaster-electric-iron-art-deco-bakelite-handle-original-cloth-cord-Laurel-Leaf-Farm-item-no-nt3324.htm

[7] http://www.sp-paper.jp/english/case/use59.html

[8] http://someinterestingfacts.net/how-is-paper-made-step-by-step/

[9] https://www.britannica.com/science/stress-physics

Investigating Growing plants in Different Kinds of Light

Mobina Ebrahimi Fakhar Tehran / Iran

ARTICLE INFO

Participant in IYNT 2016 (Junior)

Selected by Ariaian Young Innovative Minds Institute , AYIMI

http://www.ayimi.org ,info@ayimi.org

ABSTRACT

The advantages and disadvantages of the artificial lightening experiments test by comparing the effect of full spectrum light bulb and light-emitting diode (LED) lamps on different samples (i.e. plants). Utilized full spectrum light is comparable with our universe sun spectrum, and only its intensity is lower. Utilized LED lamps cannot be so useful because plants need different kinds of spectra and cannot grow with limited number of spectra. Each limited range spectrum effects on the growth of special part of plant. Chlorophyll is not the same in all plants. Different chlorophyll, absorb different spectra.

Keywords : *: Artificial Lightening, Growing plant, Spectra, Cholorophyll*

1. Introduction

Our life completely depends on plants because they keep us alive by making food. They need light to produce food by action of light on their cells containing chlorophyll ($C_{55}H_{72}O_5N_4Mg$). This process is called photosynthesis (an example of energy transformation). Plants usually use sunlight for photosynthesis but it is not always possible all around the clock. Hence, we can use artificial lights when the sunlight is not available.

The effect of artificial lights on growth of plants has been experimented. Blue and red light have been used to help the growth of leaves and flower, respectively [1]. Artificial lights can be used to grow plants in areas that are not suitable for plants such as dark places. Another advantage of the artificial lights is that they can be used in the desired season, for example in winter that the intensity of sunlight is low [2]. But using LED light bulbs, with limited spectrum range, is not always a good idea to grow plants because most plants need full spectrum lights and other energies [3].

We used both LED and full spectrum light bulbs to stimulate the sunlight and also use the advantages of artificial lights. The utilized LED frequencies were in the range of the 430–770 THz (about 1.6 – 3.2 eV, i.e. visible spectrum). Results shown that the light wavelength ($\lambda = \frac{c}{f}$, where f and c are frequency and light velocity, respectively) has directly influence on the growth of a particular plant. Chlorophyll is an important pigment in the process of photosynthesis. It is a photoreceptor that is found in the chloroplast of green plants. Chlorophyll A and chlorophyll B are the two major types of chlorophyll. Chlorophyll C and chlorophyll D are less common and are found in different algae.

Chlorophyll A is the most prevalent type of chlorophyll. This type of chlorophyll absorbs red, blue and violet wavelength. Chlorophyll B is found primarily in plants as well, but this type absorbs blue light only and is yellow in pigment [4]. Different types of spectra have different effects on the growth of plants [5].

Visible light waves are the only electromagnetic waves human eyes can see. These waves are seen as the colors of the rainbow. Each color has a different wavelength. Red has the longest wavelength and violet has the shortest wavelength. When all the waves are seen together, they make white light. When white light shines through a prism, the white light is broken apart into the colors of the visible light spectrum [6].

2. Experiment

Potting soil was put into the plant pots, and a bean seed was buried under half an inch in each pot. LED lamps (blue, red, green, colors) and full spectrum light bulbs (incandescent and fluorescent lamps) were placed over the boxes (Figs. 1 and 2) .

Fig. 1: plant under fluorescent lamp

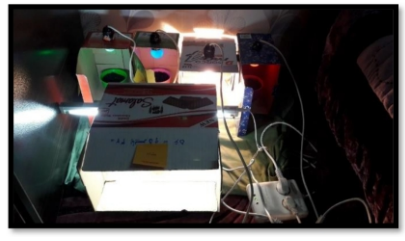

Fig. 2: Lamps are above the boxes

The boxes were sealed to prevent the light to escape. Lights were turned on/off every morning/evening at certain times. Another important point which must be considered is the different intensities of the LED lamps. In here, to have a good and acceptable estimation the growth parameter was normalized to the utilized intensities. The bean seeds under fluorescent lamp, grew in a really good way and became very strong, healthy, and green plant. So fluorescent is a good light source for plants (Fig. 3). Blue

LED was very useful for plant`s height but the plant didn`t become strong and green. But the plant`s leaves didn`t grow as good as its height (Fig. 4).

Fig.3: Plant under fluorescent lamp, day 1 to 13

Fig. 4: Plant under blue LED, day 1 to 13

The plant that was under red LED, didn`t become high. But it`s leaves grew in a suitable way (Fig.5). although Incandescent lamp has most of the necessary spectra of plant, because of making the area so hot, it cannot be a good light source (Fig. 6). Green LED is not a good light source, because the plant cannot grow in a good way and it became yellow and weak. Because green spectrum is the reflection of green color of plant`s leaves which don't have a lot of effect on plant`s growth (Fig. 7).

Fig. 5: Plant under red LED , day 1 to 13

Fig. 6: Plant under incandescent lamp , day 1 to 13

Fig. 7: Plant under green LED , day 1 to 13

3. Results

Plants prefer full spectrum artificial light (fluorescent lamp), because full spectrum light gives the full range of required energy to survive a plant. However, sometimes a bulb can be better than sunlight because most part of the light that plant receives from sunlight is not necessary. It means that some wavelengths are not absorbed by plants and they only reflect from the surface. Some other wavelengths have only an influence on the growth of special parts. At the blue, plants receive the materials for being high, while the red have influence on plants leaves [1], and at white (fluorescent lamp), plant would have the best growth.

Incandescent light bulbs give off too much heat for most plants, and although they meet the red light needs, they do not supply enough blue rays. Fluorescent tubes are better light sources and last about 10 times as long as an incandescent bulb . Because bean could grow better with blue and red lights, therefore, we can say that bean has chlorophyll A and chlorophyll B. (Fig. 8) there are some differences about the leaves of plants. The leaves of a plant that grew with fluorescent light is thicker and veins are less obvious. The leaves of a plant that grew with red LED were thinner than others (Fig. 9). There are also some differences about plant`s leaves size. Leaves of a plant that grew by fluorescent lamp were bigger than others.

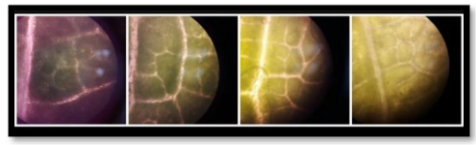

Fig .8: From left, plant under fluorescent light, blue LED, green LED, red LED

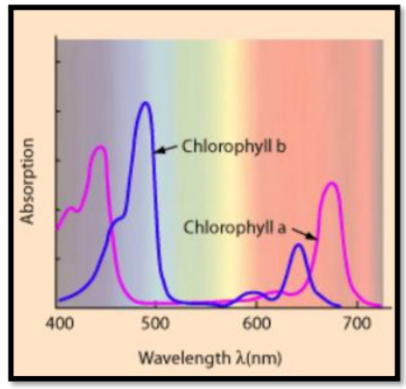

Fig. 9: Chlorophyll A and B absorb red and blue wavelength

4. Conclusion

Fluorescent bulb is the best choice for artificial lightening (beans) because it acts like sunlight and the plant can use all needed spectra. Gradually, artificial lightening can replace sunlight because it is more available and more manageable and also Artificial lightning is sometimes better than sunlight because all part of the light that plant receives from sunlight is not necessary. Using LED light bulbs cannot be so useful because plants use each spectrum for special usage but sometimes a special plant grows better with special spectrum. The difference between growth of different plants under different spectrums is because of the chlorophyll of plants. Green plants mostly, have chlorophyll A and B, which absorb red and blue spectra.

References

[1] M. Simpson et al., does the watt size of a light bulb affect a plant`s growth.

[2] A. Taylor et al., The differences between natural and artificial lights.

[3] http://www.education.com

[4] https://www.hyperphysics.phy

[5] https://www.wikipedia.org

[6] https://www.NASA.gov

Investigating an Intriguing Effect When One or Several Highly Elastic Balls Collide on Each Other or on the Surface

Artin Radmatin[a], Kiana Kamalipoor Shiraz[b]

a) Valeh school; b) Farzanegan 2 school , Tehran / Iran,

ARTICLE INFO

a)Gold medalist in ISAC Olympiad 2023(Junior)

b) Bronze medalist in IYNT 2018

Awarded by Ariaian Young Innovative

Minds Institute , AYIMI

http://www.ayimi.org ,info@ayimi.org

ABSTRACT

When two objects collide in a short time, they exert forces on each other, they can either stick together or bounce off one another. In this study by different balls such as basketball, volleyball, soccer ball, tennis ball and ping-pong ball elastic collision when the objects separate after impact and don't lose any of their kinetic energy and momentum is conserved is compared with inelastic collision which the total kinetic energy is not constant are studied . The time of collision and different materials are studied and the results and data are analyzed to find these collisions deeper.

Keywords : *: Elasticity , Collision , kinetic energy, momentum, time of collision*

1. Introduction

Momentum is a quantity that describes the amount of force required to stop an object. Also there are two types of collisions related to the momentum: elastic and inelastic.

Elasticity is the reversible deformation property of the environment and materials which in elastic collision the total kinetic energy of the two things before and after colliding is equal but in inelastic collision this energy is not constant. In the real world, there are no purely elastic or inelastic collisions.

Perfectly elastic collisions can happen only with subatomic particles. Everyday observable examples of perfectly elastic collisions don't exist, some kinetic energy is converted into heat transfer due to friction but when the surfaces are nearly frictionless ,collisions between everyday objects can be considered as elastic.

Examples of elastic collisions are seen in a game of billiards and Newtonian pendulum. When a moving ball hits a stationary billiard ball, the moving ball stops when it hits, but transfers all of its momentum to the other ball, resulting in the stationary ball spinning at the initial speed of the moving ball again it is supposed the friction can be neglected.

Also it should be noticed that if an isolated system is subject only to conservative forces, then the mechanical energy (sum of the kinetic energy(K) and potential energy (U)) $E=U+K$, is constant.

In this study all the impacts are free fall which refers to the movement of any object that is only under the force of gravity which has two different modes :

- With air resistance: In this mode two opposite forces enter the object, the first is gravity and the other is friction. The force of constant gravity is downward, but the force of friction is variable and upward and depends on the speed of the object .
- Without air resistance: In this mode the only force on the object when falling is its weight, and according to Newton's second law, the acceleration on the object will be downward, which is known as gravitational acceleration.

2. Theory

Momentum describes the motion of objects when collide to each other. In an elastic collision, where kinetic energy is conserved, the total momentum of the system as the conservation of momentum, before the collision is equal to the total momentum after the collision (Eqs. 1, 2).

$$\mathbf{p}_1 + \mathbf{p}_2 = \mathbf{p'}_1 + \mathbf{p'}_2 \tag{1}$$

$$m_1\mathbf{v}_1 + m_2\mathbf{v}_2 = m_1\mathbf{v'}_1 + m_2\mathbf{v'}_2 \tag{2}$$

But in an inelastic collision kinetic energy is not conserved and is one in which objects stick together after impact, and the maximum amount of kinetic energy is lost. This lack of conservation means that the forces between colliding objects may convert kinetic energy to other forms of energy, such as potential energy or thermal energy. For example two objects that have equal masses head toward each other at equal speeds and then stick together. The two objects come to rest after sticking together, conserving momentum but not kinetic energy after they collide. Some of the energy of motion gets converted to thermal energy, or heat (Eqs. 3, 4).

$$m_1\mathbf{v}_1 + m_2\mathbf{v}_2 = m_1\mathbf{v'}_1 + m_2\mathbf{v'}_2 \tag{3}$$

$$m_1\mathbf{v}_1 + m_2\mathbf{v}_2 = (m_1 + m_2)\,\mathbf{v'} \tag{4}$$

In inelastic collisions, v′ is the final velocity for both objects as they are stuck together, either in motion or at rest.

3. Materials and Methods

3.1. Practical Experience: Elastic Collision in Basketball Game

In Basketball game, two parameters should be fixed for the best condition of playing:

- Ground Elasticity
- Ball Elasticity

These two parameters are very important because the elasticity of the ground and ball should be fixed in a condition which after ball collision with ground, the ball returns to the normal height .In basketball game, the material which is used for ball is leather which has high

elasticity to have a good return height and also the ground material is a maple wood which has a middle elasticity so with the collision of the ball with ground, the ball will have a logical return height .

Table 1: Different types of balls

Balls			Collision Surfaces	
Type	Ball's Material	Mass (g)	Hard	Soft
Basketball	Leather and Rubber	534.3	Granite	Grass
Soccer Ball	PVC	424.5		
Volleyball	Leather	275.8		
Tennis Ball	Rubber and Cloth	55		
Ping-Pong Ball	Celluloid	1		

4. Qualitative Experiment

4.1. Test 1 – Effect of materials of surface and balls on time which balls need to run out kinetic energy

In this test, all 5 balls were released separately from constant height (167 cm from collision surface), once on hard surface and once on soft surface. After releasing, time which took from the first collision of ball with surface up to when it stops was measured.

Table 2: Effect of the material of surface and ball on time which balls need to run out kinetic energy (Test 1)

Tests	Basketball	Football	Volleyball	Tennis ball	Table tennis ball
On Grass	3.49 s	1.65 s	3.39 s	2.57 s	1.38 s
On Granite	4.99 s	1.92 s	4.11 s	3.68 s	10.59 s

4.2. Test 2 - Quantitative height measuring after first collision

In this test, 2 modes were designed to measure height which balls get after first collision.

4.2.1. Test 2.1 – Effect of the materials of surface and ball on return height

In this test, all 5 balls were released separately from constant height (167 cm from collision surface), once on hard surface and once on soft surface. After releasing, height which ball return after first collision was measured.

Table 3: Effect of surface material and ball material on return height (Test 2.1)

Tests	Basketball	Football	Volleyball	Tennis ball	Table tennis ball
On Grass	80 cm	37 cm	72 cm	63 cm	35 cm
On Granite	92 Cm	52 cm	78 cm	71 cm	97 cm

4.2.2. Test 2.2 – Effect of ball temperature on return height

In this test, tennis ball was released from constant height (167 cm from collision surface), on hard surface, once with 24 and once with -8 ℃ . After releasing, height which ball return after first collision was measured.

Table 4: Effect of ball temperature on return height(Test 2.2)

Tests	Tennis ball in 28°C	Tennis ball in -8°C
On Granite	28 cm	71 cm

4.3. Test 3 - Qualitative height measuring after first collision

In this test, 2 modes were designed to measure height which balls get after first collision

4.3.1. Test 3.1- Effect of two balls on top of each other releasing height on return quality

In this test, Tennis ball on Basketball was released concurrent from 3 different heights (49 cm, 88 cm, and 170 cm from collision surface), once on hard surface and once on soft surface. After releasing, height which tennis ball returned, because it cannot be measured, effect of changing releasing height on return quality was analyzed.

4.3.2. Test 3.2- Effect of putting 3 balls on each other on return quality

In this test, Tennis ball on Volleyball on Basketball was released concurrent from constant height (167 cm from collision surface), on soft surface. After releasing, height which tennis ball returned, because it cannot be measured, effect of putting 3 balls on each other on return quality was analyzed.

5. Quantitative Experiment

When a highly elastic super ball collides with a rigid surface how can one determine the collision time? In this problem we want to find the collision time by different methods. The definition of collision time is the time when the ball touches the surface till leaves the surface (Fig. 1).

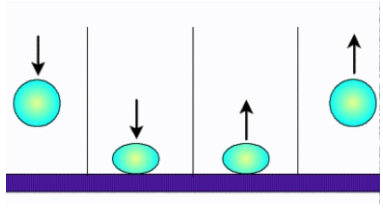

Fig. 1: Highly elastic super ball collides with a rigid surface

In inelastic collision the height of a ball when it falls, h_1 is not the same as the height it returns back, h_2 (Fig. 2).

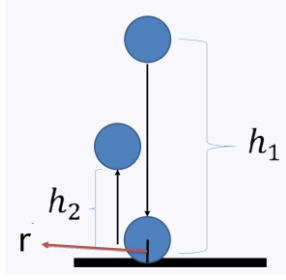

Fig. 2: Impact and return height of a ball in an inelastic collision

By the theory and experiment the collision time is measured (Eqs. 5-9).

$$mgh = \frac{1}{2}mv^2 + mgr \quad (5)$$

$$v_1 = \sqrt{2g(h_1 - r)} \quad (6)$$

$$v_2 = \sqrt{2g(h_2 - r)} \quad (7)$$

$$\left|\frac{m(v_2 - v_1)}{\Delta t}\right| = F \quad (8)$$

$$\left|\frac{mv_1(e-1)}{F}\right| = \Delta t \quad (9)$$

where;

mgr= kinetic energy
mgh = gravitational energy
h_1= Height which leaves the ball
h_2= Height which the ball comes up

Then the ratio of velocity of return ball to falling (Eq. 10) is measured.

$$\frac{v_2}{v_1} = e = \sqrt{\frac{h_2 - r}{h_1 - r}} \quad (10)$$

Theory and experiment will give the collision time as Δt when the ball is releasing from different heights (Eq. 11) (Fig. 3).

$$\left|\frac{mv_1(e-1)}{F}\right| = \Delta t \quad (11)$$

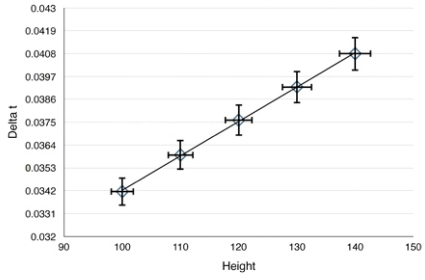

Fig. 3: The collision time vs height

we found that whenever we release the ball from higher height the time of the collision (Δt) will be more.

In the next experiment we tried the same thing on different surfaces (asphalt , stone , ceramic) (Fig. 4).

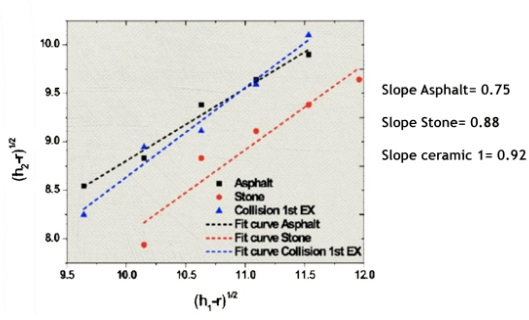

Fig 4: Collision on different materials

According to Equation (10) , in conclusion we can say that the time of a collision is different in different materials and in our experiment is like below:

Ceramic surface > stone surface > asphalt surface

6. Results and Analysis

Data which table 2 shows, basketball on the soft surface took more time to run out kinetic energy comparing with hard surface so soft surface took more energy from the basketball, so it can be said:

Granite surface has more elasticity than grass surface.

For analyzing the effect of ball material on time which balls need to run out kinetic energy , 5 balls were tested on hard surface and as data of table 2 shows , the order of the elasticity of the balls from the most to the least are:

1-Ping-Pong Ball
2-Basketball
3-Volleyball
4-Tennis Ball
5-Football

So due to table 1 (ball's material column), celluloid has the most elasticity and PVC has the least and the elasticity of materials from the most to the least can be mentioned as follows:

1-Celluloid
2-Leather and Rubber
3-Leather
4-Rubber and Cloth
5-PVC

Of course, it is obvious that the mass of the ball is also effective and depends on the material and dimensions of the ball which will be studied in our next project completely.

Data in table 4 shows, tennis ball with 24 ℃returns more comparing with tennis ball with -8 ℃ so a ball that has been placed in a cold space returns a lower height because in a cold object, due to the low molecular movement, part of the energy is used to reach environment temperature which reduces the kinetic energy for the ball's return after hitting the surface.

Qualitative analyzing shows when we drop two balls together (same balls) from a higher height, the top ball goes much higher because it stores more energy and therefore transfers more energy and the tennis ball it rises with more kinetic energy, so it will have a greater height.

By quantitative experiments we found that the collision time is increased as the height increased too.

Also in different materials the time of collision in ceramic is more than two other stone and asphalt surfaces.

6. Discussion

Elastic collisions are known as collisions which kinetic energy is equal before and after the collision but there is no purely elastic collision in the real world due to the usual wasting energy in converting potential energy into kinetic energy. So in this study , when collisions occur , due to the air resistance it is not exactly elastic collision .

Also this relationship between elasticity of ball and surface should be fixed for ball games as like as basketball. Because in sports like basketball, controlling the time and height of the ball's return after hitting the ground is an important factor in maintaining and improving the quality of the game.

Acknowledgments

1-Thanks from ISAC Olympiad organizer

2-Thanks from Mr.Arjmand- Head of research, creativity and skill department of Valeh

3-Thanks from Dr. Izadi - Head of Ariaian Young Innovative Minds Institute (AYIMI)

References

[1] Gibbs, Keith 2020.Dropping balls: School physics Blog (https://www.schoolphysics.co.uk/)

[2] David-Halliday-Robert-Resnick-Jearl-Walker-10ed.pdf

[3] https://openstax.org/books/physics/pages/8-3-elastic-and-inelastic-collisions

Microscopic Swimmers

Abedeh Tormi, Farzanegan 2 school , Tehran / Iran, abedehtormi@gmail.com

ARTICLE INFO

Participated in IYNT 2022 Georgia

Awarded by Ariaian Young Innovative Minds Institute , AYIMI

http://www.ayimi.org ,info@ayimi.org

ABSTRACT

In this study flagella and Cilia movements and their function for the cell are investigated. The locomotion of bacterial or eukaryotic cells that use natural flagella to move in a liquid is studied experimentally and theoretically .For sampling, we used two areas with natural ponds in Tehran and Mashhad, named Jajroud River in Tehran and Golestan Dam in Mashhad. The samples were immediately transferred to the laboratory for analyzing.

Keywords : *: Flagella, Cilia, Bacterial , Eukaryotic Cells*

1. Introduction

What is flagella ? It is a hair-like organ in microorganisms and which creates the ability of movement and chemotaxis for the cell which has a wave-like movement in one direction (Fig. 1).

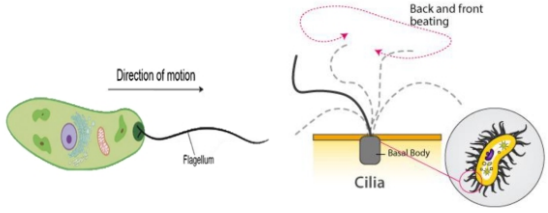

Fig. 1: Flagella and its movement

What is cilia and what is the difference between flagella and cilia? Its function for the cell is like a sensor which has a forward and backward movement (Fig. 2).

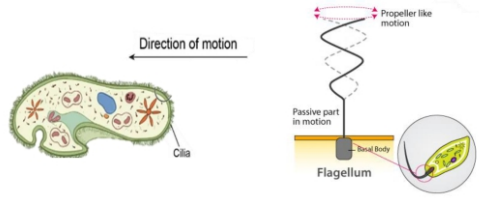

Fig. 2: Cilia and its movement

In eukaryotic cells we can find flagella like male gametes in animals, male gametes in early plants and some protozoa and algae (Fig. 3).

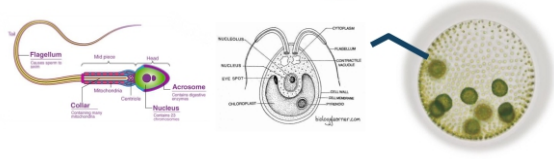

Fig. 3: Flagella in eukaryotic cells

Prokaryotic cells bacteria have flagella (Fig. 4).

Fig. 4: Flagella in prokaryotic cells

There are different types of movement in cells , whip and rotational.

Eyokaryotes : The flagella has whip movement (Fig. 5a)

Prokaryotes : The movement of the flagellum is rotational and this rotation can be clockwise and counter clockwise (Fig. 5b).

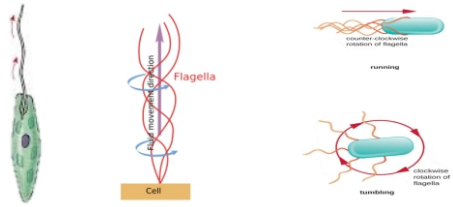

(a) (b)

Fig. 5: a) The flagella whip movement; b)The rotational movement of the flagellum

When rotation of flagella is clockwise it pulls the microorganism and has a backward movement and for counterclockwise rotation it pushes microorganism and has a forward motion (Fig. 6).

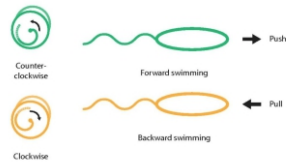

Fig. 6: clockwise and counterclockwise rotation

2. Experiments

In our experiments for sampling, we used two areas with natural ponds in Tehran and Mashhad, named Jajroud River in Tehran and Golestan Dam in Mashhad.

For this purpose, sterile glass containers were used and after collecting the samples, the samples were immediately transferred to the laboratory.

Microscopic studies are needed to detect all types of microorganisms (bacteria, protozoa and algae). Some of these microorganisms require their own staining methods for better identification under the microscope.

After staining the target microorganisms, the prepared slides are examined under the microscope with different magnifications. Also, some microorganisms can be identified completely without staining under the microscope (Fig. 7).

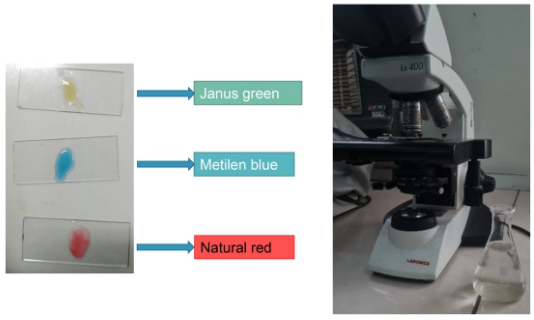

Fig. 7: Staining and studying the samples under the microscope

For paramecium staining, first we poured the sample on the slide and then Janus green, Metilen blue and neutral red colors are used for staining. In this staining, pulsating vacuoles and food vacuoles are seen in red and cilia in light blue.

In the microscopic study of the samples, several characteristics were investigated: the movement of bacteria, the possible presence of protozoa and stained paramecium slides. Also we did this experiment with raw milk and found bacteria that are swimming in the raw milk (Fig. 8).

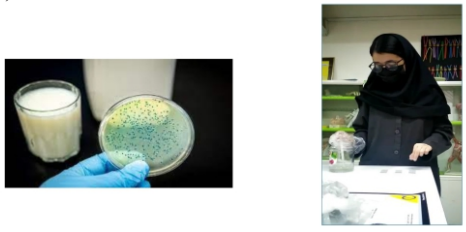

Fig. 8: Bacteria are swimming in the raw milk

Three sample were taken from jajrud river : surface ,middle and bottom of the river. We know that microorganisms use cilia, flagella and Pseudopod to swim in the liquid and you can see Paramecium Cillia and bactria using flagella , sperm using flagella and Pseudopod Amoeba (Fig. 9).

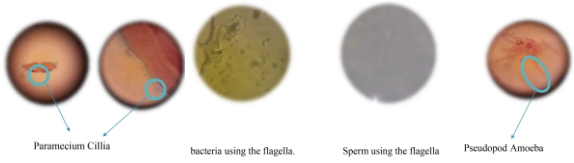

Fig. 9: Swimming of microorganisms in liquids

We used tracker to track The movement of one of the bacteria and the results showed the speed of bacteria is unstable and when it has purposeful movement we can see swimming and tumbling (Fig. 10).

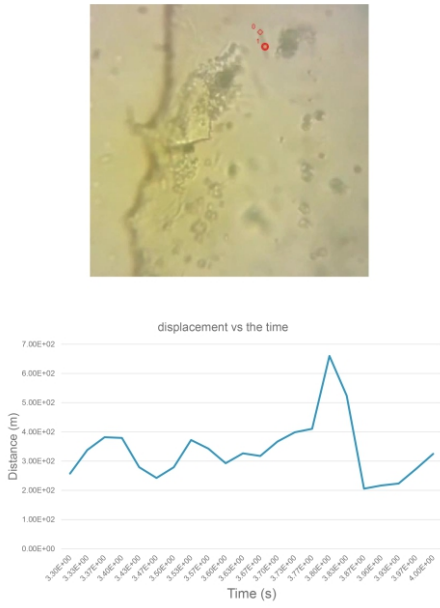

Fig. 10: Tracking the movement of one of the bacteria

3. Results and Conclusion

Based on our tests and experiments the bacteria have two kinds of movement (Fig 11).

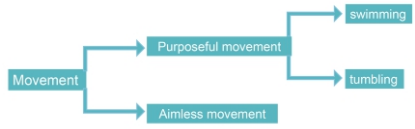

Fig. 11: Movement of bacteria

Also a wide range of microorganisms (prokaryotes and eukaryotes) have flagella. These creatures can swim using flagella because of their living conditions in water and humid environments.

A large number of microorganisms without flagella are able to move and swim using other structures.

References

[1] Bacterial Flagella Stain Protocol by Jay Mellies , 08 September 2008

[2] The surprisingly diverse ways that prokaryote move by Ken F. Jarrell*and Mark J. McBride / June 2008

[3] Tracking the Movement of a Single Prokaryotic Cell in Extreme Environmental Conditions

[4] The surprisingly diverse ways that prokaryotes move7

[5] https://www.britannica.com/science/cilium

Arrester Bed

Lucas Hinsching Mostafá, Brazil, lucasmostafa@gmail.com

ARTICLE INFO

Participated in IYPT 2023

Awarded by Ariaian Young Innovative Minds Institute , AYIMI

http://www.ayimi.org ,info@ayimi.org

ABSTRACT

A sand-filled lane results in the dissipation of the kinetic energy of a moving vehicle. What length is necessary for such an arrester bed to entirely stop a passively moving object (e.g. a ball)? What parameters does the length depend on? To study this phenomenon several experiments have been done and the results are compared with theory to find the best situation in reality.

Keywords : *: Moving vehicle, arrester bed, length, parameters*

1. Introduction

The arrester bed is used in roads to decelerate cars or trucks that lost control. Some studies were made so that this deceleration would be maximized, and accidents minimized, therefore, what the problem proposes is an analysis of this behavior.

For the model used in the following, we considered the object to be either a cylinder or a sphere. As seen in some preliminary observations and that can also be concluded intuitively, the main analysis should be the relationship between the sand and the object parameters.

2. Theory

2.1. Cylinder's Coordinates and Properties

For the phenomenon there are two main forces that lead the motion, the shear stress $(\vec{\tau})$ and the normal tension $(\vec{\sigma})$ which are the rolling friction and the normal for the interaction between objects and granular soils (Fig. 1).

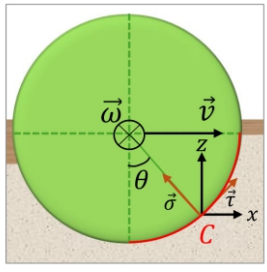

Fig. 1: Diagram of forces (shear stress and normal tension)

Other important parameters are the angular velocity $(\vec{\omega})$, linear velocity $(\vec{v})$, Coordinates *X, Z* and θ, as well as the contact surface C (Fig. 2).

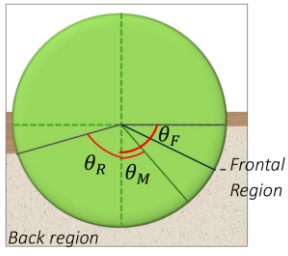

Fig. 2: Definition of frontal and back region and maximum theta

As we defined theta, some specific values will be important, such as the ones of initial (θ_F) and final contact (θ_R) with the sand, and one in which the normal tension is maximum (θ_M).

After defining the latter thetas it is possible to describe the sinking depth *(Z)* as a function of them(Eq. 1).

$$\theta_M \leq \theta \leq \theta_F\colon\ z = R(\cos(\theta) - \cos(\theta_F)) \tag{1}$$

To get to a motion equation it is better to separate them in the *Z* and *X* axis, which can be done decomposing the normal tension and the shear stress as the equation (2).

$$\overrightarrow{\sigma_z} = (\sigma\, cos(\theta) + \tau\, sin(\theta))\hat{z} \tag{2}$$

As said, now it becomes possible to achieve the motion equations by integrating the resultant of them $(\overrightarrow{\sigma_T} = \overrightarrow{\sigma_z} + \overrightarrow{\sigma_x})$ all over the contact surface C (Eq. 3).

$$\begin{pmatrix} F_x \\ F_z \end{pmatrix} = \int_C \overrightarrow{\sigma_T}, \hat{n}\, bR\, d\theta \tag{3}$$

With *b* being the cylinder width and *R* the radius. Separating the forces at *X* and *Z* and using the definition of torque the three equations of motions are found (Eqs. 4-6).

$$m\ddot{x} = \int_C (\tau\, cos(\theta) - \sigma\, sin(\theta)\, Rb)d\theta \tag{4}$$

$$m\ddot{z} = \int_C (\sigma\, cos(\theta) + \tau\, sin(\theta)\, Rb)d\theta - mg \tag{5}$$

$$I\dot{\omega} = \int_C R\tau(\theta)Rbd\theta \tag{6}$$

2.2. Pressure Model and Distribution

During the preliminary observations it was possible to observe a relevant dependence on the sand properties, and to find the normal tension and the shear stress, we chose the model of Beker.

This model was proposed in such a way that the pressure exerted by a flat surface on a granular soil would be proportional to the sinking depth multiplied by factors that include both the sand and the surface properties described in the following equation (Eq. 7).

$$\sigma = \left(ck_c + \rho k_\phi \mathrm{b}\right)\left(\frac{\mathrm{z}}{\mathrm{b}}\right)^{\mathrm{n}} \tag{7}$$

In which σ is the normal tension, *c* is the tension of ground cohesion; is the sand density ρ and k_c are the constants for

a single combination of a granular soil and a flat surface that can be found experimentally; b is the cylinder width; z is the sinking depth and n is the sinking exponent.

The tension of ground cohesion is a parameter that measures how strong is the interaction between the particles of sand, which is assumed to be 0 for dry sand, yielding in a n between 0.5 and 2.0.

Using the equation of the Beker model with the expression of the sinking depth found before we get an expression for σ_1 which is the normal tension at the frontal region (Eq. 8) $(\theta_m < \theta < \theta_f)$.

$$\sigma_1 = (\rho k_\phi b)\left(\frac{R}{b}\right)^n (\cos(\theta) - \cos(\theta_f))^n \quad (8)$$

As shown in the figure (3), there is a pressure distribution that follows a mountain shape on the cylinder, therefore a simetry between the frontal and back region can be stablished around the point of maximum normal tension.

Mathematically we can find a theta from $\theta_M < \theta < \theta_R$ that is equivalent to another one in $\theta_m < \theta < \theta_f$ and get the other values of normal tension as follows (Eq. 9).

$$\sigma_2 = (\rho k_\phi b)\left(\frac{R}{b}\right)^n \left(\cos\left(\theta_F - (\theta_F - \theta_M)\frac{\theta}{\theta_M}\right) - \cos(\theta_f)\right)^n \quad (9)$$

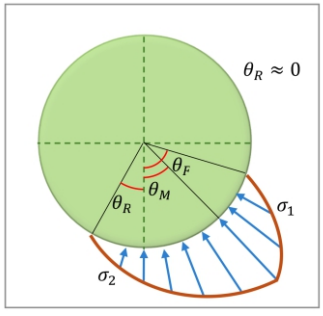

Fig. 3: Diagram of pressure distribution (blue arrows)

2.2.1 Shear Stress

Similarly to the rolling friction, for the cylinder to roll there must be friction and thus, it dependent on the normal, or in this case, the normal tension.

For that some parameters were added, such as the parameter of shear deformation (k) and the angle of ground friction (ϕ), which are found experimentally and vary from soil to soil, and the last one, the distance of ground displacement j, as observed, some particles of sand are pushed backwards due to the rolling motion of the cylinder, and j is the distance traveled by these particles. However, as stated before, one of our considerations is that the sand is dry and therefore c is negligible . So the equation becomes(Eqs. 10-11).

$$\tau(\theta) = (c + \sigma(\theta)\tan\phi)(1 - e^{-j/K}) \quad (10)$$

$$\tau(\theta) \approx (\sigma(\theta)\tan\phi)\left(1 - e^{-j/K}\right) \quad (11)$$

To calculate j we define it throughout the slipping speed which is given by $v_s = \omega R - \dot{x}\cos\theta$ achieving the integral form (Eqs. 12-13).

$$j = \int_\theta^{\theta_F} (\omega R - \dot{x}\cos\theta)\frac{d\theta}{\omega} \quad (12)$$

$$j = R(\theta_F - \theta) - \frac{\dot{x}}{\omega}(\sin(\theta_F) - \sin(\theta)) \quad (13)$$

2.2.2. Angle of Maximum Pressure

As the shear stress has two defined regimes which depend on the angle theta it must be defined, that is what we will explore a little bit.

For that we used a paper by Jo-Woung Wong and A.R. Reece as a reference. The equation that will describe the behavior of the angle of maximum normal tension is as equation (14).

$$\theta_m = \left(a_1 + a_2\frac{b}{R}\right)\theta_f \quad (14)$$

which the effect of the ratio b/R gets clearer with the following diagrams (Figs 4a,b and c).

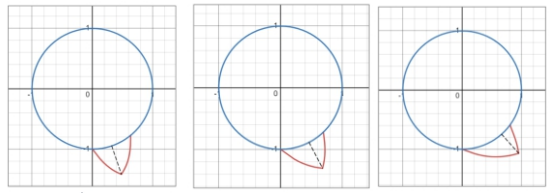

(a) (b) (c)

Fig. 4: a) b/R=0.5; b) b/R=1.5 ; c) b/R=2.5

Therefore as the ratio gets greater the angle increases and therefore is closer and closer to the horizontal axis, leading to a greater resistance force. It is important to notice that the parameters a_1 and a_2 fixed values for the material used in the cylinders:

$$a_1 = (0.30 \pm 0.04); a_2 = (0.15 \pm 0.01)$$

2.3. Motion Equations

As all the normal tension and the shear stress which were unknown before are now explained and found mathematically, we can return to the initial equations for $\ddot{x}, \ddot{z}$ and $\ddot{\theta}$ to substitute σ and τ to get a complete solution of the phenomenon.

The equations for the x, z and θ coordinates then become(Eqs. 15-17).

$$m\ddot{x} = Rb\int_C \sigma(\theta)\left(-A_1(\theta) - B_1(\theta)e^{-\frac{\dot{x}}{\omega K}(\sin(\theta)-\sin(\theta_f))}\right)d\theta \quad (15)$$

$$m\ddot{z} = \int_C \sigma(\theta)\left\{A_2(\theta) + B_2(\theta)e^{\frac{\dot{x}}{\omega K}(\sin(\theta)-\sin(\theta_f))}\right\}d\theta - mg \quad (16)$$

$$I\dot{\omega} = R^2 b\int_C \sigma(\theta)\left[A_3(\theta) - B_3(\theta)e^{\frac{\dot{x}}{\omega K}[\sin(\theta)-\sin(\theta_f)]}\right]d\theta \quad (17)$$

In which the coefficients A_ and B_ were used to shorten the solution. An interesting thing that can be observed with mathematical development is that the integral in the mg really fast, therefore the cylinder achieves a constant sinking depth in the soil surface from the fact that the resultant force in z is nude in most of the motion.

2.4. Parameter calculation k_ϕ

This parameter relates the amount of contribution that the density and the size parameter of the cylinder will contribute to the normal tension exerted on the object.

This can be made by linearizing the equation for pressure using logarithm (Eq. 18).

$$\log(\sigma) = \log(\rho k_\phi b) + n\log\left(\frac{z}{b}\right) \quad (18)$$

By plotting the linearized form of the equation the graph

is found, and by comparing the fit values with the coefficients we find the value of n and ρk_ϕ (Fig. 5).

$$n = (1{,}38 \pm 0{,}03) \qquad \rho k_\phi = (10{,}4 \pm 0{,}32)Pa$$

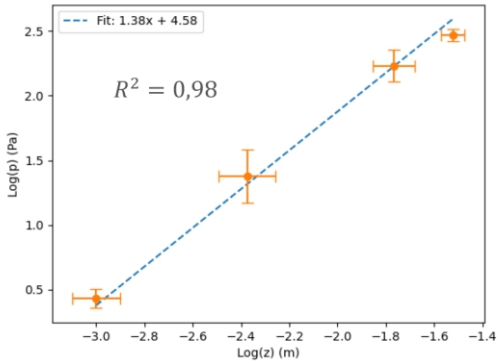

Fig. 5: Linearized graph of pressure

3. Experimental Setup

In the experimental setup the following materials were used:

- Cylinders made of ABS of different dimensions, some only changed height, others, width
- Ramp made of MDF for launch, which was standardized by using tweezers.
- Acrylic box of dimensions 50* 10 * 5 cm^3
- Different types of sand, such as natural quartz and dolomite, in which some only the density changed (black basalt and dolomite) and other only the size change, e.g. dolomite.
- Cellphone camera
- Ruler

4. Results

The analysis of the data taken using tracker and comparing to the predicted behavior of the equations of motion found theoretically leads to some interesting conclusions regarding the influence of some parameters.

The first one was the cylinder mass, in which we maintained the geometrical proportions constant, but changed the material. It can be thought that the change of the material would yield in a change of friction and therefore interfere in the system, it showed to be a false statement, since the properties of the sand have a much greater relevance on the phenomenon.

As seen, if the mass increases the distance traveled by the objects decreases, since the more massive the objects gets the greater the resistive forces get, because it is sinking more in the soil. Note that the continuous line is a theoretical plot and the points are experimental data with the respective error bars.

Another analysis made was of the diameter of the cylinder, which was changed with easily since the cylinder were made on a 3D printer. From the graph, it is possible to assert that as the diameter is bigger, also is the resistance forces, since an increase in the diameter leads to an increase in the shear tensor.

Finally, the last parameter we can vary of the cylinder is the height *b*. This variation would lead to an increase in the area of contact between the soil and the object and thus, increase the resistance forces and the displacement will decrease (Figs. 6-8).

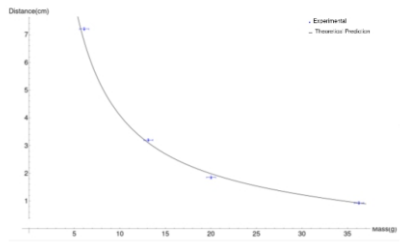

Fig. 6: Graph of Distance per mass; experimental and theoretical comparison

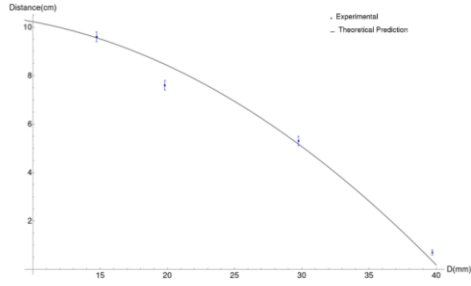

Fig. 7: Graph of Distance per Diameter; experimental and theoretical comparison

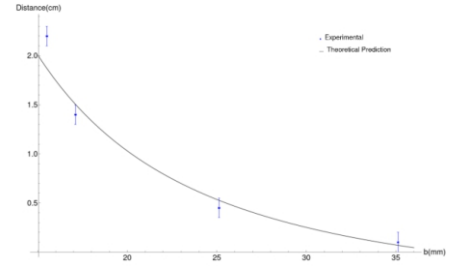

Fig. 8: Graph of Distance per Cylinder height; experimental and theoretical comparison

Another possible analysis due to the experimental setup is the variation of the density of the particles of sand. As can be observed, as the density increases the displacement decreases, but the most interesting is that some points have a huge deviation from the theoretical predication, which comes from the fact that these particles of sand are too big (between 3.00 to 5.00 mm for the most deviated point). Therefore our theory only holds for certain sizes of particle, and the behavior of a granular soil does not maintain for great values (Fig. 9).

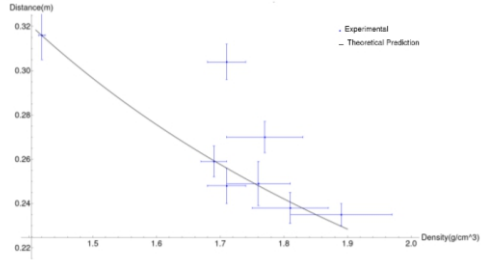

Fig. 9: Graph of Distance per Soil Density'; experimental and theoretical comparison

To check on the validity of our theory with another approach, we compared the prediction of the loss of kinetic energy with the experimental data, as it was one of the topics the problem statement stood up (Fig. 10).

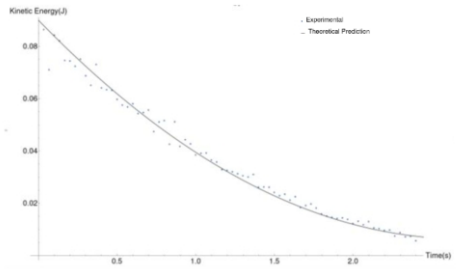

Fig. 10: Graph of the Kinetic energy per time; theoretical and experimental comparison

As said before, another possible object to analyze this situation is the sphere, and so we compared experimentally what would happen for this geometry. From the data we can see that the cylinder presences a resistance force greater than the sphere does, and so the latter has a longer displacement.

5. Conclusion

This work presented an analysis of the behavior of the arrester beds that can be seen on the roads and help prevent accidents due to its deceleration characteristics. For the theoretical approach we used a model of tensors and found equations for the axis we defined. For later development we made some experiments and took data so that it was possible to compare the theoretical predictions with the real data (Fig. 11).

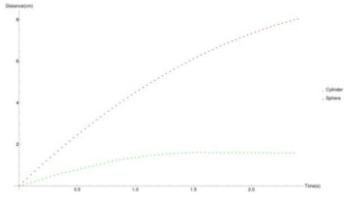

Fig. 11: Graph of a experimental comparison between the displacement of a cylinder and a sphere

Therefore we explored both the parameters of the cylinder and of the granular soil that would affect the displacement of the object during the phenomenon.

References

[1] Coutermarsh, B. (2007). Velocity effect of vehicle rolling resistance in sand. Journal of Terramechanics, 44(4), 275–291.

[2] De Blasio, F.V., Saeter, M.B.: Rolling friction on a granular medium. Phys. Rev. E 79, 022301 (2009)

Ariaian Young Innovative Minds Institute, AYIMI
Unit 14, No. 32, Malek Ave., Shariati St.
Post Code: 1565843537
Tel - Fax: +9821-77522395, 77507013
Tehran/ Iran
URL: http://www.ayimi.org
http://journal.ayimi.org
Email: info@ayimi.org